



UNIVERSITY OF AMSTERDAM

MSC PHYSICS

TRACK: THEORETICAL PHYSICS

MASTER THESIS

Black hole radiation and energy conservation

by

Bram van Overeem

10222332

July 2017

60 ECTS

Supervisor:

DR. JAN PIETER VAN DER SCHAAR

Second reviewer:

DR. BEN FREIVOGEL

INSTITUTE FOR THEORETICAL PHYSICS

Abstract

In this thesis we address the issue of enforcing energy conservation throughout the Hawking emission process for black holes. In order to do so, we include an important back reaction effect: the self-gravitational interaction of the radiation. Restricting to spherically symmetric field configurations, we show that the inclusion of this effect leads to a modified emission probability, which no longer corresponds to a strictly thermal spectrum. Instead, the probability is related to the change in the black hole's Bekenstein-Hawking entropy as a result of the emission. The analysis seems to show explicitly that one may interpret Hawking radiation as originating from a tunneling process. We clarify how the derivation of Hawking radiation as such a quantum mechanical tunneling process emerges from reducing the field theory to an effective particle description. Subsequently, we generalize this derivation to include charged radiation. In addition, the results in this thesis are discussed in the context of the weak gravity conjecture and related to the fragmentation of AdS_2 .

Acknowledgements

First and foremost, I would like to sincerely thank my supervisor Jan Pieter van der Schaar for his guidance, encouragement and inspiring views on physics. I would also like to thank Ben Freivogel for agreeing to take on the role as second reader. Furthermore, I thank Lars Aalsma for many enlightening discussions and for taking the time to work with me to find new solutions. Finally, I wish to thank my fellow students, in particular Antonio, Bahman, Charlie, Heleen, Thanasis and Vincent, for making the past two years such an inspiring and enjoyable experience.

Contents

1	Introduction	1
2	Black holes in general relativity	6
2.1	Properties of black holes and event horizons	7
2.2	Black hole mechanics	10
2.3	The Schwarzschild black hole	12
2.4	The Reissner-Nordstöm black hole	14
2.5	Painlevé coordinates	18
3	Quantum field theory in curved spacetime	20
3.1	Scalar field quantization in curved spacetime	21
3.2	The concept of particles and their gravitational creation	25
4	Black hole radiation and its consequences	27
4.1	Hawking's derivation of black hole radiation	27
4.2	Hawking's result and black hole thermodynamics	34
4.3	Black hole puzzles, paradoxes and conjectures	35
5	The effect of energy conservation on black hole radiation	39
5.1	Outline of the approach	40
5.2	Results for massless radiation	41
5.3	Results for massive, charged radiation	58

6	Black hole radiation as tunneling	62
6.1	The tunneling of massless particles through the horizon	64
6.2	Generalization to massive and charged radiation	68
6.3	Hawking radiation as tunneling and thermodynamics	73
7	The WGC, black hole radiation and AdS (in)stability	75
7.1	The weak gravity conjecture	76
7.2	AdS as near horizon geometry	80
7.3	The weak gravity conjecture and AdS (in)stability	85
7.4	AdS ₂ fragmentation	87
8	Conclusions	89
A	Conformal diagrams	92
B	Solving to the Klein Gordon equation in a Schwarzschild geometry	97
C	Evaluating contour integrals	100
C.1	One pole on the real axis	100
C.2	Issues with logarithms	101
	Bibliography	103

Chapter 1

Introduction

At present, quantum gravity remains an unresolved problem of fundamental physics. Despite notable progress, physicists have yet to succeed in developing a broadly accepted and consistent theory that reconciles and unites Einstein's theory of general relativity with the principles of quantum mechanics.¹ Independently and at their respective scales, these two theoretical frameworks have proved to be spectacularly successful. Nevertheless, they are fundamentally very different and the quantization of gravity is accompanied by many difficulties, both conceptual and technical.

Still, we may try to learn about the quantum properties of gravity by taking an approach other than its full quantization. One such approach is to consider a semiclassical theory in which we study quantum fields, but treat gravity classically. This approach leads us to the subject of quantum field theory (QFT) in curved spacetime, a framework that allows us to make progress, even without a full quantum theory of gravity at our disposal. A striking example is presented by the semiclassical study of black holes, which reveals their curious quantum mechanical properties. As will become clear throughout this thesis, black holes form a setting in which the tension between the theories of general relativity and quantum fields is clearly exposed. As such, they make a great 'laboratory' for theoretical physicists to study the properties of (quantum) gravity.

Classically, black holes are regions of spacetime from which nothing can ever escape. They

¹It should be noted that many candidate theories of quantum gravity have been proposed, the most successful and probably most promising of which is string theory. Despite its numerous successes, this theory is still very much a work in progress.

possess a horizon, acting as a surface from beyond which there is no coming back. But in 1974, Hawking showed that the inclusion of quantum effects greatly alters this picture [1]. Using methods of QFT in curved spacetime, he demonstrated that quantum effects actually cause a black hole to radiate a thermal flux of particles, with a temperature²

$$T_H = \frac{\kappa}{2\pi}, \quad (1.1)$$

now known as the Hawking temperature. The radiation effect, too, is named after its discoverer: *Hawking radiation*.

Hawking's famous demonstration of black hole radiance followed earlier work [2, 3, 4, 5] on a striking mathematical analogy between black hole mechanics and regular thermodynamics. His result allowed this to become a truly physical analogy and led to the conclusion that black holes are thermodynamic objects. In this context Hawking's result directly implied that one must associate an entropy to a black hole, proportional to its area

$$S_{BH} = \frac{A}{4}, \quad (1.2)$$

called the *Bekenstein-Hawking entropy*.³ Thus, already when one semiclassically includes quantum effects, one discovers strong hints for an unexpected fundamental connection between gravity, thermodynamics and quantum theory. This in turn may provide a clue as to how to understand the nature of black holes in a theory of quantum gravity.

The semiclassical study of black holes, however, features some paradoxes and contradictions. For example, according to (1.2), one associates a huge entropy with a black hole, which seems to be at odds with the *no hair theorem* in relativity.⁴ How should one think of this entropy and what are the microstates that make up for this huge entropy? In the context of string theory progress has been made in understanding the microscopic origin of the Bekenstein-Hawking entropy [6], but many of its aspects remain unclear. Probably the most puzzling consequence of black hole radiation is what is called the *black hole information paradox*. If Hawking's derivation is correct, and one may treat quantum gravity as an effective field theory in regions where the curvature is small, then this seems to imply that the quantum evolution in black hole backgrounds ceases to be unitary [7]. This is obviously something

²Throughout this thesis we work with units in which $\hbar = c = G_N = k_B = 1$, unless stated otherwise.

³The idea that black holes must have an entropy proportional to their area was already proposed by Bekenstein [4, 5]. Hence the name Bekenstein-Hawking entropy. Hawking's results fixed the proportionality constant.

⁴This theorem will be discussed in the next chapter.

that is hard to live with and it is now generally believed that also in the process of black hole evaporation information is conserved. It remains unclear, however, in what way.

The information paradox demonstrates a clear conflict between the theories of general relativity and quantum mechanics. As such, it might also be regarded as a potential key to their unification. Similarly, other open problems encountered in semiclassical black hole physics can be thought of as hints with regard to the quantum nature of gravity. Indeed, black hole thought experiments have been vital in getting to our present understanding. The study of Bekenstein-Hawking entropy, for example, led to the holographic principle [8, 9]. Further considerations of this concept [6] and the information paradox in turn contributed to the AdS/CFT correspondence [10].

Features of quantum gravity are thus often inferred from known black hole physics. In this context, we wish to mention a particularly interesting conjecture regarding the properties of (quantum) gravity: the *weak gravity conjecture* [11]. This conjecture can essentially be recast in a form in which it states that in any consistent theory, charged black holes must be able to dissipate their charge as they evaporate down to the Planck scale. It can therefore be regarded as an example of how one attempts to learn about quantum gravity and its low energy realizations through (semiclassical) physics of black holes.

With the above, we hope to have convinced the reader a lot is still to be learned from the physics of black holes at its current state. Over the past decades, our comprehension of black holes has developed substantially. However, some aspects, particularly those involving the evaporation of black holes, remain far from fully understood. With this in mind we focus on attempting to gain a better understanding of the Hawking process. Standard derivations of black hole radiation employ strictly semiclassical methods: the background geometry is treated as fixed and one calculates the response of quantum fields to this geometry. In this approximation, one does not enforce energy conservation and the radiation is strictly thermal. It seems clear that in order to better understand the Hawking process, one wishes for a description that, as opposed to standard derivations, allows the geometry to fluctuate and thereby enforces energy conservation.

The question of how to incorporate energy conservation or, more generally, gravitational back reaction in the black hole radiation problem has not yet been solved in a satisfactory way. In the context of what we discussed above, there are two possible approaches to attack this gravitational back reaction problem. Firstly, in the ideal case one could develop a theory

of quantum gravity and use its machinery to calculate the desired properties of black holes. Instead, we will focus on the second approach, which is to take the semiclassical derivation as a starting point and to derive gravitational corrections to the process of black hole radiation.

Such an approach is possible if we restrict to spherically symmetric setups. In order to compute corrections, we will need to move beyond the free field approximation and allow the geometry to change in response to the emission of matter. Another way to look at this, is that we should include the self-gravitational interaction of the radiated matter. An approach that allows for the inclusion of these effects was suggested by Kraus and Wilczek [12, 13]. Building on this approach, a large part of this thesis is devoted to an analysis of the modification of the spectrum of black hole radiance due to self-gravitational interaction, the simplest and probably (quantitatively) most important effect of back reaction.

As we will discover, this energy conserving analysis is intimately connected to the tunneling picture that is generally drawn to heuristically describe Hawking radiation. Our analysis seems to imply that one may indeed naturally interpret Hawking radiation as originating from the quantum mechanical tunneling of particles and anti-particles across the horizon. Building partially on results of Kraus and Wilczek [12, 13], the derivation of Hawking radiation along these lines has already been pioneered in [14]. It was shown that indeed, energy conservation, or gravitational self-interaction of the emitted matter, is of crucial importance for the consistency of this picture. This thesis also covers the derivation of black hole radiation along the lines of this natural tunneling picture. In addition to the above, we set out to clarify how this approach emerges from the field theory and aim at generalizing it.

This thesis is organized as follows. The next two chapters aim to provide the reader a basic understanding of the physical concepts that will be used in the following chapters. Chapter 2 gives a review of some classical black hole physics, after which chapter 3 introduces the reader to the theory of quantum fields in curved spacetime. In chapter 4 we put into practice what we have learned in the previous two chapters to derive black hole radiation, using the strictly semiclassical approach followed by Hawking. Furthermore, we briefly review black hole thermodynamics and some of the yet unresolved puzzles known to semiclassical black hole physics. Starting from chapter 5, we get to the main part of research. This chapter consists of a detailed calculation of the black hole emission spectrum, including effects resulting from self-gravitation. It will be shown that properly taking into account these effects leads to a modification of the emission spectrum. In the analysis performed in

chapter 5, a quantum mechanical tunneling calculation seems to emerge when we truncate the field theory to an effective particle description. In chapter 6 we discuss the derivation of Hawking radiation as such a quantum mechanical tunneling process, which was suggested in [14]. We then generalize this procedure to massive and charged radiation. In chapter 7 we review the weak gravity conjecture and the closely related (in)stability of AdS vacua, and discuss our results in this context. Finally, in chapter 8 we review our main conclusions.

Chapter 2

Black holes in general relativity

In general relativity, the standard gravitational action is the Einstein-Hilbert action

$$S_{EH} = \frac{1}{16\pi} \int d^4x \sqrt{-g} R, \quad (2.1)$$

where $g = \det g_{\mu\nu}$ and R is the Ricci scalar. Varying the Einstein-Hilbert action with respect to the metric one can show that it yields as its equations of motion the famous Einstein equations¹

$$R_{\mu\nu} - \frac{1}{2} R g_{\mu\nu} = 8\pi T_{\mu\nu}. \quad (2.2)$$

Here $R_{\mu\nu}$ is the Ricci tensor and $T_{\mu\nu}$ is the energy-momentum tensor. We may think of the Einstein field equations as a set of differential equations for the metric field $g_{\mu\nu}$. The equations therefore dictate how the dynamics of the metric (i.e. the curvature of spacetime) respond to the presence of energy-momentum.

The Einstein equations (2.2) are notoriously hard to solve. The set of equations becomes more tractable once we impose certain symmetries on the metric. The most obvious setup to consider is a spherically symmetric gravitational field. The study of such setups in general relativity leads to a remarkable prediction: the existence of black hole solutions. Physically, a black hole is a region from which nothing can classically escape. Black holes are prominently present in modern science; not only in physics, but also in astronomy and mathematics. As

¹For a derivation of the Einstein equations from the Einstein-Hilbert action see e.g. [15]. Here we have set the cosmological constant Λ to zero.

was clarified in the introduction, to theoretical physicists black holes are mysterious objects of great interest.

In order to understand Hawking radiation and the concepts applied in the remainder of this thesis, one has to be familiar with some aspects of black hole physics. In this section we review these aspects. In doing so we are only concerned with classical considerations of general relativity. We begin with the discussion of some general properties of black holes and their horizons. This discussion will be necessarily brief and focuses on conveying the main ideas, instead of providing rigorous proofs.² Next, we review two black hole solutions that will be used extensively in the remainder of this thesis: the Schwarzschild and Reissner-Nordström geometries. In chapters 5 and 6, we will use a particular set of coordinates, named Painlevé coordinates, when working with these geometries. We end this chapter with a review of this set of coordinates.

2.1 Properties of black holes and event horizons

To start with, we want to define what we mean when speaking of a black hole. In the classical theory of general relativity, a black hole is a region that is physically characterized by the fact that the gravitational field is so strong that it is impossible for anything to escape. It is this notion that we would like to make more precise. To do so, we make a restriction, which is to only consider spacetimes that are *asymptotically flat*.

Asymptotically flat spacetimes are spacetimes that become like Minkowski spacetime as $r \rightarrow \infty$. Technically, a spacetime possesses the property of asymptotic flatness if in its conformal (or Penrose) diagram specific infinities match with the conformal structure of Minkowski spacetime. We refer the reader unfamiliar with conformal diagrams to appendix A for a review of conformal diagrams, conformal infinity, etc. Conformal infinity is subdivided into five different regions: future and past timelike infinity, i^+ and i^- , spatial infinity i^0 , and future and past null infinity, \mathcal{I}^+ and \mathcal{I}^- . i^+ , i^- and i^0 are spacetime points, while \mathcal{I}^+ and \mathcal{I}^- are null surfaces. In an asymptotically flat spacetime, i^0 , \mathcal{I}^+ and \mathcal{I}^- fit the Minkowskian structure. Consequently, an asymptotically flat spacetime has a conformal

²We have in no way aimed to provide a complete overview of classical black hole physics. For those interested in the complete picture, including all details we refer to e.g. [16, 17, 18, 19]

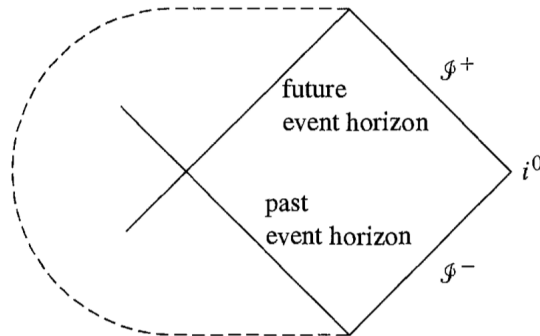


Figure 2.1: An asymptotically flat spacetime has a conformal diagram in which i^0 , \mathcal{I}^+ and \mathcal{I}^- match with the Minkowskian structure. The rest of the spacetime, represented by region within the dashed line, can have different structures, examples of which we will encounter later. (Figure taken from [15])

diagram of the general form depicted in figure 2.1.

In spacetimes that are asymptotically flat, something has ‘escaped’ the black hole if it reached the asymptotic part of this spacetime. We are now able to give a definition of a black hole in an asymptotically flat spacetime $(M, g_{\mu\nu})$. In such a geometry the black hole region \mathcal{B} is $\mathcal{B} = M - J^-(\mathcal{I}^+)$. Here $J^-(\mathcal{I}^+)$ is the causal past, J^- ,³ of future null infinity \mathcal{I}^+ . Looking at figure 2.1 we then see that the hole’s future event horizon is the boundary of the causal past of future null infinity $J^-(\mathcal{I}^+)$.⁴ Thus by definition the event horizon is a null hypersurface. This definition also clarifies why, classically, there is no way out of a black hole. The future event horizon is the hypersurface that separates the spacetime points starting from which timelike curves can reach infinity from the points starting from which they cannot. This final region is the black hole.

The question is now: how do we locate an event horizon? In this thesis we are interested in stationary⁵, asymptotically flat black hole spacetimes that contain an event horizon with the topology of a sphere. In such spacetimes, it can be shown that the event horizon is the hypersurface located at r_h , such that $g^{rr}(r_h) = 0$ (in regular spherical coordinates) [15].

³The causal past of a point x , $J^-(x)$, is the set of all spacetime points that causally precede x .

⁴There is a similar definition for the past event horizon, as the boundary of the causal future of past null infinity $J^+(\mathcal{I}^-)$.

⁵A stationary spacetime is a spacetime that has a Killing vector field that is timelike near infinity. If that Killing vector field is orthogonal to a family of spacelike hypersurfaces, the spacetime is called static.

The properties of event horizons are especially interesting to study, since it is believed that ‘generic’ solutions to the Einstein equations have singularities that are hidden behind horizons. This idea is made explicit in the *cosmic censorship conjecture*, stating that in general relativity reasonable initial states will never lead to the formation of *naked singularities*. Naked singularities are singularities that are not hidden within an event horizon. Signals starting from such a naked singularity have no problem reaching \mathcal{I}^+ .

As we only consider stationary geometries, the spacetimes we encounter possess a Killing vector $\xi = \partial_t$ that is timelike near infinity. We will see that at the event horizon of such spacetimes, ∂_t will switch from being timelike to spacelike, meaning that at the horizon ∂_t is null. A null hypersurface along which some Killing vector field ξ^μ is null, is called a *Killing horizon*. Although an event horizon does not in general need to be a Killing horizon, it will be for the spacetimes under our consideration. In this thesis we study spacetimes for which the event horizon is a Killing horizon for the Killing vector field $\xi^\mu = (\partial_t)^\mu$ [2, 16].⁶

To every Killing horizon, and hence to the event horizons in this thesis, one can associate a so called *surface gravity*. The Killing vector field ξ^ν for which a hypersurface Σ is a Killing horizon will be normal to Σ , since null vectors are orthogonal to themselves. This means that along Σ , the Killing field ξ^μ obeys the geodesic equation

$$\xi^\nu \nabla_\nu \xi^\mu = -\kappa \xi^\mu. \quad (2.3)$$

The term on the right appears since the integral curves of the Killing field might not be parametrized affinely. κ is what we call the surface gravity. To find an expression for κ , remember that ξ^μ is normal to the hypersurface Σ , meaning the field obeys the condition $\xi_{[\mu} \nabla_\nu \xi_{\sigma]} = 0$. Using this condition in combination with the Killing equation $\nabla_{(\mu} \xi_{\nu)} = 0$, we can derive

$$\kappa^2 = -\frac{1}{2}(\nabla_\mu \xi_\nu)(\nabla^\mu \xi^\nu), \quad (2.4)$$

where the right hand side is to be evaluated at Σ . The surface gravity κ is constant over Σ . Its value seems to be arbitrary, as one can always scale the Killing field by some real constant. However, for stationary, asymptotically flat spacetimes we can normalize the Killing vector $\xi = \partial_t$ by demanding

$$\xi_\mu \xi^\mu = -1, \quad \text{for } r \rightarrow \infty. \quad (2.5)$$

⁶For an account of the assumptions under which this holds and a general proof, see e.g. [16, 18].

Another generic black hole feature we wish to mention is the following. It is well known that a stationary black hole is characterized by only a small number of parameters. This is a surprising feature, since we generally think of stationary black holes as the end state of the gravitational collapse of matter. The specific set of parameters characterizing the hole depends on the matter fields that we include in the theory. In the remainder of this thesis the only non-gravitational long range field that is considered is an electric one. Under these conditions the *no hair theorem* holds for stationary, asymptotically flat black holes: these black hole solutions coupled to electromagnetism are completely characterized by three parameters: mass, electric charge and angular momentum (see e.g. [16, 20]).

2.2 Black hole mechanics

If one considers black holes in the classical theory of general relativity they obey certain mechanical laws which are mathematically almost identical to the laws of ordinary thermodynamics. The surprising appearance of this similarity suggests that black holes behave thermodynamically. In this section we will shortly review the analogies between three laws of black hole mechanics and thermodynamics at the classical level.⁷

2.2.1 Three laws of black hole mechanics

The first of the laws of black hole mechanics has already briefly been discussed in section 2.1 and is the statement that the surface gravity κ is constant on the future event horizon of a stationary black hole spacetime [2, 3].⁸ Anticipating on the correspondence with thermodynamics we name this law the zeroth law of black hole mechanics.

Using the geometric formula for A , the area of the black hole horizon, one can obtain what is known as the first law of black hole mechanics. If one perturbs a stationary black hole of mass M , charge Q and angular momentum J so that it becomes a black hole with $M + \delta M$, $Q + \delta Q$ and $J + \delta J$, then

$$dM = \frac{\kappa}{8\pi}dA + \Omega_H dJ + \Phi_H dQ, \quad (2.6)$$

⁷For details on all laws and their proofs, we refer to [18].

⁸The spacetime should also obey the dominant energy condition.

where Φ_H and Ω_H are the electric potential and angular velocity respectively, both evaluated at the event horizon [3].

The second law of black hole mechanics states that in a physical process the surface area A of a black hole's event horizon is a non-decreasing function of time.⁹ This law was derived by Hawking, directly from the Einstein equations [21]. For example, a (geometric) calculation shows that if two black holes of areas A_1 and A_2 merge, the final black hole will have an area $A_3 > A_1 + A_2$ [22].

2.2.2 Relation to thermodynamics

The three laws of black hole mechanics that were discussed in the previous section look remarkably similar to the laws of thermodynamics. At rest, a black hole has energy $E = M$. If we consider a thermodynamic system with that energy (and the same angular momentum and charge as the black hole) then the first law of thermodynamics is equal to the first law of black hole mechanics if one makes the identifications

$$T = \alpha\kappa \quad \text{and} \quad S = \frac{A}{8\pi\alpha}, \quad (2.7)$$

with some constant α . Such an identification also allows one to compare the zeroth and second laws with thermodynamics. The zeroth law of black hole mechanics is now similar to the zeroth law of thermodynamics, which states that the temperature is constant for a body in thermodynamic equilibrium. The second law becomes the second law of thermodynamics, stating that the entropy of a system is non-decreasing in time.

This final correspondence had already led Bekenstein to suggest that the entropy of a black hole should be some suitable multiple of the area of its event horizon [4, 5]. However striking this mathematical analogy between simple black hole mechanics and ordinary thermodynamics is, there still seemed to be one big problem. If this proposal was correct, then black holes have a temperature, meaning they must emit radiation. But in section 2.1 we defined black holes as a region from which nothing can escape. For now, we will leave this an open problem. In section 4.2 we will see how the inclusion of quantum effects allows the two different concepts to be compiled into a consistent picture.

⁹More technically: “If $T_{\mu\nu}$ satisfies the weak energy condition, and assuming that the cosmic censorship conjecture is true then the area of the future event horizon of an asymptotically flat spacetime is a non-decreasing function of time.” [17]

2.3 The Schwarzschild black hole

Let's first consider Einstein's equations in vacuum, i.e. $T_{\mu\nu} = 0$. Taking the trace of (2.2) we find $R = -8\pi T$, where $T = T^\mu{}_\mu$, the trace of the energy momentum tensor. We can use this to rewrite the Einstein equations (2.2) as

$$R_{\mu\nu} = 8\pi \left(T_{\mu\nu} - \frac{1}{2} T g_{\mu\nu} \right). \quad (2.8)$$

Therefore, in vacuum the Einstein equations reduce to

$$R_{\mu\nu} = 0. \quad (2.9)$$

The unique spherically symmetric solution to the vacuum Einstein equations (2.9) is the Schwarzschild metric. This is the content of Birkhoff's theorem [23], and is true even if the gravitating spherical body itself is time-dependent.¹⁰ In spherical coordinates, the Schwarzschild line element is given by

$$ds^2 = -f(r)dt^2 + f(r)^{-1}dr^2 + r^2d\Omega^2, \quad f(r) = 1 - \frac{2M}{r}, \quad (2.10)$$

where $d\Omega^2$ is the metric on the unit two-sphere. M is interpreted as the mass of the gravitating object. The metric (2.10) is a static solution and as $M \rightarrow 0$ we obtain Minkowski spacetime, as expected. We also notice that the metric is asymptotically flat.

The metric coefficients diverge at $r = 0$ and $r = 2M$. $f(r)$ is obviously coordinate-dependent, so a metric divergence may just be a coordinate singularity, originating from the breakdown of the employed coordinate system. The singularity at $r = 0$ turns out to be a true curvature singularity. A sign that this is the case is the fact that one of the coordinate-independent scalars that can be constructed from the Riemann tensor diverges. One can show that as $r \rightarrow 0$, $R_{\mu\nu\rho\sigma}R^{\mu\nu\rho\sigma} \rightarrow \infty$, implying a curvature singularity at $r = 0$.

The singularity at $r = 2M$, however, turns out to be a coordinate singularity. Transforming to so called Eddington-Finkelstein coordinates one can show that at $r = 2M$ the spacetime is perfectly regular. In these coordinates it also becomes clear that the hypersurface located at $r = 2M$ is in fact an event horizon, as was claimed in section 2.1. The Schwarzschild solution therefore describes a black hole (the simplest one possible). As the event horizon

¹⁰For a proof of Birkhoff's theorem, see e.g. [16]

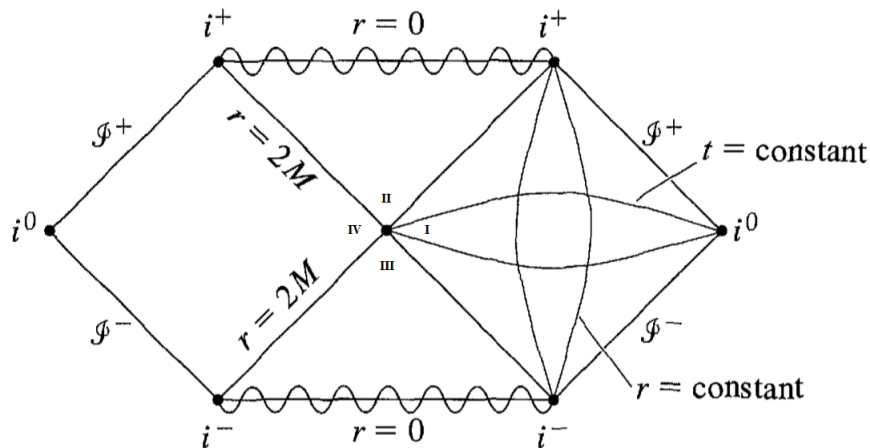


Figure 2.2: The conformal diagram of the maximally extended Schwarzschild spacetime, corresponding to an eternal black hole. (Figure taken from [15], slightly adjusted)

of the static Schwarzschild black hole is a Killing horizon, it can be assigned a surface gravity. Using equation (2.4) we obtain for the event horizon of a Schwarzschild black hole $\kappa = \frac{1}{4M}$.

By performing some clever coordinate transformations (in the same fashion as was done in appendix A for Minkowski spacetime) and analytical continuation, one discovers regions of Schwarzschild spacetime that are not covered by the original Schwarzschild coordinates (2.10). The complete spacetime is known as the maximally extended Schwarzschild solution. Its conformal diagram is depicted in 2.2.¹¹ Firstly, we notice that the structure of conformal infinity matches that of Minkowski space, confirming that the Schwarzschild geometry is asymptotically flat.

The future and past event horizons divide Schwarzschild into four regions. Region I is the asymptotically flat region that we think of as our universe, outside the black hole. Region II is the black hole. Anything that crosses the future event horizon \mathcal{H}^+ to travel from region I to II can never return. In region II every future directed trajectory ends up hitting the singularity at $r = 0$. So not only can nothing escape from the black hole, everything that is thrown in will inevitably hit the singularity. This is simply because in region II the direction of decreasing r is the timelike direction. Region III is identical to region II, but time reversed. It represents a part of the spacetime from which stuff escapes to region I, but

¹¹For all the necessary coordinate transformations and the construction of the maximally extended Schwarzschild spacetime, see e.g. [15, 17, 24].

nothing from region I can ever reach III. One might think of this as a white hole, instead of a black one. As it are the horizons that split up the spacetime, the future (past) event horizon is the boundary of region II (III). Region I and IV are not connected by any causal path. Region IV represents another asymptotically flat region, different then ours. It is a mirror image, that is the time reverse of region I.

As must be clear by now, the maximally extended Schwarzschild solution in figure 2.2 has quite some exceptional features. However, it builds on highly idealized conditions, such as perfect spherical symmetry, and the complete absence of energy-momentum. For example, if matter were to exist somewhere outside the black hole region the diagram would dramatically change. Let's consider a more realistic Schwarzschild black hole. As said before, we like to think of stationary black holes as the end point of the collapse of matter. If we consider spherical collapse, we are able to construct a new form of Schwarzschild spacetime [25]. A spherically collapsing object will be Schwarzschild in the exterior, but the interior will look nothing like figure 2.2 and highly depends on the characteristics of the collapsing body.

For pressure-free, spherical collapse, the conformal diagram looks like figure 2.3. The interior shaded region is not vacuum and hence not described by Schwarzschild. The boundary of this region is a timelike curve representing the surface of the collapsing body. The collapse eventually results in a black hole and in the existence of the corresponding horizon and singularity. But the past of such a collapse spacetime is entirely different from that of the full Schwarzschild spacetime. Regions III and IV no longer exist. Instead we have a timelike curve at $r = 0$. This curve is smooth and denotes the origin of our spherical coordinate system. The spacetime in figure 2.3 is asymptotically flat, except for the (future) region that gives rise to the event horizon.

2.4 The Reissner-Nordstöm black hole

Next, we want to consider charged black holes. To that end we work with the action for Einstein-Maxwell theory

$$S = \frac{1}{16\pi} \int d^4x \sqrt{-g} (R - F_{\mu\nu} F^{\mu\nu}). \quad (2.11)$$

Here $F_{\mu\nu}$ is the electromagnetic field strength tensor

$$F_{\mu\nu} = \partial_\mu A_\nu - \partial_\nu A_\mu \quad (2.12)$$

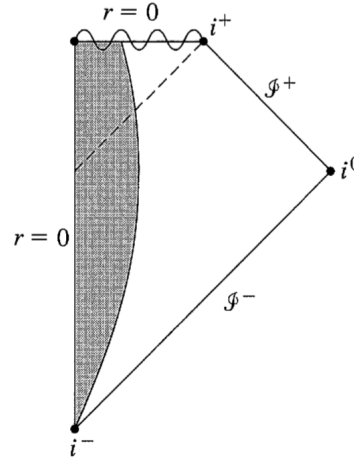


Figure 2.3: The conformal diagram of a Schwarzschild black hole, formed by gravitational collapse. In the remainder, we will also refer to this spacetime as the ‘collapse spacetime’. (Figure taken from [15])

and A_μ a 1-form potential. Maxwell’s equations are

$$\nabla_\mu F^{\mu\nu} = 0, \quad dF = 0 \quad (2.13)$$

Under these circumstances we are no longer in vacuum. The hole now has a nonzero electromagnetic field, acting as an energy-momentum source. The energy-momentum tensor for electromagnetism is

$$T_{\mu\nu} = \frac{1}{4}(F_{\mu\rho}F_\nu^\rho - \frac{1}{4}g_{\mu\nu}F_{\rho\sigma}F^{\rho\sigma}). \quad (2.14)$$

For this theory one can generalize Birkhoff’s theorem. The unique spherically symmetric solution of the Einstein-Maxwell equations is given by the Reissner-Nordström metric, which reads

$$ds^2 = -f(r)dt^2 + f(r)^{-1}dr^2 + r^2d\Omega^2, \quad f(r) = 1 - \frac{2M}{r} + \frac{Q^2}{r^2}. \quad (2.15)$$

Here, we only considered black holes that carry electric charge. The magnetic charge is theoretically possible, but set to zero. M is once again interpreted as the mass of the black hole. For the fieldstrength and potential we have

$$A_\mu dx^\mu = -\frac{Q}{r}dt \quad \Rightarrow \quad F_{rt} = \frac{Q}{r^2} \quad (2.16)$$

This is an electric field in the radial direction. The right hand side of the Maxwell equation 2.13 is zero, so all the charge is carried by the black hole. Using Gauss law one can check that the parameter Q in (2.15) and (2.16) is the hole’s electric charge (see e.g. [15, 26]).

The Reissner-Nordström solution has some properties in common with the Schwarzschild solution discussed in the previous section. The solution is static and has a timelike Killing vector $\xi = \partial_t$. Again the solution is asymptotically flat and has a curvature singularity at $r = 0$, as can be seen from computing $R_{\mu\nu\rho\sigma}R^{\mu\nu\rho\sigma}$. However, the structure of the horizon is not as simple as for the Schwarzschild black hole. Demanding $f(r_h) = 0$ we find this is solved by

$$r_{\pm} = M \pm \sqrt{M^2 - Q^2}, \quad (2.17)$$

which can have either 2, 1, or 0 solutions. At r_{\pm} we again have coordinate singularities, since the curvature and field strength are perfectly smooth here. We review all three possibilities one by one.

i) Superextremal: $M < |Q|$

In this first case, called superextremal, $f(r)$ has no real roots. $f(r)$ is always positive and therefore the metric in spherical coordinates (2.15) is completely regular up to the singularity at $r = 0$. Throughout the entire spacetime, r is spacelike and t timelike. Of course, the singularity still exists, but it is now a timelike line. So the singularity is not necessarily in anyone's future. Because of that and the absence of an event horizon, an observer should have no trouble travelling to the singularity and coming back afterwards. The Reissner-Nordström solution with $M < |Q|$ is a naked singularity. Such a solution would violate the cosmic censorship conjecture discussed in section 2.1 and is generally believed to be unphysical.

ii) Subextremal: $M > |Q|$

This situation we do consider physical and is called subextremal. The conformal diagram for a subextremal Reissner-Nordström black hole is shown in figure 2.4. The function $f(r)$ now has two real roots and therefore two coordinate singularities located at $r = r_{\pm}$, which define hypersurfaces referred to as the outer and inner horizon. These surfaces are both null and act as horizons. The singularity at $r = 0$ is again a timelike line, instead of a spacelike surface for the Schwarzschild solution. The function $f(r)$ is positive both outside r_+ and inside r_- . In between those surfaces, $f(r) < 0$. This means that for an observer falling into the Reissner-Nordström black hole, r_+ will be like the event horizon $r = 2M$ in Schwarzschild solution. At this surface r becomes timelike, so just as in Schwarzschild, one is bound to move in the direction of decreasing r . However, at r_- the coordinate r becomes spacelike again, so the observer is no longer necessarily infalling. Consequently, as was expected from

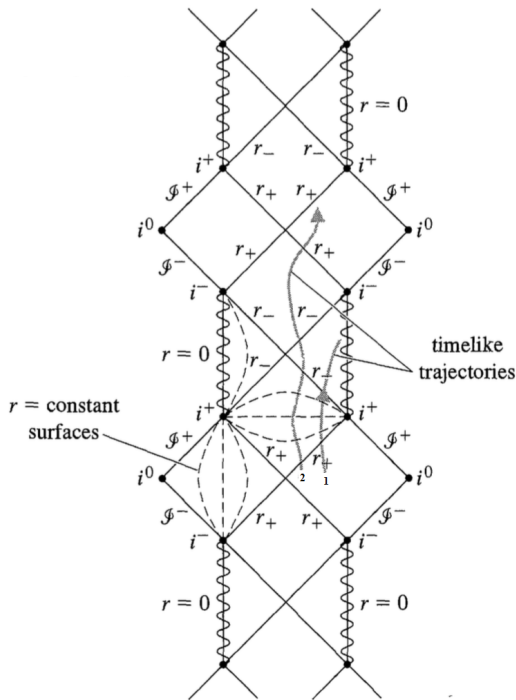


Figure 2.4: The conformal diagram for the maximally extended Reissner-Nordström spacetime. (Figure taken from [15], slightly adjusted)

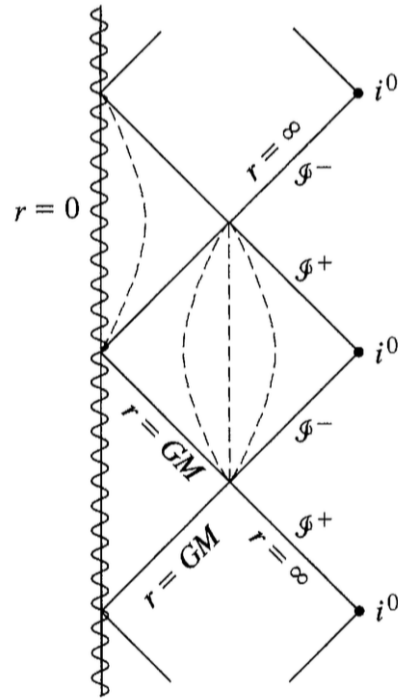


Figure 2.5: The conformal diagram for the extremal Reissner-Nordström black hole. (Figure taken from [15])

the fact that the singularity is now a timelike line, an observer is not doomed when falling into the black hole. After passing r_- he can choose die in the singularity, which corresponds to the trajectory 1 in figure 2.4. Instead he could choose trajectory 2 and proceed in the direction of increasing r to pass through the null surface $r = r_-$ again. Then r becomes timelike again, but as a consequence the observer is now compelled to move outwards. This only stops after one emerges from the event horizon r_+ . This is like being spit out of a white hole, in a different asymptotically flat region as the one where the observer started his journey. The observer could now start this adventure again by falling into the black hole (which is now a different one than the first one) an arbitrary number of times. Just like in the Schwarzschild case, it is (unfortunately) very likely that only a small non-spherically symmetric perturbation or presence of matter will dramatically alter the geometry.

iii) Extremal: $M = |Q|$

A charged black hole satisfying the relation $M = |Q|$ is referred to as an extremal Reissner-

Nordström black hole. Its conformal diagram is shown in figure 2.5. In this case the function $f(r)$ becomes a perfect square

$$f(r) = \left(1 - \frac{Q}{r}\right)^2. \quad (2.18)$$

The two horizons now coincide at $r = Q$. The hypersurface at this radius is an event horizon and at this surface r is null. However, r never becomes timelike in this spacetime. Just as in the other two cases, the singularity at $r = 0$ is a timelike line. Consequently, once again one can avoid hitting it. Once an observer has past the horizon, he can decide to either get crushed in the singularity, or turn around and continue to an arbitrary number of copies of the asymptotically flat region. Anticipating on what will follow in this thesis, it is important to note that for the extremal Reissner-Nordström black hole the surface gravity vanishes: $\kappa = 0$.

2.5 Painlevé coordinates

As we recall from the above, the metric for the Schwarzschild and Reissner-Nordström black holes has the form

$$ds^2 = -f(r)d\tilde{t}^2 + f(r)^{-1}dr^2 + rd\Omega^2, \quad (2.19)$$

where

$$f(r) = \begin{cases} 1 - \frac{2M}{r} & \text{Schwarzschild} \\ 1 - \frac{2M}{r} + \frac{Q^2}{r^2} & \text{Reissner - Nordström} \end{cases} \quad (2.20)$$

and \tilde{t} is the ‘Schwarzschild/Reissner-Nordström’ time. The time coordinate \tilde{t} corresponds to a timelike Killing vector and the metric (2.19) is static. One of the drawbacks of this metric is that it is only valid up to the horizon. It only covers a small region of spacetime and at the horizon the metric diverges. In this thesis will be concerned with horizon-crossing phenomena. Therefore, we need coordinates which, unlike the above, are well-behaved at the horizon. Another drawback is that in these spherical coordinates, the metric is static. In such a static metric one can never expect to find radiation, since this is a manifestly time-reversal asymmetric process. Therefore, in early derivations of Hawking radiation, time-reversal symmetry had to be broken by hand through the introduction of a collapsing surface, as we will see in chapter 4.

Instead of the line element (2.19), we will use *Painlevé coordinates* [27], rediscovered in [28], which do not suffer from the drawbacks mentioned above. In order to obtain this line element we introduce a new time-coordinate, given by $t = \tilde{t} - g(r)$, leading to the line element

$$ds^2 = -f(r)dt^2 - 2f(r)g'(r)dtdr + (f(r)^{-1} - f(r)g'(r)^2)dr^2 + r^2d\Omega^2, \quad (2.21)$$

where $'$ denotes a partial derivative with respect to r . The function g only depends on r and not on t . Therefore the metric remains stationary (i.e. time-translational invariant). This means the time direction is still a Killing vector. We now want our metric to be regular at the horizon. Since a radially freely-falling observer falling through the black hole horizon does not detect anything abnormal there, we can choose the proper time of such an observer as our time coordinate. Consequently, constant-time slices should be flat, meaning that the factor in front of dr^2 should be 1. This provides us with the condition

$$f(r)^{-1} - f(r)g'(r)^2 = 1 \quad \Rightarrow \quad g'(r) = \pm \frac{\sqrt{1 - f(r)}}{f(r)}. \quad (2.22)$$

So for Schwarzschild-like black holes the Painlevé coordinates are obtained by the transformation

$$dt = dt_r + \frac{\sqrt{1 - f(r)}}{f(r)} dr. \quad (2.23)$$

The black hole line element in Painlevé coordinates reads

$$ds^2 = -f(r)dt^2 \pm 2\sqrt{1 - f(r)}dtdr + dr^2 + r^2d\Omega^2. \quad (2.24)$$

This metric has a number of attractive features. First of all, there is no coordinate singularity at the horizon. Second, it makes manifest that the spacetime is stationary (non-static). The generator of t is a Killing vector, so it can be used to compute global charges such as the mass in a natural way. This Killing vector becomes spacelike across the horizon. Thirdly, by construction constant-time slices are just flat Euclidean space. And finally, an observer at spatial infinity does not make any distinction between these coordinates and the static ones. The function $f(r)$ goes to 1 at spatial infinity, so there is no distinguishing between the two time coordinates there. Coordinates similar to the ones discussed in this section and useful for ‘radiation-type’ problems, like the one we will consider, have been found in the context of de Sitter space [29, 30] and black holes in AdS [31, 32].

Chapter 3

Quantum field theory in curved spacetime

In our discussion on black hole physics in chapter 2 we restricted to considerations of classical general relativity. We now wish to move on to a quantum theory. In principle, this means one should consider black holes is a theory of quantum gravity. However, many aspects of such a theory are still poorly understood. Fortunately, it is possible to include quantum effects without appealing to quantum gravity. Einstein gravity has two sides to it. On the one hand we have the curvature of spacetime and its effect on matter. On the other hand it describes the effect of energy-momentum on the dynamics of the metric. As John Wheeler famously put it: *"Spacetime tells matter how to move; matter tells spacetime how to curve."* Quantum gravity aims at quantizing the whole picture. Instead, we will just quantize half of it. We take the (general relativity) framework of matter fields propagating in curved spacetime and treat those matter fields quantum mechanically. This leads to the theory of quantum fields in curved spacetime. Quantum field theory in curved spacetime is a semiclassical theory, in which we study quantum fields on a fixed (i.e. classical) background.¹

To obtain a more fundamental theory of quantum gravity, one must also treat the metric quantum mechanically. However, within the regime where effects of the curved spacetime might be significant, but quantum gravity effects may be ignored, it is believed that the theory of quantum fields in curved spacetime provides an accurate description. In particular, we expect the theory to be accurate in describing the quantum phenomena arising in the

¹Meaning we take the metric to be fixed, rather than obeying some dynamical equations.

context of black holes, as long as the back reaction of the quantum fields on the black hole background is small.²

The idea of building quantum field theory on the spacetime of general relativity is simple, but leads to some interesting and puzzling predictions. Throughout the treatment of quantum fields in flat space, Poincaré invariance plays an important role. In curved spacetime we do not have Poincaré symmetry at hand. At first sight, this does not seem to be that much of a problem. One can still formulate a classical field theory and formally quantize it in an arbitrary spacetime, without the need for Poincaré symmetry. The difference between quantum fields in flat and curved spacetimes arises in the characterization of the quantum states and observables, and their interpretation. We will see that as we lose Poincaré symmetry, some of the concepts that seemed crucial in Minkowskian quantum field theory, like those of 'vacuum' and 'particles', lose their privileged status.

In this chapter we set out to provide a short introduction to the quantization of fields in curved spacetime. In the context of the free massive scalar field we discuss the inherent ambiguity of notions like 'vacuum' and 'particle' that will be encountered. Throughout this chapter, we will be necessarily brief. For a more complete discussion of quantum fields in curved backgrounds we refer to [33, 34, 35, 36].

3.1 Scalar field quantization in curved spacetime

To a large extent, the formal quantization of fields in curved spacetime runs parallel to quantization in flat spacetime. In short, one just recasts the theory in covariant form. In this section we consider a real, massive scalar field. The approach extends to tensor and spinor fields in a straightforward fashion [33]. In a spacetime of arbitrary dimension n and a metric $g_{\mu\nu}$ with signature $(- + \dots +)$ the action for the scalar field ϕ is

$$S = \int d^n x \frac{1}{2} \sqrt{-g} [-g^{\mu\nu} \partial_\mu \phi \partial_\nu \phi - m^2 \phi^2 - \xi R \phi]. \quad (3.1)$$

²Anticipating on the next chapter: by a small back reaction, we mean that the change of T_H as a result of the emission of a quantum is small. In general, this means $M_{BH} \gg \omega_k$, where ω_k is the energy of the emitted quantum. Furthermore, for this semiclassical theory to be accurate, one must refrain from describing phenomena near the singularity, where curvatures are of the Planck scale and one does need quantum gravity, as the quantum nature of the metric becomes important.

Here $g = \det g_{\mu\nu}$ and m is to be understood as the mass of the field quanta. The coupling with the gravitational field is accounted for with the last term. R is the Ricci curvature scalar³ and ξ is a dimensionless constant. The partial derivatives appear since for scalar fields $\nabla_\mu \phi = \partial_\mu \phi$. The corresponding equation of motion for the scalar field is

$$[\square - m^2 - \xi R] \phi = 0, \quad \square \equiv \frac{1}{\sqrt{-g}} \partial_\mu (\sqrt{-g} g^{\mu\nu} \partial_\nu). \quad (3.2)$$

There are two commonly used values for ξ . Firstly, one can set $\xi = 0$. This is referred to as minimal coupling and leads to the Klein-Gordon equation, which is the simplest equation of motion possible. Second is the so-called conformal coupling, $\xi = \frac{(n-2)}{4(n-1)}$. If the coupling takes this value and one considers the massless limit, then the action is conformally invariant.

One can now define the conserved Klein-Gordon inner product for a pair of solutions of the generally covariant Klein-Gordon equation (3.2)

$$(\phi_1, \phi_2) = -i \int \sqrt{-h} (\phi_1 \partial_\mu \phi_2^* - \phi_2^* \partial_\mu \phi_1) d\Sigma^\mu, \quad (3.3)$$

where $d\Sigma^\mu = n^\mu d\Sigma$. Here $d\Sigma$ is the volume element in a given spacelike hypersurface and n^μ is the timelike unit vector normal to this hypersurface. h is the determinant of h_{ij} , the induced metric on the hypersurface Σ . The value of this inner product is independent of the hypersurface on which it is evaluated.

There always exists a complete set of positive norm mode solutions $\{u_i\}$ to the wave equation (3.2). Then $\{u_i^*\}$ forms a complete set of negative norm mode solutions. We can normalize these such that $\{u_i, u_i^*\}$ is a complete set of mode solutions to (3.2), orthonormal in the Klein-Gordon inner product (3.3):

$$(u_i, u_j) = \delta_{ij}, \quad (u_i^*, u_j^*) = -\delta_{ij}, \quad (u_i, u_j^*) = 0. \quad (3.4)$$

Since they form a complete set, we can expand the field operator ϕ in terms of these modes as

$$\phi(x) = \sum_i \left[a_i u_i(x) + a_i^\dagger u_i^*(x) \right]. \quad (3.5)$$

We can now quantize the field using canonical methods. We choose a foliation of the spacetime into spacelike hypersurfaces. Let Σ be a particular hypersurface that has a corresponding normal unit vector n^μ characterized by a constant value of the time coordinate t . The

³The Ricci scalar appears here as it is the only possibility for a local, scalar coupling of to gravity with the appropriate dimensions [33].

derivative of ϕ in this normal direction is then $\dot{\phi} = n^\mu \partial_\mu \phi$, and one defines the canonical momentum by

$$\pi = \frac{\delta \mathcal{L}}{\delta \dot{\phi}}. \quad (3.6)$$

We now impose the canonical commutation relation

$$[\phi(\vec{x}, t), \pi(\vec{x}', t)] = i\delta(\vec{x}, \vec{x}'). \quad (3.7)$$

From (3.7) the commutation relations for the coefficients in (3.5) are determined to be

$$[a_i, a_j^\dagger] = \delta_{ij}, \quad [a_i, a_j] = [a_i^\dagger, a_j^\dagger] = 0. \quad (3.8)$$

We interpret a_i^\dagger and a_i as creation and annihilation operators respectively. This way we can define a vacuum state $|0_a\rangle$, such that $a_i|0_a\rangle = 0, \quad \forall i$. Starting with this vacuum state we can go on to construct an entire Fock space by acting on the vacuum with creation operators.

Up to now the approach runs pretty much parallel to the well-known flat spacetime procedure. We formulated a classical theory and quantized it in an arbitrary spacetime, much like one does in Minkowski spacetime, without the need for Poincaré symmetry. At this moment, however, we run into an inherent ambiguity in the curved spacetime procedure [37].

Let's take a closer look at our mode solutions u_i . In Minkowski space we have a natural set of such modes. There, ∂_t is a timelike Killing vector associated with the Poincaré symmetry in Minkowski spacetime. We naturally take the positive frequency solutions to be $u_i \propto e^{-i\omega t}$. These modes are eigenfunctions of the Killing vector ∂_t with eigenvalues $-i\omega$ for $\omega > 0$ (which we call positive frequency). Consequently, u_i^* are negative frequency eigenfunctions.⁴ This time coordinate t in Minkowski space is not unique, since we may still perform Lorentz transformations. However, the vacuum state is invariant under the action of the Poincaré group, and so is the set of all inertial observers. Therefore, irrespective of the inertial frame for which t is the time coordinate, this approach defines the same vacuum state. Since in Minkowski spacetime all inertial observers agree on this vacuum, they will automatically agree on the particle content of any given quantum state.

In curved spacetime Poincaré symmetry is lost and consequently, there is generally no natural choice of modes. In general, there is no Killing vector at hand that can be used to

⁴Note that, although $\omega > 0$, we call these modes negative frequency, because the derivative pulls down a factor $+i\omega$.

define positive frequency modes. In fact, general relativity is a generally covariant theory, implying that any time coordinate forms a sensible choice with respect to which one could define particles. Even if the spacetime does have some restricted symmetry and there exist (asymptotic) Killing vectors, these do not play a similarly crucial role as in Minkowski space.

In short, the practical lesson is the following: when moving from a flat to a curved spacetime we lose every reason to prefer a particular set of modes over any other set. As a consequence, there is no unique notion of the vacuum state in curved spacetime and hence the concept of particle comes to be ambiguous, in the sense that it becomes an observer-dependent notion.

Let's now make this observer-dependency explicit. The above means that instead of $\{u_i, u_i^*\}$, we could equally well have chosen a second orthonormal set of mode solutions to (3.2), $\{v_i, v_i^*\}$. In terms of these modes we can again expand the field operator

$$\phi(x) = \sum_i \left[b_i v_i(x) + b_i^\dagger v_i^*(x) \right]. \quad (3.9)$$

This field expansion in turn defines a new vacuum $|0_b\rangle$ by $b_i|0_b\rangle = 0 \quad \forall i$, and correspondingly a new Fock space. As we will see, two observers who define particles with respect to different sets of modes will in general disagree on the particle content of a given state.

Both sets of modes form complete sets. This means we can expand both sets of modes in terms of the other

$$v_i = \sum_j (\alpha_{ij} u_j + \beta_{ij} u_j^*) \quad (3.10)$$

and

$$u_i = \sum_j (\alpha_{ij}^* v_j - \beta_{ij} v_j^*). \quad (3.11)$$

These relations are Bogoliubov transformations and the matrices α_{ij} and β_{ij} are known as Bogoliubov coefficients [38]. Using (3.10) and (3.11) and orthonormality of the modes (3.4) these coefficients are found to be

$$\alpha_{ij} = (v_i, u_j), \quad \beta_{ij} = -(v_i, u_j^*). \quad (3.12)$$

If we equate the two expansions (3.5) and (3.9) and use the above, we obtain

$$a_i = \sum_j (\alpha_{ji} b_j + \beta_{ji}^* b_j^\dagger), \quad b_i = \sum_j (\alpha_{ij}^* a_j - \beta_{ij} a_j^\dagger). \quad (3.13)$$

From these relations it follows directly that the two Fock spaces based on the different choices of modes u_i and v_i are different when $\beta_{ij} \neq 0$. This is because the coefficients β_{ij} describe the mixing of creation and annihilation operators as one transforms between the two bases. The Bogoliubov coefficients furthermore have the following normalization properties

$$\sum_k (\alpha_{ik}\alpha_{jk}^* - \beta_{ik}\beta_{jk}^*) = \delta_{ij}, \quad (3.14)$$

$$\sum_k (\alpha_{ik}\beta_{jk}^* - \beta_{ik}\alpha_{jk}^*) = 0. \quad (3.15)$$

From (3.13) it follows that as long as $\beta_{ij} \neq 0$, the $|0_a\rangle$ and $|0_b\rangle$ vacua will not be annihilated by b_i and a_i respectively. In fact, the expectation value of the ‘ a ’ number operator $N_i = a_i^\dagger a_i$ for the number of u_i -mode particles in the ‘ b -vacuum’ $|0_b\rangle$ is

$$\langle 0_b | N_i | 0_b \rangle = \sum_j |\beta_{ji}|^2. \quad (3.16)$$

This means that the vacuum corresponding to the v_j modes contains $\sum_j |\beta_{ji}|^2$ particles in the u_i mode. This shows explicitly what we claimed to be true before: in curved spacetime the vacuum state and particle content become observer-dependent notions. What one observer considers to be the empty vacuum state may contain particles according to a second observer.

3.2 The concept of particles and their gravitational creation

In the previous section, we have learned that the notions of particle and vacuum are ambiguous in curved spacetime. But could we not just use a particle detector to eliminate this ambiguity? Such a detector should not care about the particular modes we choose to use for our field theory. The point is, however, that that the state of motion of the particle detector itself affects whether or not particles are detected. A detector moving on a certain trajectory defines positive and negative frequency modes with respect to the proper time τ measured along that trajectory. Suppose one could find a set of modes satisfying

$$\frac{D}{d\tau} u_i = -i\omega u_i, \quad (3.17)$$

then one could calculate the amount of particles observed by the detector. In general, however, it is impossible to find such modes over all of spacetime.

Just like any general curved spacetime, Minkowski space does not have a unique vacuum. What makes Minkowski space different, is that there exists a conventional vacuum state, upon which all inertial detectors throughout the spacetime agree. Even in flat space, a situation in which two observers accelerate with respect to each other, suffers from the same ‘particle’ ambiguities as the curved spacetime case [37, 39].

The key lesson is that, in a general curved spacetime, the concept of particles has no universal significance. It is precisely this non-uniqueness of positive frequency modes that allows for particle creation by gravitational fields. Consider for example a spacetime which is asymptotically flat in the far past and future, but curved in between. In the past and future we now have natural sets of modes: the Minkowskian ones. Now let $\{u_i\}$ be positive frequency solutions in the past (in-region) and $\{v_i\}$ be positive frequency solutions in the future (out-region). We can then choose these sets to be orthonormal with respect to the generalized Klein Gordon inner product, like (3.4). These modes are defined by their asymptotic properties in two different regions of spacetime, but they are solutions of the wave equation in the entire spacetime. Therefore, they both constitute a basis all over spacetime and we may expand the field operator in both sets of modes everywhere in spacetime and express the in-modes in terms of the out-modes and vice versa, like in equations (3.10) and further.

We can now describe the particle creation by time-dependent gravitational fields. We define the in-vacuum, $|0_{in}\rangle$ by $a_i|0_{in}\rangle = 0 \forall i$. This state is like the natural Minkowski vacuum and has an intuitive physical meaning; it is the state with no particles present initially, in the asymptotic past. Now we turn on a gravitational field. Adopting the Heisenberg picture of quantum mechanics, the state chosen in the far past, $|0\rangle_{in}$, remains the state of the system for all time. But the number operator which counts particles in the out-region (distant future) is $N_i = b_i^\dagger b_i$. So the mean number of particles in the out-region is

$$\langle 0_{in} | N_i | 0_{in} \rangle = \sum_j |\beta_{ji}|^2. \quad (3.18)$$

This is non-zero whenever any of the β_{ji} Bogoliubov coefficients is non-zero. In that case an inertial observer in the distant future detects particles in the vacuum defined in the far past, implying that particles are created by the gravitational field. This gravitational creation of particles leads to the most important prediction done by the theory of quantum fields in curved spacetime: the existence of Hawking radiation.

Chapter 4

Black hole radiation and its consequences

In the previous two chapters we have discussed both black holes and quantum fields in curved spacetime. We now combine these concepts by studying quantum fields in black hole spacetimes. This leads us to the discovery of the Hawking effect [1, 25]. Hawking famously discovered that whereas classically, nothing can ever possibly escape from black holes, they do emit a thermal spectrum of particles once quantum effects are taken into consideration. This predicted thermal radiation by black holes is what we call Hawking radiation. Hawking's discovery allows for the formulation of a consistent picture of black hole thermodynamics, a problem left open in section 2.2. But in addition, we will see that it also has puzzling consequences and leads to paradoxes.

In this chapter, we first apply what we have learned in the preceding part of this thesis to derive the Hawking radiation by black holes. In doing so, we will follow Hawking's original work [1, 25]. For the sake of simplicity, free fields and the Schwarzschild black hole are considered. After completing this derivation, we discuss aspects of black hole thermodynamics and shortly review some of the puzzles posed by the semiclassical theory of black holes.

4.1 Hawking's derivation of black hole radiation

Before diving into the details of the calculations, we outline the approach. The original derivation considers the classical spacetime that describes the gravitational collapse of matter

into a Schwarzschild black hole. We then consider the propagation of a free quantum field in this spacetime. Prior to the collapse, the field is in the vacuum state. We now evaluate the field's particle content at infinity at late times. This is done by propagating the positive frequency mode at late times backwards in time. We can then determine its negative and positive frequency parts in the far past. This analysis shows that the number of particles we expect at infinity corresponds to a Planckian flux of particles. The produced particles are interpreted as black hole radiation.¹

4.1.1 Field quantization in a collapse spacetime

We will consider the creation of particles in the spacetime of a Schwarzschild black hole formed by gravitational collapse. The structure of this spacetime has been reviewed in section 2.3 and its conformal diagram is shown in figure 2.3. For simplicity, we consider a minimally coupled massless scalar field ϕ , just like in chapter 3. ϕ satisfies the wave equation (3.2) with $\xi = 0$. At past null infinity \mathcal{I}^- , the geometry is asymptotically flat and we can expand the field operator as

$$\phi = \sum_i (a_i f_i + a_i^\dagger f_i^*), \quad (4.1)$$

where $\{f_i\}$ is a complete set of positive frequency solutions² to the wave equation that is orthonormal at \mathcal{I}^- . As before, a_i and a_i^\dagger are naturally interpreted as annihilation and creation operators at \mathcal{I}^- . This defines the vacuum at \mathcal{I}^- , $|0_-\rangle$, as $a_i|0_-\rangle = 0$. Although the modes are defined by their properties on \mathcal{I}^- , they are solutions of the wavefunction in the entire spacetime. Consequently, ϕ can be expressed as (4.1) everywhere.

The other asymptotically flat region is at future null infinity \mathcal{I}^+ . In this region, we can play a similar game and expand the field operator as³

$$\phi = \sum_i (b_i p_i + b_i^\dagger p_i^* + c_i q_i + c_i^\dagger q_i^*). \quad (4.2)$$

¹It is also worth mentioning that the analysis only relies on the properties of the field in the region that is exterior to the black hole. Furthermore, no gravitational field equations are used.

²with respect to the canonical affine parameter on \mathcal{I}^-

³ \mathcal{I}^+ is not a Cauchy surface. Therefore, if we want to define a complete set of modes at late times, we should also define modes on \mathcal{H}^+ .

Here $\{p_i\}$ are solutions of the wave equations that are purely outgoing, i.e. they can escape to \mathcal{I}^+ . On the other hand, $\{q_i\}$ are solutions with no outgoing component, i.e. they cannot escape to \mathcal{I}^+ , because they remain trapped within the future event horizon \mathcal{H}^+ . These two sets of modes again form an orthonormal set, this time at \mathcal{I}^+ and \mathcal{H}^+ respectively. We require that $\{p_i\}$ contains only positive frequency solutions with respect to the canonical affine parameter on \mathcal{I}^+ . The b_i and b_i^\dagger , and c_i and c_i^\dagger now act as annihilation and creation operators at \mathcal{I}^+ and \mathcal{H}^+ respectively. We can define the vacuum at \mathcal{I}^+ , $|0_+\rangle$, as $b_i|0_+\rangle = 0$. We are interested in calculating the emission of particles to \mathcal{I}^+ . Since the $\{q_i\}$ are zero at \mathcal{I}^+ , the choice of $\{q_i\}$ does not affect our calculation.⁴

As was discussed in section 3.1, we can express $\{p_i\}$ as linear combinations of $\{f_i, f_i^*\}$

$$p_i = \sum_j (\alpha_{ij} f_j + \beta_{ij} f_j^*), \quad (4.3)$$

leading to relations between the different creation and annihilation operators

$$b_i = \sum_j (\alpha_{ij}^* a_j - \beta_{ij}^* a_j^\dagger). \quad (4.4)$$

We want to calculate the possible gravitational creation of particles, so we take as the initial state the vacuum state $|0_-\rangle$, with no particles on \mathcal{I}^- . Hence, this is the state which contains no ‘incoming’ particles. In analogy with what was discussed in section 3.2, this initial vacuum state will not be the vacuum state to an observer at \mathcal{I}^+ , since in general $\beta_{ij} \neq 0$. An observer at \mathcal{I}^+ will find a non-zero expectation value of the number operator in the initial state

$$\langle 0_- | b_i^\dagger b_i | 0_- \rangle = \sum_j |\beta_{ij}|^2. \quad (4.5)$$

So in order for us to find the amount of particle creation in this spacetime (which will be interpreted as black hole radiation), we ‘simply’ calculate the coefficients β_{ij} .

In a collapsing background we can actually solve the massless Klein-Gordon equation (3.2) at $r \rightarrow \infty$ ⁵. This is done in appendix B and the resulting mode solutions are

$$f_{\omega'lm} = \frac{F_{\omega'}(r)}{r\sqrt{2\pi\omega'}} e^{i\omega'v} Y_{lm}(\theta, \phi) \quad (4.6)$$

$$p_{\omega lm} = \frac{P_\omega(r)}{r\sqrt{2\pi\omega}} e^{i\omega u} Y_{lm}(\theta, \phi), \quad (4.7)$$

⁴See for more details on this [40].

⁵since we are interested in late time radiation

where Y_{lm} are the spherical harmonics and u and v are called the advanced and retarded time. In terms of r and t they read

$$u = t + r + 2M \log \left| \frac{r}{2M} - 1 \right| \quad (4.8)$$

$$v = t - r - 2M \log \left| \frac{r}{2M} - 1 \right|. \quad (4.9)$$

u is an affine parameter on \mathcal{I}^+ and v on \mathcal{I}^- . $F_{\omega'}(r)$ and $P_{\omega}(r)$ are integration ‘constants’ with a small r -dependence. The index i for a state used in section 4.1.1 is determined uniquely by the quantum numbers ω , l and m , so we denote $f_i \rightarrow f_{\omega lm}$. The frequencies ω' and ω are (energy) eigenvalues

$$i\partial_t f_{\omega' lm} = \omega' f_{\omega' lm}, \quad i\partial_t p_{\omega lm} = \omega p_{\omega lm}. \quad (4.10)$$

We can take the continuous limit of expressions (4.3), (4.4) and (4.5). Since we consider a spherically symmetric setup, we may drop the l and m indices and the p_{ω} solutions can be represented as

$$p_{\omega} = \int_0^{\infty} (\alpha_{\omega\omega'} f_{\omega'} + \beta_{\omega\omega'} f_{\omega'}^*) d\omega' \quad (4.11)$$

and we find

$$b_{\omega} = \int_0^{\infty} (\alpha_{\omega\omega'}^* a_{\omega'} + \beta_{\omega\omega'}^* a_{\omega'}^{\dagger}) d\omega' \quad (4.12)$$

and

$$N_{\omega} = \int_0^{\infty} |\beta_{\omega\omega'}|^2 d\omega'. \quad (4.13)$$

We wish to evaluate the Bogoliubov coefficients $\alpha_{\omega\omega'}$ and $\beta_{\omega\omega'}$. In order to do so, we substitute (4.6) into (4.11) (omitting the angular part because of spherical symmetry) and then multiply both sides of the equation by $\int_{-\infty}^{\infty} e^{-i\omega''v}$. This is essentially a Fourier transformation. Evaluating this expression, we arrive at

$$\int_{-\infty}^{\infty} dve^{-i\omega''v} p_{\omega} = \int_{-\infty}^{\infty} dve^{-i\omega''v} \int_0^{\infty} \left(\alpha_{\omega\omega'} \frac{F_{\omega'}}{r\sqrt{2\pi\omega'}} e^{i\omega'v} + \beta_{\omega\omega'} \frac{F_{\omega'}}{r\sqrt{2\pi\omega'}} e^{-i\omega'v} \right) d\omega' \quad (4.14)$$

$$= 2\pi \int_0^{\infty} \left(\frac{F_{\omega'}}{r\sqrt{2\pi\omega'}} \delta(\omega' - \omega'') \alpha_{\omega\omega'} + \frac{F_{\omega'}}{r\sqrt{2\pi\omega'}} \delta(\omega' + \omega'') \beta_{\omega\omega'} \right) d\omega'. \quad (4.15)$$

Since $(\omega' + \omega'') \neq 0$ we obtain for $\alpha_{\omega\omega'}$ (and for $\beta_{\omega\omega'}$ along the same lines)

$$\alpha_{\omega\omega'} = \frac{r\sqrt{\omega'}}{\sqrt{2\pi}F_{\omega'}} \int_{-\infty}^{\infty} dve^{-i\omega'v} p_{\omega} \quad (4.16)$$

$$\beta_{\omega\omega'} = \frac{r\sqrt{\omega'}}{\sqrt{2\pi}F_{\omega'}} \int_{-\infty}^{\infty} dve^{i\omega'v} p_{\omega}. \quad (4.17)$$

4.1.2 Calculation of the Bogoliubov coefficients

We now wish to calculate the Bogoliubov coefficients by evaluating expressions (4.16) and (4.17). To do so we take a closer look at the solutions p_ω . Consider a mode p_ω that has reached \mathcal{I}^+ and track it backwards. Doing this there are two parts that we can divide the wave function into. Firstly, a part $p_\omega^{(1)}$ is scattered by the Schwarzschild gravitational field outside the collapsing matter. This part ends up on \mathcal{I}^- with unchanged frequency ω . The second, more interesting, part $p_\omega^{(2)}$ enters the black hole and is partially scattered and partially reflected through the origin, before it ends up on \mathcal{I}^- . However, at the horizon u diverges, which means that the effective frequency of $p_\omega^{(2)}$ becomes arbitrarily large. This means we can treat these wave functions in the geometrical optics approximation. In this approximation the scattering of the Schwarzschild gravitational field can be neglected and all of $p_\omega^{(2)}$ is reflected through the black hole center.

We now want to analyze the form of $p_\omega^{(2)}$ at \mathcal{I}^- . Let's take a look at the Penrose diagram in figure 4.1, depicted without the collapsing body. x is a point on the horizon \mathcal{H}^+ outside the collapsing matter. We now define two null vectors. Let l^μ be a null vector that is tangent to \mathcal{H}^+ at x and let n^μ be a null vector that is normal to \mathcal{H}^+ at x and directed radially inwards. The vectors are normalized such that

$$l^\mu n_\mu = -1. \quad (4.18)$$

\mathcal{I}^+ intersects the event horizon \mathcal{H}^+ in the point we represent by the affine parameter u_0 . γ_H is a null geodesic travelling backwards from \mathcal{I}^+ . It goes along the horizon and is reflected at the center $r = 0$ before it reaches \mathcal{I}^- in the point represented by affine parameter v_0 . Since the affine parameter v becomes larger as one goes from \mathcal{I}^- to \mathcal{I}^0 , v_0 is the latest time that something can leave \mathcal{I}^- and escape to \mathcal{I}^+ after passing through the center. Paths with larger affine parameter v , will not be able to escape to \mathcal{I}^+ .

A vector $-\epsilon n^\mu$, with ϵ small and positive, will connect x on the horizon with a nearby null surface of constant u and therefore a constant ω for $p_\omega^{(2)}$. If we parallel transport the vectors n^μ and l^μ along γ_H , the vector $-\epsilon n^\mu$ generates a null geodesic γ , which again has constant phase for $p_\omega^{(2)}$. Since we consider small ϵ for the geodesic γ we can also use the geometric optics approximation. The null geodesic γ enters the collapsing body, reflects in $r = 0$ and reaches \mathcal{I}^- in v .

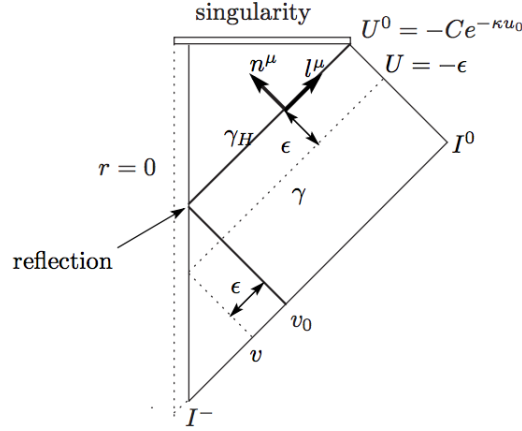


Figure 4.1: The conformal diagram for the spacetime of a Schwarzschild black hole formed by gravitational collapse, depicted without the collapsing matter. (Figure taken from [41])

If we transport l^μ and n^μ back to the point where the future and past event horizons intersect, the vector $-\epsilon n^\mu$ lies along the past event horizon, \mathcal{H}^- . Now let U be the affine parameter on \mathcal{H}^- . At the point of intersection of the future and past horizons, $U = 0$ and $\frac{dx^\mu}{dU} = n^\mu$. U is related to u on \mathcal{H}^- by

$$U = -C e^{\kappa u}. \quad (4.19)$$

Here, C is a constant and κ is the surface gravity of the hole, defined by (2.3). For a Schwarzschild black hole, $\kappa = \frac{1}{4M}$. $U = 0$ on \mathcal{H}^+ and $U = -\epsilon$ on γ . So on γ

$$u = -\frac{1}{\kappa} (\ln \epsilon - \ln C). \quad (4.20)$$

From figure (4.1) it is clear that on \mathcal{I}^- , $\epsilon = v_0 - v$. On \mathcal{I}^- , n^μ is parallel to the Killing vector ξ^μ , so

$$n^\mu = D \xi^\mu, \quad (4.21)$$

with D a constant, so

$$u = -\frac{1}{\kappa} (\ln(v_0 - v) - \ln D - \ln C). \quad (4.22)$$

Consequently, for $v > v_0$, we find that $p_\omega^{(2)}$ vanishes, since the solution cannot escape from the black hole. For $v \leq v_0$ we substitute (4.22) into the expression for $p_\omega^{(2)}$ (4.7) to obtain

$$p_\omega^{(2)} \sim \begin{cases} 0 & v > v_0 \\ \frac{P_\omega^-}{r\sqrt{2\pi\omega}} \exp\left[-i\frac{\omega}{\kappa} \ln\left(\frac{v_0-v}{CD}\right)\right] & v \leq v_0 \end{cases} \quad (4.23)$$

Here $P_\omega^- = P_\omega(2M)$. This expression (4.23) is valid only for $v - v_0$ small and positive. For large values of ω' we can use the asymptotic form of the solution. Plugging (4.23) in (4.16) and (4.17) and evaluating the expression (see appendix E in thesis), we get for large ω'

$$\alpha_{\omega\omega'}^{(2)} \approx \frac{1}{2\pi} P_\omega^- (CD)^{\frac{i\omega}{\kappa}} e^{-i\omega'v_0} \left(\sqrt{\frac{\omega'}{\omega}} \right) \Gamma \left(1 - \frac{i\omega}{\kappa} \right) (i\omega')^{-1 + \frac{i\omega}{\kappa}} \quad (4.24)$$

$$\beta_{\omega\omega'}^{(2)} \approx -i\alpha_{\omega(-\omega')}^{(2)}. \quad (4.25)$$

From (4.25) we find

$$\beta_{\omega\omega'}^{(2)} = e^{2i\omega'v_0} e^{\log(-1)(-1 + \frac{i\omega}{\kappa})} \alpha_{\omega\omega'}^{(2)}. \quad (4.26)$$

$\beta_{\omega\omega'}^{(2)}$ has a singularity at $\omega' = 0$. We analytically continue anticlockwise around this singularity and get $\log(-1) = i\pi$. Using this we find from (4.26)

$$|\beta_{\omega\omega'}^{(2)}| = e^{-\frac{\pi\omega}{\kappa}} |\alpha_{\omega\omega'}^{(2)}| \quad (4.27)$$

Suppose now that the portion of the wave that propagates through the collapsing matter, reflects in the center and reaches \mathcal{S}^- is γ_ω . This means a fraction $1 - \gamma_\omega$ is reflected by the Schwarzschild gravitational field outside the matter. The orthonormality condition is then

$$\gamma_\omega = \int_0^\infty \left(|\alpha_{\omega\omega'}^{(2)}|^2 - |\beta_{\omega\omega'}^{(2)}|^2 \right) d\omega'. \quad (4.28)$$

This means that the spectrum of particles that is produced is

$$N_\omega = \int_0^\infty |\beta_{\omega\omega'}|^2 d\omega' = \frac{\gamma_\omega}{e^{\frac{2\pi\omega}{\kappa}} - 1}. \quad (4.29)$$

This is Hawking's famous result. Comparing to ordinary thermodynamics we see the black hole behaves as a black body with temperature

$$T_H = \frac{\kappa}{2\pi}, \quad (4.30)$$

called the Hawking temperature.

There remains one issue to be resolved. The expectation value of the number of particles created at \mathcal{S}^+ in the range of frequencies ω to $\omega + d\omega$ is $d\omega \int_0^\infty |\beta_{\omega\omega'}|^2 d\omega'$. Now since $|\beta_{\omega\omega'}| \propto 1/\sqrt{\omega'}$ the integral diverges logarithmically. This results in an infinite number of particles created. This divergence corresponds to the fact that we evaluate a finite rate of emission for an infinite time. One can show that indeed, the particles created produce a steady flow at \mathcal{S}^+ . One way to go is to do an analysis that involves introducing wavepackets. This is the way in which Hawking himself proceeded. A simpler way to go is described in [33].

4.2 Hawking's result and black hole thermodynamics

Let's now look back at our review of the mathematical analogy between the laws of black hole mechanics and ordinary thermodynamics in section 2.2. The only thing that was holding this mathematical analogy from being an actual physical analogy was the absence of a black hole temperature. We now see how this issue is resolved when one moves away from the strictly classical picture. As we have learned in the previous section, semiclassical black holes do radiate with a thermal spectrum at the black body temperature given by (4.30). This allows for the concepts of black hole mechanics and thermodynamics to be consistently compiled into a one picture. Thus, we can conclude that a black hole is indeed a thermodynamic object. Equation (4.30) determines the value of the constant in (2.7) at $\alpha = 1/2\pi$, thereby confirming what Bekenstein had proposed earlier: black holes have an entropy proportional to their area. This Bekenstein-Hawking entropy is

$$S_{BH} = \frac{A}{4}. \quad (4.31)$$

The derivation in section 4.1 took place in the spacetime of a black hole formed by gravitational collapse. However, the same effect occurs for eternal black holes. The time-dependency of the metric turns out to have nothing to do with Hawking radiation. After Hawking's original derivation, numerous other derivations of the effect have been proposed, generalizing the concept in different directions. A few notable derivations can be found in [42, 43, 44, 45, 46]. The above is in no way intended to be a full overview of all known derivations or generalizations, but serves as an illustration of the fact that the Hawking effect is by now very well established.

In all cases one obtains a radiation spectrum

$$N_\omega = \frac{\gamma_\omega}{e^{\frac{2\pi(\omega-\mu)}{\kappa}} \pm 1}, \quad (4.32)$$

where the minus (plus) sign corresponds to bosons (fermions). It can be shown that the radiation is indeed truly thermal [47]. Linking with thermodynamics, μ is a chemical potential. For Reissner-Nordström black holes in 4d, $\mu = q\Phi_H$, where q is the charge of the emitted particle and Φ_H is the electrostatic potential at the horizon. So, Φ_H appears as a chemical potential causing particles with the same sign of charge as the hole to be preferentially emitted. A charged black hole will therefore preferably radiate away its charge.

4.3 Black hole puzzles, paradoxes and conjectures

The semiclassical theory of black holes and in particular the Hawking effect, is elegant, but it is full of conceptual problems. The study of semiclassical black holes clearly reveals the tension and conflicts between the theories of general relativity and quantum mechanics. Therefore, the puzzles and paradoxes we encounter may also carry important clues for how one should think about unifying the two. We will very briefly discuss two of these issues. Here, we present them in simplified form, as they serve to provide a taste of what puzzles semiclassical black holes bring along and why a better understanding of Hawking radiation may prove useful.

4.3.1 The entropy puzzle

From the above, we have learned that a black hole has an entropy $S = \frac{A}{4}$. This entropy will be huge and this poses a puzzle. We know from statistical physics that the entropy of a system is $S = \log N$, where N is the number of accessible states. If we plug in some numbers, we find that for a solar mass Schwarzschild black hole

$$N = e^{S_{BH}} \sim 10^{10^{77}}. \quad (4.33)$$

This is a huge number and it is not immediately clear where to look for the microstates that make up this number. The enormous entropy of a black hole seems to be at odds with the no hair theorem from general relativity, discussed in section 2.1. In the context of string theory we have developed some understanding of the microscopic origin of the Bekenstein-Hawking entropy [6], but many of its aspects remain poorly understood. One could think that the discrepancy described above should not matter too much and that the entropy is at the singularity in one way or another. But this does not solve the problem. As we will see, this possibility leads to an even more serious problem if one includes the Hawking effect.

4.3.2 The black hole information paradox

Let's again take a Schwarzschild black hole as an example. Its temperature is inversely proportional to the hole's mass. So, as the hole radiates, its temperature rises. If we consider an isolated black hole, this will become a runaway process and the hole will eventually

completely evaporate in a finite time. This presents a problem. Consider a black hole and let it evaporate completely. According to what we discussed in section 4.1 the radiation is purely thermal. This means it is characterized by one parameter, T_H , and is uncorrelated. So, once the black hole has completely evaporated, all that is left is this thermal Hawking radiation. The information that specified the matter forming the hole seems lost. This is known as the information paradox [7].

Being a bit more precise, the paradox can be stated as follows. Imagine some matter in a pure state and collapse it so that it forms a black hole. If we now let this hole evaporate completely, all that will eventually be left is the Hawking radiation that is in a mixed state. This means that the result of the evaporation process is that a quantum state that was initially pure evolved into a mixed state. This process is not unitary and therefore violates a quantum mechanical principle.

The information paradox has remained a challenge since Hawking's first derivation of black hole radiation. An overview of the complete discussion on this topic and its suggested resolutions is far outside the scope of this thesis. For a more precise and complete review, see e.g. [48, 49, 50]. Roughly, the paradox leaves three possibilities, in which most scenarios somehow end up.

Information loss This is the resolution Hawking himself originally concluded [7] and means the rules of quantum theory as we know them do not apply in all situations. Treating gravity as an effective theory in regions of small curvature, seems to lead logically to the loss of information. However, this non-unitary evolution violates the fundamentals of quantum mechanics, and is widely regarded as highly undesired. This should change the framework of quantum mechanics and we would then expect to see this non-unitary evolution elsewhere. Moreover, it is claimed that such evolution results in severe violations of the conservation of energy [51].

Remnants Another possible solution is that black holes do not evaporate entirely, but end up as Planck sized remnants in which the information is stored. The existence of stable or long-lived remnants, however, provides severe difficulties [52]. For remnants there is no connection between the density of states and S_{BH} . Moreover, we can start with a black hole that is arbitrarily large. This means that the number of states that are available to a remnant is arbitrarily large. Due to the unbounded number of

states that is available to the remnant, the virtual effects due to them diverge, even at zero temperature. The same goes for the amplitudes for their pair production. For a particularly nice argument against the existence of remnants, see [53].

Information conservation via Hawking radiation This seems to be the most desired resolution. However, it is not known how this Hawking radiation would be able to carry the information. This solution seems to imply that gravity as an effective field theory breaks down in regimes where one would normally expect it to be valid.

The development of the AdS/CFT correspondence has shed some light on the information paradox. According to this duality the evaporation of a black hole should be dual to a process in the dual gauge theory. Since in this gauge theory evolution is unitary, i.e. pure states cannot evolve into mixed states, so should the process of black hole decay be. So, AdS/CFT implies that the last of the three scenarios should be true. It is still unclear, however, where the original argument by Hawking was wrong or how exactly the information is carried away by the radiation. It has been argued that if we demand no information to be lost, this means the effective theory breaks down dramatically at the horizon, leading to the *firewall puzzle* [54]. Efforts to deal with this puzzle have, again, led to many new ideas, spreading into many different directions.

4.3.3 Preview: the weak gravity conjecture

We wish to close this chapter by mentioning the *weak gravity conjecture* (WGC) [11]. It is by nature different from the two puzzles described above. Instead of being a problem posed by semiclassical physics of black holes, the WGC is a conjecture on the properties of quantum gravity and its low energy realizations, which was originally based on semiclassical black hole physics.

Consider a black hole that is charged under some $U(1)$ gauge field. We would like it to be able for such a black hole to dissipate all its charge in evaporating down to the Planck scale. Suppose that this would not be possible. Then as a result, the spectrum will contain a huge number of remnants. Such remnants, as discussed in section 4.3.2, are highly undesired.

Now, in order to allow such a black hole to evaporate, at least one superextremal state must exist. Let's make this as explicit as possible. We consider, as before, a $U(1)$ gauge theory

and we label the charged states by an index i . Each state i represents a particle of mass m_i and charge q_i . We can define a charge-to-mass ratio

$$z_i = \frac{q_i}{m_i} M_p, \quad (4.34)$$

which is dimensionless. Now, consider a black hole of mass M and charge Q and let it evaporate only into particles i , with highest z_i . Using charge conservation, we know that in evaporating all its charge, the black hole emits $\frac{Q}{q_i}$ particles. After evaporation the rest mass of the final state is $\frac{m_i Q}{q_i}$. Energy conservation tells us this must be less than the initial rest mass: $\frac{m_i Q}{q_i} < M$. Defining the black hole charge-to-mass ratio analogous to (4.34) as $Z = \frac{Q}{M} M_p$, we find that for a black hole to be able to dissipate its charge we must have a state obeying $z_i > Z$. Since for an extremal black hole $Z = 1$, it is stable unless the theory contains a state with $z_i > 1$.

Thus, in order to allow all black holes to radiate away their charge as they evaporate to the Planck scale, the theory must contain a state that obeys

$$z_i > 1 \quad \Rightarrow \quad \frac{m}{q} \leq M_p. \quad (4.35)$$

Another way of stating this is by demanding that ‘gravity is the weakest force’. The WGC promotes this to a principle and suggests that (4.35) is to be understood as a consistency relation on a theory of quantum gravity and all its EFTs.

Recalling that $T_H \sim \kappa$, we notice a problem. In section 2.4 we learned that for extremal Reissner-Nordström black holes the surface gravity, and hence the temperature, vanishes. Hawking’s strictly semiclassical derivation of the radiation spectrum therefore does not allow extremal black holes to decay. However, in this regime we do not expect this strictly semiclassical approximation to be accurate, as back reaction effects become important.⁶

⁶For this approximation to hold we assume the backreaction effects are small. By this, we also mean that the change in T_H as a result of emitting a single quantum is small. This does not hold for black holes very near extremality [55].

Chapter 5

The effect of energy conservation on black hole radiation

As was discussed in the previous section, all standard derivations of black hole radiation reproduce the same result of a strictly thermal radiation spectrum characterized by the Hawking temperature T_H . These standard derivations employ strictly semi-classical methods: the background geometry is treated as fixed and one calculates the response of quantum fields to this geometry. Since one considers a fixed background, energy conservation is not enforced in these calculations. This can for example be seen from the collapse geometry we used to derive the radiation in the previous chapter. The radiation is caused by the changing metric of the collapsing body, but at late times it matches a steady flux. This implies a violation of energy conservation, strongly indicating that we cannot ignore the problem of back reaction.

The question of how to incorporate energy conservation or, more generally, gravitational back reaction in the black hole radiation problem has not yet been solved in a satisfactory way. To address questions of this type one must go beyond the approximation of a fixed background and allow the geometry to fluctuate. In general, however, this means one has to treat the geometry as a quantum variable and hence requires a theory of quantum gravity.

Luckily, if one considers only spherically symmetric field configurations, i.e. s-wave emission, energy conservation in the radiation process can be accounted for without the need for quantum gravity. In such setups, the gravitational field has no dynamical degrees of freedom

and can be integrated out.¹ In [12, 13] Kraus and Wilczek developed an approach to include self-gravitational effects in a spherically symmetric radiation process. Contrary to the regular method of quantizing a field on a fixed background, this procedure allows the geometry to fluctuate in response to the emission. Consequently, the energy of the complete system is conserved throughout the procedure.

In this chapter we propose an improved version of the method suggested in [12, 13] to calculate the black hole emission probability, with self-gravitational effects included. We treat both massless and charged radiation from the Schwarzschild and Reissner-Nordström black holes and find that the refined procedure results in a modified radiation spectrum, that deviated from a strictly thermal one.

5.1 Outline of the approach

The actual computation that will be performed in this chapter can get rather detailed and complex. For the sake of the overall picture, we start with a short outline of the approach and a discussion of the underlying logic.

The starting point is the full action describing a relativistic particle interacting with gravity. This action contains a large number of degrees of freedom, making it difficult to solve concrete problems like that of black hole radiation. To make the problem more manageable, we consider spherically symmetric configurations only. By doing so, we focus on the degrees of freedom most relevant to the emission process.

After truncating to s-wave emission, we can treat the particle as a spherical shell. There effectively remains only one degree of freedom: the position of this shell. One can isolate this true degree of freedom to obtain an effective action for a self-gravitating shell interacting with the black hole. The next step would then be to quantize this effective action in order to obtain a corrected field equation. However, full quantization appears to be too difficult. Next, we use the WKB approximation to quantize the action semi-classically. Doing this, one obtains a Hamilton-Jacobi equation for the action, which in the WKB approximation equals the phase of the wave function. Solving this differential equation we find an expression for the phase of the wave function, providing us with the corrected proper modes.

¹This is a consequence of Birkhoff's theorem.

Now that we have an expression for the proper modes, we move on to determining the state of the quantum field following the gravitational collapse of matter into a black hole. We are eventually interested in the late-time radiation. As is usually done, we demand that an observer freely falling through the horizon sees nothing singular, and that the positive frequency modes are unoccupied in the far past. Performing the regular second quantized analysis, consisting of the calculation of the Bogoliubov coefficients, we find at late times a mixture of positive and negative frequency modes. The produced particles are interpreted as black hole radiation.

5.2 Results for massless radiation

We start by discussing the radiation of massless scalar particles from the Schwarzschild black hole. We carry out the full calculation in detail and obtain an interesting modification of the radiation rate, which is no longer strictly thermal and instead relates to the change in Bekenstein-Hawking entropy as a result of the emission.

5.2.1 The effective action of a self-gravitating shell

The full action for a particle interacting with gravity reads

$$S = -m \int \sqrt{-\hat{g}_{\mu\nu} d\hat{x}^\mu d\hat{x}^\nu} + \frac{1}{16\pi} \int d^4x \sqrt{-g} R. \quad (5.1)$$

Here, a hat means the quantity is to be evaluated at the position of the particle. Starting from this action, we can work towards an effective action for a self-gravitating massless particle in the s-wave, interacting with a black hole. This is done in the Hamiltonian formulation [56, 57, 58] of spherically symmetric gravity [59, 60]. There is only one true physical degree of freedom in our problem. Due to the fact that Einstein gravity is a theory of constraints, the action (5.1) seems to contain more. To isolate the true degree of freedom one must solve these constraints. In general (and in our case for sure), this is easier done with Hamiltonian methods [12].

In the Lagrangian formalism, the constraints are expressed in terms of the variables $\hat{r}, \dot{\hat{r}}, g_{\mu\nu}, \dot{g}_{\mu\nu}$. Applying these constraints to spherically symmetric vacuum solutions results in the Schwarzschild

geometry with some mass parameter M .² In this formalism, M is constrained to be time-independent and it turns out only a subset of the shell trajectories are allowed by the constraints. But in order to quantize the theory, we need an action that is valid for arbitrary shell trajectories. In the Hamiltonian formulation, on the other hand, the constraints are expressed in terms of the variables $\hat{r}, p, g_{ij}, \pi_{ij}$. Applying the constraints we again obtain Schwarzschild geometry with mass parameter M , only this time M is allowed to be time-dependent. Hence, in the Hamiltonian formulation an arbitrary shell trajectory is compatible with the constraints. This makes the transition to a quantum theory a lot more convenient.

We will not go through the entire procedure to obtain the effective action for a shell interacting gravitationally with a black hole.³ Instead, we will limit to an outline of the method and use the result derived in [12]. The recipe used is:

1. Write the metric in ADM form and restrict to spherically symmetric geometries. This means we only consider emission in the s-wave. We thereby focus on the most relevant degrees of freedom in the emission process, since the radiation of black holes into scalar particle primarily takes place in the s-wave.
2. Rewrite the action in canonical (Hamiltonian) form.
3. Identify the constraints by varying the action.
4. Solve these constraints and plug the solutions back into the action.
5. Pick the Painlevé gauge, discussed in section 2.5, to obtain the effective action.

The effective action for a self-gravitating, massless shell interacting with a Schwarzschild black hole can be written in canonical form as [12]

$$S = \int dt (p_c \dot{\hat{r}} - M_+). \quad (5.2)$$

Here, we have chosen to fix the black hole mass M and allow the mass as seen from infinity (including the shell contribution), M_+ , to vary (in order to satisfy the constraints, see step 4). Note that we could equally well have chosen the total mass to be fixed and the black hole mass to vary. We will elaborate on this in section 5.2.6.

²This is the content of Birkhoff's theorem, discussed in chapter 2.

³This requires substantial prior knowledge of the Hamiltonian formulation of gravity, a review of which is beyond the scope of this thesis.

As the action is written in canonical form, we can identify M_+ as the Hamiltonian. p_c is the canonical momentum conjugate to \hat{r} , the position of the shell, and reads

$$p_c = \sqrt{2M\hat{r}} - \sqrt{2M_+\hat{r}} - \eta\hat{r} \log \left| \frac{\sqrt{\hat{r}} - \eta\sqrt{2M_+}}{\sqrt{\hat{r}} - \eta\sqrt{2M}} \right|, \quad (5.3)$$

where $\eta = \pm 1$ for outgoing and ingoing shells respectively. In what follows, we focus on outgoing shells, i.e. $\eta = +1$.

5.2.2 Quantizing the effective action

Now that we obtained the effective action (5.2), we wish to quantize it. We have

$$M_+ = M - p_t, \quad (5.4)$$

where p_t is the negative of the energy of the shell.⁴ Using (5.4) we can rewrite the action as

$$S = \int dt(p_c\dot{\hat{r}} + p_t). \quad (5.5)$$

We have dropped the term $\int dtM$, since this merely contributes a constant shift.

We want to proceed by quantizing the massless, gravitating shell surrounding a black hole. Full quantization, however, appears to be very difficult. The gravitational field of the shell itself is included in the effective action (5.5), meaning we lost locality. Simply substituting $p \rightarrow -i\partial_r$ and $p_t \rightarrow -i\partial_t$ will not do, since we do not know how to manipulate (5.3) before making such substitutions.

Our goal is to determine the late-time black hole radiation. Fortunately, for this problem we can circumvent the difficulties that arise in the quantization of the action. The quanta emitted from the black hole experience an ever increasing redshift as they escape to infinity. So if we trace back the radiation towards the black hole horizon, the wavelengths become arbitrarily small. For the short wavelength solutions to the wave equation, the geometrical optics, or WKB approximation provides an accurate description and enables (semi-classical) quantization.

⁴We write our equations in terms of p_t to follow the conventions in [12]. This makes a comparison between our analysis and the one performed there easier.

In the WKB approximation we can write the wavefunction of the shell as

$$\phi(t, r) = e^{iS(t, r)}. \quad (5.6)$$

In this approximation the ambiguities when inserting the substitutions $p \rightarrow -i\partial_r$ and $p_t \rightarrow -i\partial_t$ are absent. Instead, derivatives acting on ϕ just bring down powers of $i\partial S$. Therefore, we proceed quantization by substituting

$$p_c \rightarrow \frac{\partial S}{\partial r}, \quad p_t \rightarrow \frac{\partial S}{\partial t}. \quad (5.7)$$

These substitutions lead to a Hamilton-Jacobi equation for S of the form $\frac{\partial S}{\partial r} = p_c$, where p_c is a function of $\frac{\partial S}{\partial t}$. The solution to this equation is simply given by the classical action, computed along classical trajectories. We take $\hat{r}(t)$ to be a solution of the equations of motion found from (5.5), i.e. a classical trajectory. Then the quantized action reads

$$S(t, \hat{r}(t)) = S(0, \hat{r}(0)) + \int_0^t dt [p_c(\hat{r}(t))\dot{\hat{r}}(t) + p_t]. \quad (5.8)$$

One can check that indeed (5.7) holds. Now that we have a quantized action, there are two issues that remain to be discussed: the nature of the trajectories \hat{r} and the specification of the initial conditions.

The trajectories extremizing the action (5.5) turn out to be the null geodesics of the black hole metric with mass parameter M_+ . Let's show this. Since the Lagrangian has no explicit time dependence, the Hamiltonian $-p_t$ is conserved. We may use Hamilton's equations $\dot{r} = \frac{\partial H}{\partial p}$, with $H = -p_t$ and p_c given in (5.3). We obtain for the trajectory extremizing the action in (5.5)

$$\dot{r} = 1 - \sqrt{\frac{2M_+}{r}}. \quad (5.9)$$

Now, let's find the expression for a null geodesic in the Schwarzschild metric with mass parameter M_+ , to show that this equals (5.9). From the geodesic equation and metric compatibility we know that the quantity

$$g_{\mu\nu} \frac{dx^\mu}{d\lambda} \frac{dx^\nu}{d\lambda} = \epsilon \quad (5.10)$$

is constant along a path. For null paths $\epsilon = 0$ and the condition simplifies to $ds^2 = 0$. If we plug in the line element of the Schwarzschild black hole in Painlevé coordinates (2.24), with mass parameter M_+ , this leaves us with the condition

$$ds^2 = 0 \quad \Rightarrow \quad \dot{r}^2 + 2\sqrt{1 - f(r)}\dot{r} - f(r) = 0, \quad (5.11)$$

with solutions

$$\dot{r} = \pm 1 - \sqrt{1 - f(r)} = \pm 1 - \sqrt{\frac{2M_+}{r}}. \quad (5.12)$$

Under the assumption that t increases towards the future, the plus and minus sign correspond to outgoing and ingoing trajectories respectively. Therefore, the trajectories extremizing the action (5.9) are outgoing null geodesics in the Schwarzschild geometry with mass parameter M_+ .

What is left is to determine the initial condition. As we will see in the next section, the solutions that we need in order to describe the state of the field after the formation of a black hole have the initial condition

$$S(0, r) = kr \quad k > 0. \quad (5.13)$$

For the WKB approximation to remain valid, k must be large ($k \gg 1/M$). This does not present a problem in our approach. As clarified above, the k 's relevant for the calculation of black hole radiation at late times become arbitrarily large due to infinite redshift.

We can now rewrite our effective action (5.8) as

$$S(t, \hat{r}(t)) = k\hat{r}(0) + \int_{\hat{r}(0)}^r d\hat{r} p_c(\hat{r}(t)) + p_t t, \quad (5.14)$$

where we have used (5.13), and p_c is given by (5.3). In [12] the authors only keep the terms that become singular at the horizon. This is not necessary and for clarity we keep all terms, including the non-singular ones. Now from (5.7) and (5.13) we find

$$p_c(0, \hat{r}(0)) = \frac{\partial S}{\partial r}(0, \hat{r}(0)) = k. \quad (5.15)$$

So, focusing on outgoing radiation, we obtain for k

$$k = \sqrt{2M\hat{r}(0)} - \sqrt{2M_+\hat{r}(0)} - \hat{r}(0) \log \left| \frac{\sqrt{\hat{r}(0)} - \sqrt{2M_+}}{\sqrt{\hat{r}(0)} - \sqrt{2M}} \right|. \quad (5.16)$$

5.2.3 Quantum field theory and black hole radiation

We now have a quantum effective action (5.14) for the shell, which includes effects due to self-gravitation. Next, we focus on discussing the emission of such shells from the black

hole. As we know by now, black hole radiation results from the fact that we have two non-matching natural vacuum states appearing in the quantization of a field in a black hole spacetime. Second quantization has us expanding the field operator in a complete set of solutions to the wave equation

$$\phi(t, r) = \int dk \left[a_k f_k(t, r) + a_k^\dagger f_k^*(t, r) \right]. \quad (5.17)$$

In a stationary black hole spacetime, we have to consider two inequivalent sets of modes that both appear to be natural:

- modes natural from the standpoint of an observer making measurements at infinity, and
- modes natural from the standpoint of an observer freely falling through the black hole horizon.

As Schwarzschild is asymptotically flat, the natural modes for an observer at infinity are those that are positive frequency with respect to the timelike Killing vector ∂_t . We write these modes as $u_k(r)e^{-i\omega_k t}$ and the expanded field operator reads

$$\phi(t, r) = \int dk \left[a_k u_k(r) e^{-i\omega_k t} + a_k^\dagger u_k^*(r) e^{i\omega_k t} \right]. \quad (5.18)$$

The modes $u_k(r)$ are singular at the horizon. Therefore, the freely falling observer would find an infinite energy-momentum density in the vacuum state $|0_u\rangle$ defined by $a_k|0_u\rangle = 0$. This cannot be the state resulting from collapse, because we expect the freely falling observer to notice nothing unusual when crossing the horizon. To describe the state resulting from collapse, we use the modes that are positive frequency with respect to this freely falling observer, $v_k(t, r)$, and that are well behaved through the horizon. Expanding the field operator in terms of these modes, we write

$$\phi(t, r) = \int dk \left[b_k v_k(t, r) + b_k^\dagger v_k^*(t, r) \right]. \quad (5.19)$$

This expansion defines a new natural vacuum state $|0_v\rangle$ defined by $b_k|0_v\rangle = 0$.

Since both sets of modes form complete sets, we can expand one set in terms of the other. This means⁵

$$v_k(t, r) = \int dk' \left[\alpha_{kk'} u_{k'}(r) e^{-i\omega_{k'} t} + \beta_{kk'}^* u_{k'}^*(r) e^{i\omega_{k'} t} \right] \quad (5.20)$$

⁵following the conventions of [12].

so that the a_k and b_k operators are related by Bogoliubov transformations

$$a_k = \int dk' [\alpha_{kk'} b_{k'} + \beta_{kk'} b_{k'}^\dagger]. \quad (5.21)$$

From (5.20) and (5.21) we obtain expressions for these Bogoliubov coefficients

$$\alpha_{kk'} = \frac{1}{2\pi u_k(r)} \int_{-\infty}^{\infty} dt e^{i\omega_k t} v_{k'}(t, r) \quad (5.22)$$

and

$$\beta_{kk'} = \frac{1}{2\pi u_k(r)} \int_{-\infty}^{\infty} dt e^{i\omega_k t} v_{k'}^*(t, r). \quad (5.23)$$

The average number of particles measured by the observer at infinity in the v -vacuum, $|0_v\rangle$, is

$$N_k = \langle 0_v | a_k^\dagger a_k | 0_v \rangle = \int dk' |\beta_{kk'}|^2. \quad (5.24)$$

If we were to consider the radiation from a black hole for an infinite amount of time, N_k would obviously become infinite. Instead, we wish to obtain the rate of emission. In order to do so we use the density of states $\frac{d\omega}{2\pi}$. If $|\alpha_{kk'}/\beta_{kk'}|$ is independent of k' (as we will see is the case), we can use

$$\int dk' (|\alpha_{kk'}|^2 - |\beta_{kk'}|^2) = 1 \quad (5.25)$$

to obtain the flux of outgoing particles with frequencies between ω_k and $\omega_k + d\omega_k$ at infinity

$$F_\infty(\omega_k) = \frac{d\omega_k}{2\pi} \frac{\gamma(\omega_k)}{\left| \frac{\alpha_{kk'}}{\beta_{kk'}} \right|^2 - 1}. \quad (5.26)$$

We have included a grey body factor $\gamma(\omega_k)$. As particles travel outwards a fraction $1 - \gamma(\omega_k)$ will be reflected back into the black hole due to spacetime curvature. (5.26) identifies the ratio of the coefficients as effective Boltzmann factor and the probability for emission as

$$\Gamma \sim \left| \frac{\beta_{kk'}}{\alpha_{kk'}} \right|^2. \quad (5.27)$$

5.2.4 The corrected radiation probability

From (5.27) we know that it is the norm of the ratio of the Bogoliubov coefficients $\left| \frac{\beta_{kk'}}{\alpha_{kk'}} \right|$ that determines the rate of emission. In order to calculate this ratio, we need an expression for $v_k(t, r)$, the modes that are positive frequency with respect to the freely falling observer and which extend smoothly through the horizon. In section 5.2.2, we used the WKB approximation to find an expression for the solutions to the wave equation. We now use these solutions as the (corrected) proper modes.

The integrals (5.22) and (5.23) determining the Bogoliubov coefficients are to be evaluated at constant r . We are evaluating $v_k(t, r)$ in the WKB approximation. This approximation is most accurate as close to the horizon as possible. But we also need to watch the other modes, $u_k(r)$. These break down for $r < 2(M + \omega_k)$. We therefore evaluate the integrals just outside the black hole horizon at $r = 2(M + \omega_k)$, leaving us with the modes

$$v_{k'}(t, 2(M + \omega_k)) = e^{iS(t, 2(M + \omega_k))}. \quad (5.28)$$

In fact, the exact position of r turns out not to matter that much, as long as it is outside $r_h(M + \omega_k) = 2(M + \omega_k)$. Furthermore, the exact form of the $u_k(r)$ modes is irrelevant for our purposes, since the factors in (5.22) and (5.23) containing these modes cancel when we take the ratio.

Now what about the initial condition to be imposed on the $v_k(t, r)$ modes? We want these modes to be regular at the horizon. The metric near the horizon is a smooth function of t and r . Therefore, we can define a set of modes regular at the horizon by setting their behavior on the spacelike surface $t = 0$ to be

$$v_k(0, r) \approx e^{ikr} \quad \text{as} \quad r \rightarrow 2M \quad (5.29)$$

Since we are evaluating the modes $v_k(t, r)$ in the WKB approximation, this sets an initial condition for the action

$$S(0, r) = kr, \quad k > 0. \quad (5.30)$$

We recognize this as the initial condition we imposed in (5.13). The above is the underlying logic.

Now that we have an expression for the modes, we can rewrite the integrals (5.22) and (5.23) for the Bogoliubov coefficients as

$$\begin{aligned}\alpha_{kk'} &= \frac{1}{2\pi u_k(r)} \int_{-\infty}^{\infty} dt e^{i\omega_k t + iS(t, 2(M+\omega_k))} \\ \beta_{kk'} &= \frac{1}{2\pi u_k(r)} \int_{-\infty}^{\infty} dt e^{i\omega_k t - iS(t, 2(M+\omega_k))}.\end{aligned}\quad (5.31)$$

Since the prefactor will drop out in the ratio, we will only be concerned with evaluating the integral. We evaluate these integrals in the saddle point approximation. This approximation gives us

$$\alpha_{kk'} = \frac{1}{2\pi u_k(r)} e^{i(\omega_k t_0 + S(t_0, r))} \int_{-\infty}^{\infty} dt e^{\frac{i}{2} S''(t_0, r)(t-t_0)^2} \quad (5.32)$$

$$\beta_{kk'} = \frac{1}{2\pi u_k(r)} e^{i(\omega_k t_0 - S(t_0, r))} \int_{-\infty}^{\infty} dt e^{-\frac{i}{2} S''(t_0, r)(t-t_0)^2}, \quad (5.33)$$

where $r = 2(M + \omega_k)$. The integral with the second derivative at the saddle point is just some Gaussian integral that will give us a prefactor of no interest. From now on we ignore it, meaning that in this approximation we take the coefficients to be given by their saddle point values. The saddle point is found by setting the derivative of the integrand in (5.31) with respect to t equal to zero. Therefore, the saddle point equation is

$$\omega_k \pm \frac{\partial S}{\partial t}(t, r) = 0, \quad (5.34)$$

where the plus and minus sign correspond to $\alpha_{kk'}$ and $\beta_{kk'}$ respectively. From section 5.2.2, we know

$$\frac{\partial S}{\partial t} = p_t = M - M_+, \quad (5.35)$$

leading to the rewritten saddle point equation

$$M_+ = M \pm \omega_k. \quad (5.36)$$

This equation tells us that for $\alpha_{kk'}$ the saddle point trajectory has energy ω_k and for $\beta_{kk'}$ the saddle point trajectory has negative energy $-\omega_k$.

Remember that the emission rate is given by the norm of the ratio of the Bogoliubov coefficients. This means only real parts of the exponent are relevant and (leaving for now the prefactors) we want to compute

$$|\alpha_{kk'}| = e^{-\text{Im}(\omega_k t_0 + S(t_0, r))}, \quad |\beta_{kk'}| = e^{-\text{Im}(\omega_k t_0 - S(t_0, r))}. \quad (5.37)$$

Now, let's take a closer look at the exponent

$$\begin{aligned} -\text{Im}(\omega_k t_0 \pm S(t_0, r)) &= -\text{Im} \left[\omega_k t_0 \pm k\hat{r}(0) \pm \int_{\hat{r}(0)}^r d\hat{r} p_c(\hat{r}(t_0)) - \omega_k t_0 \right] \\ &= \mp \text{Im} \int_{\hat{r}(0)}^r d\hat{r} p_c(\hat{r}(t_0)), \end{aligned} \quad (5.38)$$

where the minus (plus) sign corresponds to $\alpha_{kk'}$ ($\beta_{kk'}$). In the first line we used (5.14) and (5.36) and in the second line we used that $\hat{r}(0) \in \mathbb{R}$. From (5.38) it follows that we are left with calculating

$$|\alpha_{kk'}| = e^{-\text{Im} \int_{r(0)}^r p(r) dr} \quad \text{and} \quad |\beta_{kk'}| = e^{\text{Im} \int_{r(0)}^r p(r) dr}. \quad (5.39)$$

Note that for the two coefficients, $\hat{r}(0)$ has different expressions and M_+ different values.

We wish to solve close to the horizon. For a black hole the event horizon coincides with the surface of infinite redshift. We can therefore plug the saddle point expression for M_+ corresponding to each of the trajectories in equation (5.16) and solve for $k \rightarrow \infty$, which yields

$$\alpha_{kk'} : \quad \hat{r}(0) = 2(M + \omega_k) + \mathcal{O}(e^{k/M}) \quad (5.40)$$

$$\beta_{kk'} : \quad \hat{r}(0) = 2(M - \omega_k) - \mathcal{O}(e^{k/M}). \quad (5.41)$$

We now have all the ingredients needed to calculate the rate of massless radiation from a Schwarzschild black hole. Here, we do this by evaluating the integrals in (5.39) explicitly. First of all, note that for $\alpha_{kk'}$, $\hat{r}(0) = r$ and the action vanishes. Therefore, $|\alpha_{kk'}| = 1$. In practice, the exact position of r does not matter too much, as long as it is outside of the horizon. The physical reason why the imaginary part of the action vanishes, is that the region considered for r lies completely outside the horizon (as a result of which, the branch points of the logarithm lie outside the integration interval).

For $\beta_{kk'}$, $\hat{r}(0)$ is inside the horizon. Looking at the expression for p in (5.3) we observe that only the logarithmic term may yield an imaginary contribution. The emission rate is now given by

$$\Gamma \sim \left| \frac{\beta_{kk'}}{\alpha_{kk'}} \right|^2 = e^{2\text{Im} \int_{r(0)}^r p(r) dr}. \quad (5.42)$$

Performing the integral in the exponent, we find

$$\text{Im} \int_{r(0)}^r p(\hat{r}) d\hat{r} = -\text{Im} \int_{r(0)}^r \hat{r} \log \left| \frac{\sqrt{\hat{r}} - \sqrt{2M_+}}{\sqrt{\hat{r}} - \sqrt{2M}} \right| d\hat{r} = 2\pi(M - \omega_k)^2 - 2M^2. \quad (5.43)$$

Therefore, we finally obtain the corrected probability for a Schwarzschild black hole of mass M to emit a quantum of energy ω

$$\Gamma_\omega \sim \left| \frac{\beta_{kk'}}{\alpha_{kk'}} \right|^2 = e^{4\pi(M - \omega_k)^2 - 4\pi M^2} = e^{-8\pi\omega_k(M - \frac{\omega_k}{2})} = e^{\Delta S_{BH}}. \quad (5.44)$$

Substituting this expression in (5.26) gives us for the flux of radiation at infinity

$$F_\infty(\omega_k) = \frac{d\omega_k}{2\pi} \frac{\gamma(\omega_k)}{e^{8\pi\omega_k(M - \frac{\omega_k}{2})} - 1}. \quad (5.45)$$

For details of the final step in equation (5.43), we refer to appendix C.

It is important to mention that the result in (5.44) differs from the result obtained in [12]. In [12] the authors seem to disregard the final term in the action (5.14). Moreover, they treat the action as if it were purely real, which it is not. As they do not treat the action properly, their analysis runs into trouble as they calculate the Bogoliubov coefficients. This is also the reason why in their analysis, one does not recognize the appearance of what effectively is a tunneling calculation. The fact that one does so in our analysis is discussed in the next chapter. As a result of the above, the authors of [12] miss the fact that the corrected emission probability is related to the change in the black hole's entropy, a feature that seems to be universal.

5.2.5 Comments and interpretations

The result obtained in (5.44) demonstrates that with the inclusion of self-gravitational effects, the spectrum deviates from a strictly thermal one. To linear order in ω the rate is a Boltzmann factor $e^{-\beta\omega}$ with $\beta = 8\pi M = T_H^{-1}$. This is the inverse of the familiar Hawking temperature for a Schwarzschild black hole. Hence, to linear order we recover the familiar thermal spectrum. The quadratic correction arises from the physics of energy conservation and becomes significant for larger ω .

Furthermore, we see from (5.44) that the radiation rate can be written as the exponent of the change in the Bekenstein-Hawking entropy of the hole: $\Gamma \sim e^{\Delta S_{BH}}$. This appears consistent

with unitarity [14]. It agrees with what one would expect from a quantum mechanical microscopic theory of black holes in which there is no loss of information. From quantum mechanics we know that the rate for a process is expressed as the square of the amplitude of the process, multiplied by a phase space factor

$$\Gamma = |\text{amplitude}|^2 \times (\text{phase space factor}). \quad (5.46)$$

The phase space factor is obtained by summing over all final states and averaging over initial states. For a black hole the number of such states is just given by the exponent of the final and initial Bekenstein-Hawking entropy. Hence

$$\Gamma \sim \frac{e^{S_{final}}}{e^{S_{initial}}} = e^{\Delta S_{BH}}. \quad (5.47)$$

Our result, therefore, is in agreement with what we would expect from unitary quantum mechanics.

Another hint that the obtained result is correct can be found when one considers the limit in which the entire mass of the hole is carried away by the emission of one particle, i.e. $\omega = M$. We see from (5.44) that

$$\Gamma \sim e^{-4\pi M^2} = e^{-S_{BH}}, \quad \text{as } \omega \rightarrow M. \quad (5.48)$$

This agrees with what one would expect on physical grounds. There are $e^{S_{BH}}$ initial states in total and there can only be one outgoing state with $\omega = M$. It follows from statistical mechanics that the probability of finding this state is $\sim e^{-S_{BH}}$, just like we found in (5.48).

While the corrected emission probability seems to be in agreement with what one would expect from unitary quantum mechanics, this does not necessarily say anything about the microscopic degrees of freedom. It would be interesting to check whether the non-thermal corrections lead to correlations between the probabilities of emission of quanta with different energies. If so, this would allow for information to be encoded in the emitted radiation, which would be of particular interest in the context of the puzzles discussed in 4.3. Here, we will very briefly discuss some issues attached to this. We must warn that the remainder of this section is somewhat speculative.

In [61], this possibility was already briefly discussed. Although in this chapter we went beyond the free field approximation, it is important to keep in mind that we only considered single particle emission. It is, however, not unlikely that one could in principle calculate

the correlations (if present) between two particles emitted by the hole by extending the methods we developed. This extension would consist of including two shells, instead of just a single one. But how would one go about doing that? We can write down the action for two mutually gravitating shells in a similar way as for a single shell

$$S = \int dt [p_1 \dot{r}_1 + p_2 \dot{r}_2 - H(r_1, r_2, p_1, p_2)]. \quad (5.49)$$

We can then take the initial conditions as

$$S(0, r_1, r_2) = k_1 r_1 + k_2 r_2 \quad (5.50)$$

and obtain the quantized action $S_{k_1 k_2}(t, r_1, r_2)$ by integrating the Hamilton-Jacobi equation just like in the single particle case. If there are any correlations, the action $S_{k_1 k_2}(t, r_1, r_2)$ probably contains all information about them. But there is another problem. Treating single particle emission, we knew how to proceed to a field description. This is prescribed by (5.19) and we were then able to use the second quantized machinery to calculate emission probabilities. In the case where we consider the emission of two particles, however, it is not clear how to proceed to a field theory description. Therefore, we do not know how to properly interpret the theory and calculate emission probabilities.

Perhaps we can simplify the discussion slightly if we take the time separation between the emission of the two particles to be large. In this case the second particle will have an emission probability given by (5.44), but with a black hole mass $M - \omega_1$, where ω_1 is the energy of the particle that was emitted first. Intuitively, one would say the probabilities are correlated. Obviously, the probability of emission of the second particle depends on the energy of the particle that was emitted previously. This is simply a manifestation of the fact that we took into account a back reaction effect. It might be interesting to further investigate the possible presence of non trivial correlations in the radiation.

Another approach

Consider two quanta of energies ω_1 and ω_2 emitted one after another and compare this process to the situation in which one quantum of energy $\omega_1 + \omega_2$ is emitted. In [62] it is claimed that the probabilities are correlated as long as

$$\log(\Gamma_{\omega_1} \Gamma_{\omega_2}) \neq \log(\Gamma_{\omega_1 + \omega_2}), \quad (5.51)$$

or equivalently

$$\chi(\omega_1, \omega_2) = \log \left| \frac{\Gamma_{\omega_1 + \omega_2}}{\Gamma_{\omega_1} \Gamma_{\omega_2}} \right| \neq 0 \quad (5.52)$$

As an example, we consider massless radiation from the Schwarzschild black hole. Let us denote the probability of emission of a quantum ω from a black hole of mass M (before emission) as $\Gamma(M, \omega)$. In [62], Γ_{ω_2} in (5.52) is then interpreted to be $\Gamma(M - \omega_1, \omega_2)$. In this case we use (5.44) to obtain

$$\begin{aligned} \log(\Gamma_{\omega_1} \Gamma_{\omega_2}) &= -8\pi \left[\omega_1 \left(M - \frac{\omega_1}{2} \right) + \omega_2 \left(M - \omega_1 - \frac{\omega_2}{2} \right) \right] \\ &= -8\pi \left[(\omega_1 + \omega_2) \left(M - \frac{\omega_1 + \omega_2}{2} \right) \right] \\ &= \log(\Gamma_{\omega_1 + \omega_2}). \end{aligned} \quad (5.53)$$

Therefore, [62] concludes that there are no correlation at late times, just like for a thermal emission spectrum. Thus, it is concluded that self-gravitational effects alone do not provide a straightforward way in which information can emerge from the horizon.

However, in [63] it is argued that with this definition where $\Gamma_{\omega_2} = \Gamma(M - \omega_1, \omega_2)$, (5.52) does not properly compare the single emission of a quantum $\omega = \omega_1 + \omega_2$ with the separate emission of two quanta ω_1 and ω_2 . Their claim is that with such a definition, one "*absorbs the correlations themselves into the test for their existence*". In other words, for any two events, one would find $\chi = 0$. Instead, they claim that the proper definition is instead $\Gamma_{\omega_2} = \Gamma(M, \omega_2)$. A simple calculation shows that with this definition, one finds

$$\chi(\omega_1, \omega_2) = -8\pi\omega_1\omega_2, \quad (5.54)$$

indicating the presence of correlations in the radiation. This, of course, is only if one accepts that the quantity $\chi(\omega_1, \omega_2)$ truly does signal correlations.

To us, the validity of this entire approach is unclear. There are two questions that may be asked and to which the answer is unclear to us. Firstly, is χ , in either definition, the right quantity to signal correlators? And if so, is it applied in the correct way? As for the second question, remember that we found $\Gamma_{\omega} \sim e^{\Delta S}$. This means $\Gamma_{\omega} = A(\omega)e^{\Delta S}$, where $A(\omega)$ should in principle be a function of the particle's energy. In the above, it is somehow assumed that the terms in $\chi(\omega_1, \omega_2)$ involving this energy-dependent prefactor cancel. How this happens is also not clear to us.

5.2.6 A note on the fixing of ‘mass parameters’

In [12, 13] the authors choose to fix the mass of the black hole M and allow the mass as seen from infinity M_+ to vary. This is also the approach we followed so far in this chapter. The total energy contained in a sphere of radius r is then

$$E(r) = \begin{cases} M & r < \hat{r} \\ M_+ \equiv M - p_t & r > \hat{r} \end{cases} \quad (5.55)$$

As was claimed above, one could just as well choose this to be the other way around. This means we allow the black hole mass to vary, while the mass as seen from infinity is fixed. We would then have

$$E(r) = \begin{cases} M_- \equiv M + p_t & r < \hat{r} \\ M & r > \hat{r} \end{cases} \quad (5.56)$$

If we would use the conventions of (5.56) in the field theory analysis, we would expect to obtain the same final answer as obtained in section 5.2.4 with the use of (5.55). This is worth paying attention to and linking the two possibilities might prove useful.

The effective action (5.2) has the form

$$S = \int p_c \dot{\hat{r}} dt + [\text{boundary term}] \quad (5.57)$$

Both terms in this action should be treated differently when switching between the two different choices for fixing the mass parameters. In deriving p_c like in [12], the suitable transformations to switch from situation (5.55) to (5.56) are simply

$$M \rightarrow M_- \quad \text{and} \quad M_+ \rightarrow M. \quad (5.58)$$

This gives us

$$p_c = \sqrt{2M_- \hat{r}} - \sqrt{2M \hat{r}} - \hat{r} \log \left| \frac{\sqrt{\hat{r}} - \sqrt{2M}}{\sqrt{\hat{r}} - \sqrt{2M_-}} \right|. \quad (5.59)$$

The second term in (5.57) requires some more thinking. This term is a boundary term. Boundary terms are added in the Hamiltonian formalism in order to have a well-defined variational principle. In the Schwarzschild spacetime we are considering, spacelike slices have two boundaries. One boundary is at spatial infinity, i^0 , and the other at the horizon.

What boundary term appears in (5.57) depends on the quantities one keeps fixed at each of the boundaries. Naturally, one would say that as the boundary term is added to obtain a well-defined variational principle, it must contain a variable. This points in the direction of a similar term as before, but with M_- instead of M_+ . In [64] this boundary issue is covered and it indeed seems that in case one uses conventions (5.56) the correct boundary term is $\int M_- dt$.

The above means that we start with the action

$$S = \int dt (p_c \dot{\hat{r}} + M_-), \quad (5.60)$$

where p_c is given by (5.59). Rewriting this action using $M_- = M + p_t$, we obtain

$$S = \int dt (p_c \dot{\hat{r}} + p_t). \quad (5.61)$$

This may also be regarded as a clue that we have picked the right boundary term, since whether we fix the ADM mass or the black hole mass, $-p_t$ should be the Hamiltonian of the shell. If we now use Hamilton's equations $\dot{r} = \frac{\partial H}{\partial p}$, with $H = -p_t$, we find for the trajectories that extremize the action (5.60)

$$\dot{r} = 1 - \sqrt{\frac{2M_-}{r}}. \quad (5.62)$$

This is a null geodesic in the Schwarzschild geometry with mass parameter M_- .

We proceed by WKB quantizing the action, just like in section 5.2.2. This time, we have

$$k = \sqrt{2M_- \hat{r}(0)} - \sqrt{2M \hat{r}(0)} - \hat{r}(0) \log \left| \frac{\sqrt{\hat{r}(0)} - \sqrt{2M}}{\sqrt{\hat{r}(0)} - \sqrt{2M_-}} \right|. \quad (5.63)$$

The expressions for the Bogoliubov coefficients do not change. As in section 5.2.4, we evaluate them by their value at the saddle point

$$\alpha_{kk'} = \frac{1}{2\pi u_k(r)} e^{i(\omega_k t_0 + S(t_0, r))} \quad (5.64)$$

$$\beta_{kk'} = \frac{1}{2\pi u_k(r)} e^{i(\omega_k t_0 - S(t_0, r))} \quad (5.65)$$

The u -modes now break down at $r = 2(M - \omega)$. This will be the upper bound of our integral. Let's have a look at the saddle points. We again find

$$\omega \pm \frac{\partial S}{\partial t} = 0 \quad (5.66)$$

where the plus and minus sign correspond to $\alpha_{kk'}$ and $\beta_{kk'}$ respectively. From the quantization scheme we know

$$\frac{\partial S}{\partial t} = p_t = M_- - M, \quad (5.67)$$

leading to the rewritten saddle point equation

$$M_- = M \mp \omega_k. \quad (5.68)$$

This equation tells us that again, for $\alpha_{kk'}$ the saddle point trajectory has energy ω_k and for $\beta_{kk'}$ the saddle point trajectory has positive energy $-\omega_k$.

To find $\hat{r}(0)$ we take our expression for k (5.63) and solve for $k \rightarrow \infty$, plugging in the proper saddle point energies. This gives us

$$\alpha_{kk'} : \quad \hat{r}(0) = 2M + \epsilon_\alpha \quad (5.69)$$

$$\beta_{kk'} : \quad \hat{r}(0) = 2M - \epsilon_\beta, \quad (5.70)$$

where $\epsilon_\alpha, \epsilon_\beta > 0$.

Now, let's get back to the integrals we wish to evaluate. We want to compute

$$|\alpha_{kk'}| = e^{-\text{Im}(\omega_k t_0 + S(t_0, r))}, \quad |\beta_{kk'}| = e^{-\text{Im}(\omega_k t_0 - S(t_0, r))}. \quad (5.71)$$

Rewriting the exponent, we find that it simplifies again

$$\begin{aligned} -\text{Im}(\omega_k t_0 \pm S(t_0, r)) &= -\text{Im} \left[\omega_k t_0 \pm k \hat{r}(0) \pm \int_{\hat{r}(0)}^r d\hat{r} p_c(\hat{r}(t_0)) - \omega_k t_0 \right] \\ &= \mp \text{Im} \int_{\hat{r}(0)}^r d\hat{r} p_c(\hat{r}(t_0)), \end{aligned} \quad (5.72)$$

where the minus (plus) sign corresponds to $\alpha_{kk'}$ ($\beta_{kk'}$). We are therefore going to evaluate

$$|\alpha_{kk'}| = e^{-\text{Im} \int_{\hat{r}(0)}^r p(r) dr} \quad \text{and} \quad |\beta_{kk'}| = e^{\text{Im} \int_{\hat{r}(0)}^r p(r) dr}. \quad (5.73)$$

The parts of the integrals containing potentially imaginary terms are of the form

$$\mp \text{Im} \int_{\hat{r}(0)}^r d\hat{r} p_c(\hat{r}) = \pm \text{Im} \int_{\hat{r}(0)}^r d\hat{r} \hat{r} \log \left[\frac{\sqrt{\hat{r}} - \sqrt{2M}}{\sqrt{\hat{r}} - \sqrt{2M_-}} \right]$$

For β , one has $M_- = M + \omega$, $\hat{r}(0) = 2M - \epsilon$ and $r = 2(M - \omega)$. The branch point of the integrand do not lie in the interval of integration. Hence, the integral is purely real, leaving $|\beta_{kk'}| = 1$.

On to α , for which we have $M_- = M - \omega$, $\hat{r}(0) = 2M - \epsilon$ and $r = 2(M - \omega)$. We find

$$\text{Im} \int_{\hat{r}(0)}^r d\hat{r} \hat{r} \log \left[\frac{\sqrt{\hat{r}} - \sqrt{2M}}{\sqrt{\hat{r}} - \sqrt{2M_-}} \right] = 2\pi M^2 - 2\pi(M - \omega)^2, \quad (5.74)$$

and therefore

$$\Gamma_\omega \sim e^{\Delta S_{BH}}. \quad (5.75)$$

Thus, starting from the picture in which one fixes the mass as seen from infinity and allows the black hole mass to vary, one finds the same result as in section 5.2.4, just as we expected. In fact, as will become clear in chapter 6, this picture seems like the more natural one to adopt.

5.3 Results for massive, charged radiation

In the section 5.2 we analyzed the modification of the black hole radiation spectrum due to self-gravitational interaction, the simplest (and probably most important) back-reaction effect. However, we only considered massless radiation from the Schwarzschild black hole. In this section we extend the analysis carried out in section 5.2 to charged holes and charged radiation. For this process, the inclusion of back reaction effects may be of particular value, as this enables us to study the radiation behavior of extremal black holes. In general, the procedure runs pretty much parallel to the massless case. Therefore, we will not get into as many details as was done in the derivation for massless radiation, but rather highlight the differences.

5.3.1 Effective action and quantization

The system under consideration is now slightly different due to the incorporation of Maxwell theory. Truncating to s-waves only, the full action for a matter shell with mass m and charge

q interacting with gravitational and electromagnetic field is

$$S = \int (-m\sqrt{-\hat{g}_{\mu\nu}d\hat{x}^\mu d\hat{x}^\nu} + q\hat{A}_\mu d\hat{x}^\mu) + \frac{1}{16\pi} \int d^4x \sqrt{-g}(\mathcal{R} - F_{\mu\nu}F^{\mu\nu}). \quad (5.76)$$

Using similar techniques as in section 5.2.1, we can derive an effective action for the physical degree of freedom. We keep the black hole mass M and charge Q fixed and allow the mass M_+ and charge Q_+ as seen from infinity to vary. In the WKB approximation, this results in the quantized effective action for the hole-shell system

$$S_k^q = k\hat{r}(0) + \int_{\hat{r}(0)}^r d\hat{r} p_c(\hat{r}) - (M_+ - M)t, \quad (5.77)$$

where now ⁶

$$p_c(\hat{r}) = \sqrt{2M\hat{r} - Q^2} - \sqrt{2M_+\hat{r} - Q_+^2} - \hat{r} \log \left| \frac{\sqrt{\hat{r}} - \sqrt{2(M_+ - Q_+^2/2\hat{r})}}{\sqrt{\hat{r}} - \sqrt{2(M - Q^2/2\hat{r})}} \right| \quad (5.78)$$

and

$$k = \sqrt{2M\hat{r}(0) - Q^2} - \sqrt{2M_+\hat{r}(0) - Q_+^2} - \hat{r}(0) \log \left| \frac{\sqrt{\hat{r}(0)} - \sqrt{2M_+ - Q_+^2/\hat{r}(0)}}{\sqrt{\hat{r}(0)} - \sqrt{2M - Q^2/\hat{r}(0)}} \right|. \quad (5.79)$$

5.3.2 Bogoliubov coefficients and the radiation rate

We attempt to describe the same physical process as before, so we use the same sets of natural modes. Note that due to the fact that we consider charged states, the complete sets of modes are now $\{u_k^q, u_k^{-q*}\}$ and $\{v_k^q, v_k^{-q*}\}$. The Bogoliubov coefficients are then found to be

$$\alpha_{kk'} = \frac{1}{2\pi u_k^q(r)} \int_{-\infty}^{\infty} dt e^{i\omega_k t} v_{k'}^q(t, r), \quad \beta_{kk'} = \frac{1}{2\pi u_k^q(r)} \int_{-\infty}^{\infty} dt e^{i\omega_k t} v_{k'}^{-q}(t, r)^*. \quad (5.80)$$

Using the same logic as in equations (5.31)-(5.39), we obtain

$$|\alpha_{kk'}| = e^{-\text{Im} \int_{r(0)}^r p_\omega^q(r) dr} \quad \text{and} \quad |\beta_{kk'}| = e^{\text{Im} \int_{r(0)}^r p_{-\omega}^{-q}(r) dr}, \quad (5.81)$$

⁶Note that this expression differs from expression (2.14) for p_c in [13]. In order to make the transition from the Schwarzschild to the Reissner-Nordström black hole, one must make some substitutions. Outside the black hole, the energy contained in a spherical shell of radius r is no longer just the black hole mass M , but there is a contribution from the electric field energy. Therefore, one has to substitute $M \rightarrow M - Q^2/2r$, and hence $M_+ \rightarrow M_+ - Q_+/2r$. These substitutions seem to be intended in [13], but an error was made.

where we added sub- and superscripts to the momentum to denote the energy and charge associated to the saddle trajectories. Because of the divergence of the u -modes we evaluate the integrals just outside the horizon at

$$r = r_+(M + \omega_k, Q + q) = M + \omega_k + \sqrt{(M + \omega_k)^2 - (Q + q)^2}. \quad (5.82)$$

To obtain $\hat{r}(0)$, we solve (5.79) in the limit $k \rightarrow \infty$ and obtain

$$\alpha_{kk'} : \quad \hat{r}(0) = r_+(M + \omega_k, Q + q) + \epsilon_\alpha = M + \omega_k + \sqrt{(M + \omega_k)^2 - (Q + q)^2} + \epsilon_\alpha \quad (5.83)$$

$$\beta_{kk'} : \quad \hat{r}(0) = r_+(M - \omega_k, Q - q) - \epsilon_\beta = M - \omega_k + \sqrt{(M - \omega_k)^2 - (Q - q)^2} - \epsilon_\beta. \quad (5.84)$$

Here the ϵ 's are corrections and $\epsilon_\alpha, \epsilon_\beta > 0$. Now let's evaluate the integrals in the exponents in (5.81). For $|\alpha_{kk'}|$, we notice from (5.83) that again $\hat{r}(0) = r$, so that the integral vanishes. We are left with calculating

$$\Gamma \sim \left| \frac{\beta_{kk'}}{\alpha_{kk'}} \right|^2 = e^{2\text{Im} \int_{r(0)}^r p_{-\omega}^{-q}(r) dr}. \quad (5.85)$$

Evaluating the integral in the exponent we find

$$\begin{aligned} \text{Im} \int_{r(0)}^r p_{-\omega}^{-q}(r) dr &= -\text{Im} \int_{r(0)}^r \hat{r} \log \left| \frac{\sqrt{\hat{r}} - \sqrt{2M_+ - (Q - q)^2/\hat{r}}}{\sqrt{\hat{r}} - \sqrt{2M - Q^2/\hat{r}}} \right| d\hat{r} \\ &= \frac{\pi}{2} (r_+^2(M - \omega, Q - q) - r_+^2(M, Q)) \\ &= -\pi \left[\omega(2M - \omega) - q(Q - \frac{q}{2}) + M\sqrt{M^2 - Q^2} - (M - \omega)\sqrt{(M - \omega)^2 - (Q - q)^2} \right]. \end{aligned} \quad (5.86)$$

This leads us to the corrected probability for a Reissner-Nordström black hole of mass M and charge Q to emit a particle with energy ω and charge q

$$\Gamma \sim e^{-2\pi \left[\omega(2M - \omega) - q(Q - \frac{q}{2}) + M\sqrt{M^2 - Q^2} - (M - \omega)\sqrt{(M - \omega)^2 - (Q - q)^2} \right]} = e^{\Delta S_{BH}}. \quad (5.87)$$

It should be noted that the result in (5.87) again differs from the result obtained for charged radiation in [13]. This time, the authors seem not to make the mistakes mentioned for the massless case at the end of section 5.2.4. However, one or more other calculational mistakes were made. Their expression for p_c for example, contains an error. Therefore, also in [13] the relation between the corrected emission probability and the change in entropy is not noticed.

5.3.3 Non-thermal aspects

Again, the spectrum obtained when including self-gravitational effects deviates from a thermal spectrum. For small ω and q we can expand the exponent in (5.87) to find

$$\begin{aligned}\Delta S_{BH} &= 2\pi\omega \left(-2M - \frac{M^2}{\sqrt{M^2 - Q^2}} - \sqrt{M^2 - Q^2} \right) + 2\pi q \left(\frac{MQ}{\sqrt{M^2 - Q^2}} + Q \right) + O(\omega^2, q^2, \omega q) \\ &= -2\pi \frac{(M + \sqrt{M^2 - Q^2})^2}{\sqrt{M^2 - Q^2}} \left(\omega - \frac{Q}{M + \sqrt{M^2 - Q^2}} q + O(\omega^2, q^2, \omega q) \right).\end{aligned}\quad (5.88)$$

So, for charged radiation we find the Boltzmann factor to first order in ω and q

$$\Delta S_{BH} = -\beta \left(\omega - \frac{Q}{r_+} q \right) \quad \rightarrow \quad \Gamma \sim e^{-\beta(\omega - \Phi_{r_+} q)} \quad (5.89)$$

where

$$\beta = T_H^{-1} = \left(\frac{\sqrt{M^2 - Q^2}}{(M + \sqrt{M^2 - Q^2})^2} \right)^{-1} \quad (5.90)$$

is the inverse Hawking temperature and Φ_{r_+} is the electrostatic potential evaluated at the outer black hole horizon. Again, we find the well known thermal spectrum characterized by T_H to leading order. Higher order corrections (due to energy conservation) drive the spectrum away from thermality. Collecting all corrections the radiation rate can, again, be expressed as the exponent of the change in the Bekenstein-Hawking entropy of the hole, due to the emission.

Another feature of equation (5.87) worth mentioning is that it does not allow radiation past extremality. The emission rate has to be real, so the second square root in the exponent ensures that radiation is only possible as long as the final mass of the black hole does not fall below its charge, $M - \omega \geq |Q - q|$. Another way of stating this is that for $M - \omega \geq |Q - q|$, the pole in the integral (5.86) lies in the complex plane. Since we are integrating over the real axis, we do not obtain an imaginary part. This means our result for the radiation rate in (5.87) explicitly ensures that no naked singularities form in the Hawking process.

Chapter 6

Black hole radiation as tunneling

The expression for the emission probability given in (5.42) and (5.85) arouses interest. The expression is of the form

$$\Gamma \sim \left| \frac{\beta_{kk'}}{\alpha_{kk'}} \right|^2 = e^{2\text{Im} \int_{r(0)}^r p(r) dr}, \quad (6.1)$$

which we recognize as being the expression for a quantum mechanical tunneling probability in the WKB approximation. Therefore, $|\alpha_{kk'}|$ and $|\beta_{kk'}|$ look exactly like quantum mechanical WKB tunneling coefficients. The field theoretical approach that was taken in the previous chapter to include self-gravitating effects, essentially appears to boil down to the calculation of a quantum mechanical tunneling rate. It seems this analysis therefore shows that one can naturally interpret the emission from a black hole as resulting from the tunneling of (anti-)particles across the hole's horizon.

Hawking himself already proposed to think of black hole radiation as a tunneling process when he first derived it [1, 25]. It is such a tunneling process that is generally used to draw a heuristic picture of Hawking radiation [15]. In terms of Feynman diagrams, vacuum fluctuations can be represented by virtual pairs of particles and antiparticles that exist for an extremely short period of time before annihilating. The effect of these fluctuations is usually only indirect.¹ However, this can change in the presence of an event horizon. The idea is that when a virtual particle pair is created near the black hole horizon, one of the two virtual particles can tunnel through the horizon and materialize. Either a pair is created just inside the horizon and the positive energy virtual particle tunnels out, or a pair is created just

¹Since one needs to renormalize processes that involve virtual particles.

outside the horizon and the negative energy virtual particle tunnels inwards. It is possible for the infalling particle to have an energy that is negative as seen from infinity, since the Killing vector that is asymptotically timelike, becomes spacelike inside the horizon. In both cases the negative energy particle is absorbed by the black hole, decreasing its mass and the positive energy particle escapes to infinity, appearing as Hawking radiation.

As was discussed before, numerous derivations of Hawking radiation exist, but most of them are QFT calculations and do not correspond well with the heuristic tunneling picture. However, in the previous chapter we saw how a quantum mechanical tunneling calculation emerged by truncating our field theory approach to an effective particle description. Therefore, this approach, aimed at the inclusion of energy conservation, provides us with a starting point for a calculating that describes the Hawking effect as an intuitive tunneling process.

The derivation of Hawking radiation as such a tunneling process has been pioneered by Parikh and Wilczek [14]. This derivation indeed takes (6.1) as a starting point. Relying partially on the results of [12], they consider the tunneling of a self-gravitating shell through the horizon. In [14], no comments were made on the origins of this tunneling calculation, but they found a modification of the emission spectrum equal to the modification found using the second quantized methods in chapter 5. Of course, now that we have seen how this tunneling calculation emerges from the field theory approach, this does not come as a surprise and rather serves as consistency check.

Still, the method suggested by Parikh and Wilczek obtains these results in a neat and simple fashion by following the more intuitive tunneling interpretation of black hole radiance from the start. Particle emission by the black hole is regarded as quantum mechanical tunneling through a barrier, which only appears when enforcing energy conservation. This allows one to avoid the tedious calculations that second quantization brings along. Moreover, it elegantly shows how energy is naturally conserved in the process of particle emission. Technically, the method simply uses a different approach in evaluating the integral in (6.1). Instead of using the details of the solution, one uses Hamilton's equations to evaluate them.

In this chapter we first review the tunneling approach suggested by Parikh and Wilczek. However, in [14] they only considered massless radiation from Schwarzschild and Reissner-Nordström black holes. Following the methodological review, we generalize the procedure to the emission of massive and charged radiation from these black holes.

6.1 The tunneling of massless particles through the horizon

Despite the intuitive appeal, before 2004 black hole radiation was never derived as a tunneling process. Historically, there were two difficulties to such an approach [65]. Firstly, there seemed to be no coordinate system at hand that was well-behaved at the black hole horizon. Such coordinates are clearly needed in order to describe tunneling, a horizon-crossing phenomenon. Secondly, there was no apparent barrier for the particle to tunnel through. In a regular quantum mechanical tunneling process, one has two classical turning points. These points are then connected by a path in imaginary time. But a particle can escape classically as soon as it is only infinitesimally outside the black hole horizon. This means the classical turning points do not seem to be separated and the imaginary time trajectory that is supposed to join them does not seem to be defined. As will become clear in this section, this second hurdle can be overcome by incorporating energy conservation.

6.1.1 The WKB tunneling probability and energy conservation

As mentioned in the introduction of this chapter, Parikh and Wilczek consider the tunneling of a self-gravitating shell through the black hole horizon. Therefore, the discussion is again limited to s-wave emission. In the WKB limit, which we know from the previous chapter to be accurate for processes close to the horizon, the probability of tunneling is related to the imaginary part of the action in the classically forbidden region by²

$$\Gamma \sim e^{-2\text{Im}S} = e^{-2\text{Im} \int p_r dr}. \quad (6.2)$$

This is exactly the same expression as the one we found in (5.42) using a second quantized approach and functions as the starting point of our tunneling calculation. Instead of using tedious field theory methods we arrived at (6.2) by simple, intuitive tunneling reasoning. We have seen in chapter 5 how this expression emerged from the field theory description. Therefore, we expect to obtain the same results as in chapter 5.

²We use the action in (5.61). The second term in this action is disregarded since the Hamiltonian is conserved and integrating it over time will therefore not give any imaginary contribution. A minus sign appears in relation to (6.1), because this is ‘extracted’ from the action to fit with WKB tunneling conventions.

In the field theory approach, we used the explicit form of p_r to evaluate the integral. But as it turns out, we do not need the details of the solution to evaluate this integral, provided we use the following result from [12], proved in the previous chapter. Both inside and outside the shell, the geometry is Schwarzschild or Reissner-Nordström. The mass parameters, however, are different. A key result in [12] (that was verified in the previous chapter) is that, if one fixes the black hole mass M and allows the mass as seen from infinity to vary, the classical trajectory of a self-gravitating shell with energy ω is a null geodesic in the Schwarzschild or Reissner-Nordström metric with mass parameter $M + \omega$. Alternatively, if one decides to fix the mass as seen from infinity and to allow the black hole mass to vary, one obtains the same result, but with a mass parameter $M - \omega$. In what follows, we decide to do the last, since this is the most intuitive choice.

We wish to calculate the imaginary part of the momentum term in the action for a particle crossing the horizon outwards, from r_{in} just inside the horizon before the radiation to r_{out} just outside the new horizon after radiation. Considering the tunneling of a massless particle with energy ω in the s-wave channel we have

$$\text{Im}S = \text{Im} \int_{r_{in}}^{r_{out}} p_r dr = \text{Im} \int_{r_{in}}^{r_{out}} \int_0^{p_r} dp'_r dr. \quad (6.3)$$

We can now see how energy conservation provides us with the tunneling barrier that seemed to be absent. As the black hole radiates, it loses energy. This means its radius shrinks and it is this contraction that sets the scale for tunneling. The horizon recedes from its original radius to a new, smaller radius. The amount of contraction depends on the energy of the outgoing particle. Hence, in a sense it is the tunneling particle itself that defines the barrier. It is the (classically forbidden) region between the initial and final radii of the horizon that the tunneling particle must traverse.

We now use Hamilton's equation, $\frac{dH}{dp_r} = \frac{dr}{dt} \equiv \dot{r}$, to change the variable from momentum to energy and switch the order of integration to obtain

$$\text{Im}S = \text{Im} \int_M^{M-\omega} \int_{r_{in}}^{r_{out}} \frac{dr}{\dot{r}} dH = -\text{Im} \int_0^\omega \int_{r_{in}}^{r_{out}} \frac{dr}{\dot{r}} d\omega', \quad (6.4)$$

where we have used that $H = M - \omega$. To obtain the tunneling rate, we need an expression for \dot{r} . This describes a null geodesic in the Schwarzschild metric with mass parameter M .

and was obtained in section 5.2.2

$$\dot{r} = \pm 1 - \sqrt{1 - f(r)}. \quad (6.5)$$

Under the assumption that t increases towards the future, the plus and minus sign correspond to outgoing and ingoing radiation respectively. Here, we focus on outgoing radiation. Remember that due to self-gravitation, $f(r)$ is to be evaluated with mass parameter $M_- = M - \omega$.

Using (6.5) we can evaluate the integral in order to obtain the tunneling rate of outgoing massless particles

$$\text{Im}S = -\text{Im} \int_0^\omega \int_{r_{in}}^{r_{out}} \frac{dr}{1 - \sqrt{1 - f(r)}} d\omega'. \quad (6.6)$$

We notice this integral has a pole at the horizon, $f(r_h) = 0$, and evaluate this integral by contour integration. We deform the contour so as to ensure that the positive energy solutions decay in time, i.e. $\omega' \rightarrow \omega' - i\epsilon$. For some additional details on contour integration we refer to appendix C.

6.1.2 Massless radiation from the Schwarzschild black hole

First consider radiation from the Schwarzschild black hole. We perform the r -integral first. Making the substitution $u = \sqrt{r}$ (so $dr = 2u du$), we have

$$\text{Im}S = -\text{Im} \int_0^\omega \int_{u_{in}}^{u_{out}} \frac{2u^2 du}{u - \sqrt{2(M - \omega' + i\epsilon)}} d\omega' = 4\pi \int_0^\omega d\omega' (M - \omega'). \quad (6.7)$$

The pole lies in the upper half u -plane and we evaluate the integral by deforming the contour around it. The right sign appears in the last step because $r_{in} > r_{out}$ (and therefore $u_{in} > u_{out}$). Performing the energy integral we find

$$\text{Im}S = -2\pi\omega(\omega - 2M). \quad (6.8)$$

We could also not have switched the order of integration. This also provides us with understanding of the ordering (that provides us with the correct sign). We again evaluate the

contour with the prescription $\omega' \rightarrow \omega' - i\epsilon$. We now substitute $u \equiv \sqrt{2(M - \omega')r}$ (and thus $d\omega' = -\frac{u}{r}du$) to obtain

$$\begin{aligned} \text{Im}S &= \text{Im} \int_{r_{in}}^{r_{out}} \int_{u_i}^{u_f} \frac{u du}{r - u} dr \\ &= \pi \int_{r_{in}}^{r_{out}} r dr = \frac{\pi}{2}(r_{in}^2 - r_{out}^2) = -2\pi\omega(\omega - 2M). \end{aligned} \quad (6.9)$$

Where from the last step we may infer that $r_{in} = 2M$ and $r_{out} = 2(M - \omega)$. The limits of the intergral tell us that over the course of the classically forbidden trajectory, the particle starts just inside the initial position of the horizon at $r = 2M$ and traverses the contracting horizon to materialize just outside the final position of the horizon at $r = 2(M - \omega)$. The calculation of the imaginary contribution of the actions leaves us with a tunneling rate for massless radiation from a Schwarzschild black hole of

$$\Gamma \sim e^{-2\text{Im}S} = e^{-8\pi\omega(M - \frac{\omega}{2})} = e^{\Delta S_{BH}}. \quad (6.10)$$

In obtaining the result (6.10), we considered pair creation just inside the horizon followed by the outward tunneling of the positive energy particle. Alternatively, we could consider pair creation just outside the horizon, with the negative particle tunneling inwards through the horizon. A negative particle travels backwards in time, meaning we reverse time $t \Rightarrow -t$. For an ingoing nul geodesic, we then find

$$\dot{r} = -1 + \sqrt{\frac{2M}{r}}. \quad (6.11)$$

The ingoing negative energy sees a geometry with a fixed black hole mass [14]. Then, as we have seen in chapter 5, self-gravitation forces $M \rightarrow M + \omega$ instead of $M - \omega$. In this picture, we have

$$\text{Im}S = \text{Im} \int_0^{-\omega} \int_{r_{out}}^{r_{in}} \frac{dr}{-1 + \sqrt{\frac{2(M+\omega')}{r}}} d\omega'. \quad (6.12)$$

We now evaluate the integral by deforming the contour in order to ensure the decay of negative energy solutions, i.e. $\omega' \rightarrow \omega' + i\epsilon$. This gives

$$\text{Im}S = 4\pi\omega \left(M - \frac{\omega}{2} \right). \quad (6.13)$$

In reality, both particle and anti-particle tunneling need to be taken into account when calculating the rate of black hole radiation. To do so, one must consider the amplitudes for these processes. These, however, just concern the prefactor and are therefore ignored.

Note that there seems to be a strong resemblance between considering the particle or anti-particle tunneling in the above calculation and taking either the black hole mass or the mass as seen from infinity to vary in the field theory approach of chapter 5. Presumably, choosing the black hole mass to vary in the analysis of chapter 5 corresponds to the intuitive picture of a particle tunneling outwards, while choosing the ADM mass to vary corresponds to the inward tunneling of an anti-particle.

For massless radiation from the Reissner Nordström black hole we find, using (2.20) and (6.6)

$$\text{Im}S = -\text{Im} \int_0^\omega \int_{r_{in}}^{r_{out}} \frac{dr}{1 - \sqrt{\frac{2(M-\omega')}{r} - \frac{Q^2}{r^2}}} d\omega'. \quad (6.14)$$

Using the same pole prescription as above, we find

$$\text{Im}S = \pi \int_{r_{in}}^{r_{out}} r dr = \pi \left[\omega(2M - \omega) + M\sqrt{M^2 - Q^2} - (M - \omega)\sqrt{(M - \omega)^2 - Q^2} \right] \quad (6.15)$$

and thus

$$\Gamma \sim e^{-2\text{Im}S} = e^{-2\pi \left[\omega(2M - \omega) + M\sqrt{M^2 - Q^2} - (M - \omega)\sqrt{(M - \omega)^2 - Q^2} \right]} = e^{\Delta S_{BH}}. \quad (6.16)$$

6.2 Generalization to massive and charged radiation

In the previous section we have seen that the method developed in [14] to take into account global conservation laws in the black hole radiation process leads to a modification of the emission spectrum, in agreement with what was found in chapter 5. However, Parikh and Wilczek only consider massless radiation from Schwarzschild and Reissner-Nordström black holes. In this section, we generalize this tunneling approach. We extend the calculation in order to describe massive, charged radiation from the Reissner-Nordström black hole.

6.2.1 Radial equations of motion

When considering massive and charged radiation a few things change concerning the trajectories of the shells. First of all, being massive, the shells will no longer travel on null paths, but on timelike ones. Secondly, if the shell is charged this path will not be a geodesic. The

fact that we now consider timelike trajectories changes the expression for \dot{r} . It does not matter, however, that the trajectories under consideration are no longer geodesics. In the procedure for massless radiation, we never invoked this property and the exact form of r was never used.

To obtain the radial equation of motion, we may again use condition (5.10). For timelike paths parametrized by τ we have

$$g_{\mu\nu} \frac{dx^\mu}{d\tau} \frac{dx^\nu}{d\tau} = g_{\mu\nu} U^\mu U^\nu = -1. \quad (6.17)$$

In the massless case the condition (5.10) was all that was needed to find \dot{r} . In the massive case, however, this condition alone is not sufficient to find an expression for \dot{r} . In expanded form it reads

$$-f(r) \left(\frac{dt}{d\tau} \right)^2 + 2\sqrt{1-f(r)} \frac{dt}{d\tau} \frac{dr}{d\tau} + \left(\frac{dr}{d\tau} \right)^2 = -1. \quad (6.18)$$

To obtain the information needed to derive an expression for \dot{r} we take a look at the equations of motion derived from the action. The action for a relativistic particle in an electromagnetic potential reads

$$S[x(\tau)] = \int \left[\frac{m}{2} g_{\mu\nu} \frac{dx^\mu}{d\tau} \frac{dx^\nu}{d\tau} + q A_\mu \frac{dx^\mu}{d\tau} \right] d\tau. \quad (6.19)$$

For the Reissner Nordström black hole the electromagnetic potential is $A_\mu = (-Q/r, 0, 0, 0)$ (in both regular and Painlevé coordinates). Expanding the Lagrangian using Painlevé coordinates we find

$$\mathcal{L} = \frac{m}{2} \left[-f(r) \left(\frac{dt}{d\tau} \right)^2 + 2\sqrt{1-f(r)} \frac{dt}{d\tau} \frac{dr}{d\tau} + \left(\frac{dr}{d\tau} \right)^2 \right] - \frac{qQ}{r} \frac{dt}{d\tau}. \quad (6.20)$$

We now use the Euler-Lagrange equation to get the equation of motion for t

$$\frac{\partial \mathcal{L}}{\partial t} - \frac{d}{d\tau} \frac{\partial \mathcal{L}}{\partial \left(\frac{dt}{d\tau} \right)} = 0. \quad (6.21)$$

Since the Lagrangian has no explicit t -dependence and the canonical momentum for a generalized coordinate is defined as $\frac{\partial \mathcal{L}}{\partial \dot{q}_i} = p_i$, we have

$$\frac{\partial \mathcal{L}}{\partial \left(\frac{dt}{d\tau} \right)} = -mf(r) \frac{dt}{d\tau} + m\sqrt{1-f(r)} \frac{dr}{d\tau} - \frac{qQ}{r} = \text{constant} = p_t = -\omega. \quad (6.22)$$

Now using both equation (6.18) and (6.22) we are able to solve for $\frac{dt}{d\tau}$ and $\frac{dr}{d\tau}$:

$$\begin{aligned}\frac{dr}{d\tau} &= \pm \frac{\sqrt{(\omega - \frac{qQ}{r})^2 - m^2 f(r)}}{m} \\ \frac{dt}{d\tau} &= \frac{(\omega - \frac{qQ}{r}) \pm \sqrt{1 - f(r)} \sqrt{(\omega - \frac{qQ}{r})^2 - m^2 f(r)}}{m f(r)}.\end{aligned}\tag{6.23}$$

Combining these, we find

$$\begin{aligned}\dot{r} = \frac{dr}{dt} &= \frac{dr}{d\tau} \left(\frac{dt}{d\tau} \right)^{-1} = \frac{\pm f(r) \sqrt{(\omega - \frac{qQ}{r})^2 - m^2 f(r)}}{(\omega - \frac{qQ}{r}) \pm \sqrt{1 - f(r)} \sqrt{(\omega - \frac{qQ}{r})^2 - m^2 f(r)}} \\ &= \frac{\pm f(r)}{\frac{(\omega - \frac{qQ}{r})}{\sqrt{(\omega - \frac{qQ}{r})^2 - m^2 f(r)}} \pm \sqrt{1 - f(r)}}.\end{aligned}\tag{6.24}$$

This is the radial equation of motion we were looking for. Under the assumption that t increases towards the future, the plus and minus sign correspond to outgoing and ingoing radiation respectively.

This result relates nicely to the radial motion obtained in (6.5) for massless shells. Taking a closer look at equation (6.24) we see that

$$\dot{r} = \frac{\pm f(r)}{1 \pm \sqrt{1 - f(r)}} = \pm 1 - \sqrt{1 - f(r)} \quad \text{for } m, q \rightarrow 0,\tag{6.25}$$

equal to (6.5). Note also, that we should obtain a result similar to (6.24) from just using Hamilton's equations on the canonical momentum (5.78). Here, however, we acted as if we did not know the details of this solution, in order to stick to the strict tunneling picture.

6.2.2 The tunneling of massive, uncharged shell

As a layover we first consider massive, but uncharged radiation. In this case we can proceed through (6.2)-(6.4) exactly as in the massless case. The only thing changing is \dot{r} , which is now given by (6.24), with $q = 0$. Substituting this into equation (6.4) and evaluating the

integrals, we find

$$\begin{aligned}
\text{Im}S &= -\text{Im} \int_0^\omega \int_{r_{in}}^{r_{out}} \frac{\omega - \frac{qQ}{r} + \sqrt{1 + f(r)} \sqrt{(\omega - \frac{qQ}{r})^2 - m^2 f(r)}}{f(r) \sqrt{(\omega - \frac{qQ}{r})^2 - m^2 f(r)}} dr d\omega' \\
&= \pi \int_0^\omega \frac{(M - \omega' + \sqrt{(M - \omega')^2 - Q^2})^2}{\sqrt{(M - \omega')^2 - Q^2}} d\omega' \\
&= \pi \left[\omega(2M - \omega) + M\sqrt{M^2 - Q^2} - (M - \omega)\sqrt{(M - \omega)^2 - Q^2} \right]. \quad (6.26)
\end{aligned}$$

Hence, for massive, neutral radiation we find the same tunneling rate as for massless radiation. The poles in the integrand remain at the horizon and the residue is unchanged.

It does not come as a surprise that, in the absence of electric/magnetic charge, we obtain the same rate for the tunneling of massive and massless shells. Near the horizon the wavelengths of the emitted quanta experience an infinite blueshift. This means the wavenumber becomes arbitrarily large, $k^2 \gg m^2$. And since $\omega^2 = k^2 + m^2$, we have $\omega^2 \sim k^2$ and effectively $m^2 \sim 0$.

6.2.3 The tunneling of massive, charged shells

We now include both mass and charge. As discussed in section 6.1.1, the classical trajectory of an uncharged gravitating shell with energy ω is a geodesic in the black hole geometry with mass parameter $M - \omega$ (provided we allow the black hole mass to vary and not the mass as seen from infinity). In [13] it was shown that if one adds a charge q to the shell, this generalizes in a straightforward way. If one allows the black hole charge to vary, while keeping the total charge as seen from infinity fixed, one simply also transforms the charge parameter $Q \rightarrow Q - q$ in the line element.

By adding charge, we alter Hamilton's equations. Starting again from and (6.2) we use Hamilton's equation to obtain

$$\text{Im} \int_{r_{in}}^{r_{out}} \int_0^{P_r} dp'_r dr = \text{Im} \int_{E_i}^{E_f} \int_{r_{in}}^{r_{out}} \frac{dr}{\dot{r}} dH', \quad (6.27)$$

where \dot{r} is evaluated with parameters $M \rightarrow M_- = M - \omega'$ and $Q \rightarrow Q_- = Q - q'$. Now that we have included an electric field, H' no longer simply equals $M - \omega'$. There is an electromagnetic contribution as well. In line with what seems to be done in [13], we interpret

H' as the energy contained in a shell of coordinate radius r . According to [13] this is

$$H' = (M - \omega') - \frac{(Q - q')^2}{2r}, \quad (6.28)$$

leading to

$$dH' = dM_- - \frac{Q_-}{r} dQ_-. \quad (6.29)$$

A way to look at this is that dH is now no longer just the change in the mass, but also the change in work done by the electric field. Therefore

$$dH' = dM_- + \Phi|_{r_+} dQ_- = dM_- - \frac{Q_-}{r} dQ_-, \quad (6.30)$$

equal to (6.29).

Using this we rewrite (6.27) as

$$\text{Im}S = \int_M^{M-\omega} \int_{r_{in}}^{r_{out}} \frac{dr}{\dot{r}} dM_- - \int_Q^{Q-q} \int_{r_{in}}^{r_{out}} \frac{Q_-}{r} \frac{dr}{\dot{r}} dQ_-. \quad (6.31)$$

Or, in terms of ω' and q'

$$\text{Im}S = - \int_0^\omega \int_{r_{in}}^{r_{out}} \frac{dr}{\dot{r}} d\omega' + \int_0^q \int_{r_{in}}^{r_{out}} \frac{Q_-}{r} \frac{dr}{\dot{r}} dq'. \quad (6.32)$$

We now substitute the (outgoing) radial equation of motion (6.24) in the expression for the imaginary part of the action (6.32) to find

$$\begin{aligned} \text{Im}S &= \int_M^{M-\omega} \int_{r_{in}}^{r_{out}} \frac{\frac{(\omega - \frac{qQ_-}{r})}{\sqrt{(\omega - \frac{qQ_-}{r})^2 - m^2 f(r)}} + \sqrt{1 - f(r)}}{f(r)} dr dM_- \\ &\quad - \int_Q^{Q-q} \int_{r_{in}}^{r_{out}} \frac{Q_-}{r} \frac{\frac{(\omega - \frac{qQ_-}{r})}{\sqrt{(\omega - \frac{qQ_-}{r})^2 - m^2 f(r)}} + \sqrt{1 - f(r)}}{f(r)} dr dQ_-. \end{aligned} \quad (6.33)$$

We see that the pole is at the familiar positions $f(r) = 0$ again. Using contour integration to evaluate the r -integral (at the outer pole) we find

$$\begin{aligned} \text{Im}S &= -\pi \int_M^{M-\omega} \frac{\left(M_- + \sqrt{M_-^2 - Q_-^2}\right)^2}{\sqrt{M_-^2 - Q_-^2}} dM_- + \pi \int_Q^{Q-q} Q_- \frac{M_- + \sqrt{M_-^2 - Q_-^2}}{\sqrt{M_-^2 - Q_-^2}} dQ_- \\ &= -\pi \int_{(M,Q)}^{(M-\omega, Q-q)} \frac{2r_+}{r_+ - r_-} (r_+ dM_- - Q_- dQ_-). \end{aligned} \quad (6.34)$$

where $r_{\pm} = M_{\pm} \pm \sqrt{M_{\pm}^2 - Q_{\pm}^2}$.

Now we change the integration variable to r_+ . Since r_+ depends both on Q_- and M_- , we have

$$dr_+ = \frac{\partial r_+}{\partial M_-} dM_- + \frac{\partial r_+}{\partial Q_-} dQ_- = \frac{2r_+}{r_+ - r_-} dM_- - \frac{2Q_-}{r_+ - r_-} dQ_-. \quad (6.35)$$

Therefore, from (6.34) and (6.35) we can express the imaginary part of the action over the classically forbidden region as an integral over the recession of the outer horizon due to the tunneling of the shell

$$\text{Im}S = -\pi \int_{r_{in}}^{r_{out}} r_+ dr_+, \quad (6.36)$$

where $r_{in} = r_+(M, Q)$ and $r_{out} = r_+(M - \omega, Q - q)$. From this expression the relation with the change in entropy is immediately clear. We see

$$\Gamma \sim e^{-2\text{Im}S} = e^{\Delta S_{BH}}. \quad (6.37)$$

We may conclude that the results found in this chapter for the tunneling probabilities of shells through black hole horizons all agree with the results we obtained in chapter 5 for the corrected emission probabilities.

6.3 Hawking radiation as tunneling and thermodynamics

As expected from the result, the tunneling method is very closely related to the first law of thermodynamics, discussed in section 2.2. Let's first take radiation from the Reissner-Nordström black hole as an example. As we consider uncharged radiation, using 2.6 and $T = \frac{\kappa}{2\pi}$ and $dS = \frac{dA}{4G}$, the first law becomes

$$dS = \frac{dM}{T}. \quad (6.38)$$

Now we fixed the total mass M and vary the mass of the black hole, $M_- = M - \omega'$. Using the expression for the Hawking temperature of a Reissner-Nordström black hole (5.90) we find

$$dS = \frac{2\pi(M_- + \sqrt{M_-^2 - Q^2})^2}{\sqrt{M_-^2 - Q^2}} dM_- = -\frac{2\pi(M_- + \sqrt{M_-^2 - Q^2})^2}{\sqrt{M_-^2 - Q^2}} d\omega'.$$

This means $-\frac{1}{2}dS$ is precisely the integrand in equation (6.26). From this point of view, the calculation is like applying the first law of thermodynamics.

When considering charged radiation, the first law becomes

$$dS = \frac{1}{T} (dM - \Phi dQ). \quad (6.39)$$

Now, following the same procedure as above, but now also varying the charge of the black hole, $Q_- = Q - q'$ we obtain

$$dS = \frac{2\pi(M_- + \sqrt{M_-^2 - Q_-^2})^2}{\sqrt{M_-^2 - Q_-^2}} dM_- - \frac{2\pi(M_- + \sqrt{M_-^2 - Q_-^2})}{\sqrt{M_-^2 - Q_-^2}} Q_- dQ_-. \quad (6.40)$$

Again, we see that $-\frac{1}{2}dS$ is the integrand in equation (6.34). The fact that all integrals over ω and q that we encountered can exactly be rewritten in the form $\sim \int r_h dr_h$ can therefore be expected. In fact, following the tunneling picture seems like applying the first law of thermodynamics.

Chapter 7

The WGC, black hole radiation and AdS (in)stability

In chapters 5 and 6, we computed the probability for a Reissner-Nordström black hole to emit a charged particle, with the self-gravitational interaction of this particle included. This resulted in a modified emission probability. In this chapter, we focus on the behavior of extremal Reissner-Nordström black holes under the Hawking process. It seems as if for these holes, our results should be particularly interesting. Following strictly semiclassical methods, extremal black holes have a vanishing Hawking temperature: $T_H = 0$. Therefore, the decay of such black holes is not described by Hawking's original derivation. Rather, in order to understand how extremal black holes behave under the Hawking process, the inclusion of back reaction effects is needed.

A further study of extremal black holes is also of particular interest for two closely linked reasons. Firstly, the possibility of decay of such black holes is one of the main motivations for the weak gravity conjecture (WGC), briefly discussed in section 4.3.3. Secondly, Anti-de Sitter (AdS) space appears as the near horizon geometry of extremal black holes. Therefore, the (in)stability of an extremal black hole is intimately linked with the (in)stability of this AdS spacetime, obtained in its near horizon limit.

In this chapter we first review the WGC, mainly in the context of string theory and see how the results obtained in this thesis relate to it. We then briefly discuss AdS and show how AdS_2 emerges in the near horizon limit of a 4d Reissner-Nordström black hole. Subsequently, all concepts discussed in this chapter are merged in a discussion on the (in)stability of non-

supersymmetric AdS vacua. Finally, we shortly review the fragmentation of AdS₂ and show that our results agree with previous work on this subject.

7.1 The weak gravity conjecture

7.1.1 The string landscape and swampland criteria

String theory is the leading approach towards the unification of general relativity and quantum mechanics. It is widely accepted that it has the potential to provide a consistent description of the theory of quantum gravity. For the theory's equations to be mathematically consistent, it must live in 10 dimensions.¹ This suggests the existence of six unobserved dimensions in addition to our seemingly four dimensional world. One thinks of these 'extra' dimensions as being compactified and therefore too small to be detected (at present). However, the physics we observe in our four dimensional world depends crucially on the geometry of the six hidden ones.

When one wants to find a solution to Einstein's equations in 4d one has to compactify six dimensions. This procedure is far from unique. The fact that we have six dimensions to be compactified results in many adjustable parameters, corresponding to the topology of the compactified space, the positions of branes and the amount of flux wound around loops. It is argued that this huge diversity of string vacuum constructions leads to as many as 10^{500} possible string vacuum solutions. This results in a vast *landscape* of string vacua, each corresponding to a consistent low energy effective field theory (EFT).

A natural question to ask is whether the string landscape is as vast as admitted by EFTs that seem consistent. It was suggested that this is in fact not the case and that the landscape of consistent low energy theories one can obtain in string theory is far smaller than would have been expected by simply demanding semiclassical consistency of the theory [68, 69]. The landscape of string vacua can thus actually be pictured as an island in an even bigger *swampland* of EFTs that are semiclassically consistent, but that cannot be completed to a consistent ultra-violet (UV) theory.

¹For more on string theory, see e.g. [66, 67].

Given an EFT, one would like to be able to tell whether it could possibly arise in a theory of quantum gravity. This coincides with the problem of distinguishing the string theory landscape from the swampland. The approach towards making this distinction is to use general features emerging in all string theory vacua [68] (for some examples see [69]). Although these usually do not serve as semiclassical consistency conditions for EFTs, an EFT that arises in string theory should obey these criteria.

7.1.2 What is the weak gravity conjecture?

One such criterion is the *weak gravity conjecture* (WGC), proposed in [11] and already briefly mentioned in section 4.3.3. It promotes to a principle a notion that is certainly accurate in our world, namely that gravity is the weakest force. If true, this conjecture provides a simple but strong constraint on the low energy EFTs that may arise as the low energy limit from a consistent quantum gravity theory.

In its simplest form, the WGC states that any consistent theory of 4d gravity coupled to a $U(1)$ gauge field must contain a state with mass m and charge q such that²

$$\frac{m}{q} \leq M_p. \quad (7.1)$$

It is proposed that (7.1) is to be understood as a consistency relation for any EFT that allows a UV completion. So essentially, the WGC states that any Einstein-Maxwell theory that is quantum mechanically consistent should have superextremal particles.

The statement (7.1) concerns electrically charged particles, but it should also hold for magnetic monopoles [11]

$$\frac{m_{mag}}{q_{mag}} \leq M_p. \quad (7.2)$$

These monopoles act as a probe for the theory's UV cutoff Λ . The monopole has a mass at least of the order of the energy stored in the magnetic field it generates. This energy is linearly divergent

$$m_{mon} \approx E_{mon} = \int_{r \geq 1/\Lambda} dV \epsilon(x) = \int_{r \geq 1/\Lambda} dV \vec{B}^2 \sim q_{mag}^2 \int_{1/\Lambda}^{\infty} \frac{1}{r^2} dr = q_{mag}^2 \Lambda \sim \frac{\Lambda}{q^2}. \quad (7.3)$$

²For the purpose of clarity, we reinstate M_p in this chapter's equations.

Using (7.3) and the conjecture (7.1) we see that the WGC implies that the EFT must break down at a prematurely low scale

$$\Lambda \leq qM_p. \quad (7.4)$$

An effective field theorist would never suspect the existence of this cutoff. He would not expect the EFT to break down before reaching the regime in which gravity is strongly coupled. Hence, to him it would be natural to expect $\Lambda \sim M_p$.³ To an effective field theorist, a smaller coupling (i.e. smaller q) seems to make the theory more weakly coupled. Instead, the WGC suggests that for small q there exists a ‘new’ UV cutoff scale that is well below M_p . Moreover, the WGC relates G_N and q , two quantities that are never expected to be connected from an EFT point of view.

Using simple dimensional analysis, the WGC generalizes straightforwardly to higher dimensions [11]. In higher dimensions the WGC takes the form of an upper bound on the tension of the brane that is electrically charged under the p -form gauge field. Consider a p -form Abelian gauge field in any dimension D . Then there is an electrically charged $p-1$ dimensional object with tension

$$T_{el} \leq \left(\frac{q^2}{G_N} \right)^{1/2}, \quad (7.5)$$

where the coupling q (charge density) has dimension $\text{mass}^{p+1-D/2}$. In [71] the WGC was generalized to product gauge symmetries, resulting in the so called *convex hull condition*. Furthermore, in [72] the conjecture has been generalized to holographic setups.

If true, the WGC has some interesting consequences. For example, the bound results in tight constraints on seemingly natural models of axion inflation with super-Planckian field ranges.⁴ Another example is the application of the WGC to the study of the stability of AdS vacua. This type of application was suggested very recently [75, 76, 77], and will be discussed later in this chapter.

³Provided that the Landau pole of the $U(1)$ gauge theory is above the Planck scale. A Landau pole is a divergence of the coupling of a quantum field theory under the renormalization group flow at a finite energy scale [70].

⁴See e.g. [73] and references 7-19 in [74].

7.1.3 Why should the WGC be true?

We will not extensively go through all the work done in the search for evidence for the WGC. Instead, we will go into the original motivation that led to the proposal of the WGC in [11] and then briefly refer to some further work. Originally, the bound (7.1) was mainly motivated by arguments involving the related topics of remnants, black hole stability and the absence of global symmetries in quantum gravity.

To begin with, the WGC corresponds nicely with the well known ‘folk theorem’ stating that global symmetries are forbidden in quantum gravity. The conventional argument against having global symmetries in quantum gravity is based on black hole physics. In short, the idea is that in gravitational theories that contain global (continuous) symmetries, it is possible to construct black holes of arbitrarily large charge, which they cannot radiate away (see e.g. [78, 79, 80]). This leads to an infinite number of stable remnants. As was discussed in section 4.3.2, the mainly entropic and thermodynamical arguments against having such stable remnants are compelling. Similar problems do not exist for gauge symmetries. As one takes the limit $q \rightarrow 0$, however, a gauge symmetry becomes (indistinguishable from) a global symmetry. Something should therefore prevent us from taking this limit. This is done by the WGC, which sets a lower bound on the gauge coupling. As one takes the limit $q \rightarrow 0$, we see from (7.4) that $\Lambda \rightarrow 0$. This means one cannot take this limit smoothly.

The main original motivation to propose the WGC involves a feature that is closely related with the above and that has already been reviewed in section 4.3.3: the ability of extremal black holes to decay. Summarizing, the existence of troublesome remnants is avoided if we allow macroscopic black holes to evaporate. Since extremal black holes obey $M = QM_p$, in order for them to be able to evaporate there must exist a state with $m < qM_p$. It must be noted, however, that this original motivation for the WGC has faced some criticism (see e.g. [74] and references therein). On the other hand, there has also been a considerable amount of work in search for additional evidence for the WGC (see e.g. [78, 81, 82, 83, 84]). Despite this effort, we still lack a general proof of the weak gravity conjecture. To date the most compelling evidence for the WGC is empirical. All known examples of compactifications in string theory satisfy the conjecture.

7.1.4 The corrected radiation rate and the WGC

In (5.87), we obtained the corrected probability for a Reissner-Nordström black hole of mass M and charge Q to emit a particle of energy ω and charge q . We now want to study the behavior of an extremal Reissner-Nordström black hole under the Hawking process. In order to do so, one may take two approaches. Firstly, one could try to run through a similar analysis as was done in section 5.3, but this time starting of with an extremal black hole, i.e. one sets $M = Q$ from the start of the field theory analysis. Such an approach involves some subtleties and will not be pursued here. Instead, we take the second route, which is to take the general result obtained in (5.87), and consider it in the extremal limit. Taking the limit $M \rightarrow Q$, we obtain

$$\Gamma \sim e^{-2\pi[\omega(2Q-\omega)-q(Q-\frac{q}{2})-(Q-\omega)\sqrt{(Q-\omega)^2-(Q-q)^2}]}. \quad (7.6)$$

For $\omega > |q|$, we see that Γ becomes imaginary, which is forbidden. As discussed in section 5.3.3, this corresponds to the fact that in the case of subextremal emission, the pole in the integral (5.86) lies in the complex plane. Since we are integrating over the real axis, we do not obtain an imaginary part. Hence, Γ is nonzero only for the emission of particles with $\frac{\omega}{q} > 1$. This is equivalent to the statement we made in section 5.3.3 that our result forbids the formation of a naked singularity through the Hawking process.

In order to link this statement to the WGC, we need to relate ω to the mass m of the particle. The emitted particle obeys a dispersion relation of the form

$$\omega^2 = k^2 + m^2. \quad (7.7)$$

To an observer far away from the hole doing a particle measurement, $k \rightarrow 0$, as the particle experiences an infinite redshift effect travelling of to infinity. Therefore, to the observer at infinity $\omega \approx m$ and we may treat ω as the mass of the particle. This means that our result explicitly shows a nonzero decay probability for a 4d extremal Reissner-Nordström black hole, provided there is a state with $\frac{m}{q} > 1$, i.e. provided the WGC holds.

7.2 AdS as near horizon geometry

As we have seen, the WGC ensures that extremal black holes and branes are able to decay. In the remainder of this chapter, we will apply this conjecture to the study of the stability of AdS

vacua. These geometries are of particular interest to theoretical physicists, primarily because of their role in the widely studied AdS/CFT correspondence [10]. AdS spacetimes appear as the near horizon limit of extremal branes. Therefore, the stability of these spacetimes seems to be closely related to the stability of such branes.

7.2.1 Anti-de Sitter space in short

AdS is the maximally symmetric solution of the Einstein equations with a negative cosmological constant. In general dimensions the metric of AdS_{d+1} in global coordinates is

$$ds^2 = l^2(-\cosh^2 \rho dt^2 + d\rho^2 + \sinh^2 \rho d\Omega_{d-1}^2). \quad (7.8)$$

To gain some insight into the structure of the spacetime we wish to find the Penrose diagram representing AdS_{d+1} . We will not go into the details, but try to convey the main idea. We define a new coordinate σ by

$$\sigma = \tan^{-1} \sinh \rho. \quad (7.9)$$

We then have $d\rho = \cosh \rho d\sigma$, giving us ⁵

$$ds^2 = \frac{l^2}{\cos^2 \sigma}(-dt^2 + d\sigma^2 + \sin^2 \sigma d\Omega_{d-1}^2). \quad (7.10)$$

As our original coordinate ran between $0 \leq \rho \leq \infty$, we have $0 \leq \sigma \leq \frac{\pi}{2}$. We can therefore depict the conformal diagram of AdS_{d+1} as a solid cylinder. ρ is the radial coordinate, while the t and Ω are the coordinates on the surface, that has geometry $\mathbb{R} \times S^{d-1}$. Thus, the conformal boundary of AdS is a timelike cylinder and massless particles take a finite period of time to reach this boundary.⁶

Another set of coordinates in which AdS is often represented is that of Poincaré coordinates. For AdS_{d+1} the metric in these coordinates is

$$ds^2 = \frac{l^2}{z^2} \left(-dt^2 + dz^2 + \sum_{i=1}^{d-1} dx_i^2 \right). \quad (7.11)$$

The boundary is at $z = 0$ in these coordinates. By performing some coordinate transformations, one can show that these coordinates cover only a part of the full spacetime. They cover only a wedge of the entire cylinder, called the Poincaré patch.

⁵Since $\sinh \rho = \tan \sigma$ and $\cosh \rho = \frac{1}{\cos \sigma}$.

⁶For massive particles it is impossible to reach the conformal boundary of AdS. This is because these particles are subject to a potential of $e^{2\rho}$ at large ρ .

7.2.2 AdS in the near horizon limit

Anti-de Sitter spacetimes appear naturally as the near horizon geometries of extremal (black) branes. The metric in these near horizon limits is generally $[\text{AdS}] \times [\text{a sphere}]$. The canonical example is $\text{AdS}_2 \times S^2$, which is obtained by taking the near-horizon limit of an extremal Reissner-Nordström black hole in 4d. In this section, we will show how this particular geometry appears as we take the hole's near horizon limit.

AdS₂ from the extremal Reissner-Nordström black hole

The 4d Reissner-Nordström metric in spherical coordinates reads

$$ds^2 = -f(r)dt^2 + f(r)^{-1}dr^2 + r^2d\Omega^2, \quad f(r) = 1 - \frac{2M}{r} + \frac{Q^2}{r^2}. \quad (7.12)$$

For a non-extremal Reissner-Nordström black hole, the near-horizon region has a finite volume. This can be seen if one calculates the distance L from an arbitrary point \tilde{r} outside the black hole to the horizon r_+ along a slice of fixed t . This is⁷

$$L = \int_{r_+}^{\tilde{r}} \sqrt{f(r)} dr \sim -M \log(r_+ - r_-) \sim M \log\left(\frac{1}{QT_H}\right). \quad (7.13)$$

For a non-extremal black hole, T_H is finite, resulting in a finite volume of the near horizon region. For an extremal black hole, however, $T_H = 0$ and the volume of the near horizon region becomes infinite. This ensures that the near-horizon geometry is well defined.

In the extremal limit we have

$$M = Q \quad \Rightarrow \quad f(r) = \left(1 - \frac{Q}{r}\right)^2. \quad (7.14)$$

In this case the inner and outer horizons coincide, $r_- = r_+ = Q$, and the Hawking temperature vanishes, $T_H = \frac{r_+ - r_-}{4\pi r_+^2} = 0$. To do the near-horizon analysis we define new coordinates z and τ

$$r = Q \left(1 + \frac{\epsilon}{z}\right), \quad t = \frac{Q\tau}{\epsilon}, \quad (7.15)$$

⁷We omit the contribution from the upper limit of the integral and forget about constants.

where ϵ is an arbitrary parameter of the coordinate transformation. In these coordinates the metric (7.12) becomes

$$\begin{aligned} ds^2 &= - \left(\frac{\epsilon}{\epsilon+z} \right)^2 \left(\frac{Q}{\epsilon} \right)^2 d\tau^2 + \left(\frac{\epsilon+z}{\epsilon} \right)^2 \left(\frac{Q\epsilon}{z^2} \right)^2 dz^2 + Q^2 \left(1 + \frac{\epsilon}{z} \right)^2 d\Omega^2 \\ &= - \left(\frac{Q}{\epsilon+z} \right)^2 d\tau^2 + \left(\frac{Q(\epsilon+z)}{z^2} \right)^2 dz^2 + Q^2 \left(1 + \frac{\epsilon}{z} \right)^2 d\Omega^2. \end{aligned} \quad (7.16)$$

To obtain the near-horizon limit, we send $\epsilon \rightarrow 0$, while keeping all coordinates fixed. This forces $r \rightarrow Q$ and hence, we are zooming in on the horizon. The metric then takes the form

$$ds^2 = \frac{Q^2}{z^2} (d\tau^2 + dz^2) + Q^2 d\Omega^2. \quad (7.17)$$

This metric is $AdS_2 \times S^2$, the near-horizon geometry of the extremal Reissner-Nordström black hole. Both the AdS radius and the radius of the sphere are Q .

Recall that the spacetime is supported by some nontrivial electric field. Applying the same procedure to the field strength gives a constant electric field in the near horizon region. In Reissner-Nordström coordinates the field strength was $F_{rt} = \frac{Q}{r^2}$. Now under the coordinate transformations we obtain

$$F_{z\tau} = \frac{\partial r}{\partial z} \frac{\partial t}{\partial \tau} F_{rt} = - \frac{Q}{z^2 \left(1 - \frac{\epsilon}{z} \right)^2} = - \frac{Q}{z^2} \quad \text{if } \epsilon \rightarrow 0. \quad (7.18)$$

In these coordinates this does not seem like a constant field. To see that it actually is, define $\sigma = \frac{1}{z}$. In these coordinates we find

$$F_{\sigma\tau} = \frac{\partial z}{\partial \sigma} F_{z\tau} = Q, \quad (7.19)$$

which is a constant electric field in the near horizon region.

The near-horizon metric (7.17) is AdS_2 in the Poincaré coordinates we encountered in (7.11). As was discussed in section 7.2.1, these coordinates cover only a wedge of the entire spacetime. The fact that we recover only part of the full AdS_2 spacetime in the near horizon limit is not surprising, since the spherical coordinates we started with in (7.12) likewise cover only part of the Reissner-Nordström spacetime (see section 2.4). Just like the Reissner-Nordström spacetime is made up of many asymptotically flat regions, AdS_2 consists of many Poincaré patches. Every individual Poincaré patch of AdS corresponds to the near horizon limit in another asymptotically flat region of the full Reissner-Nordström geometry. A useful way

Reissner-Nordstrom

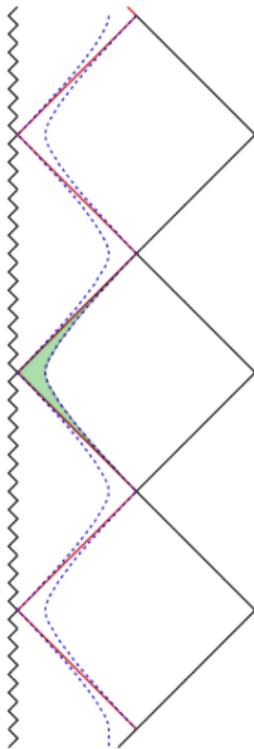
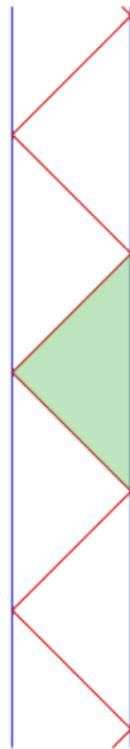
AdS₂

Figure 7.1: The figure on the left is the conformal diagram for the spacetime of an extremal Reissner-Nordström black hole, which we already encountered in figure 2.5. On the right we have the conformal diagram for AdS₂. Whereas for higher-dimensional AdS it is a cylinder, for AdS₂ it is a stripe and therefore has two boundaries. The message we try to convey with this diagram is that essentially, one can view the AdS diagram as the Reissner-Nordström diagram, but limited to the near horizon region. The boundaries of AdS₂ are represented by the dashed blue lines in the Reissner-Nordström diagram, drawn just away from the horizon. The event horizon in the Reissner-Nordström diagram coincides with the horizon of the Poincaré patch (as both coordinate systems break down there). One AdS₂ Poincaré patch is colored green in the two diagrams. As can be seen, there are many Poincaré patches, corresponding to the different asymptotically flat regions in the left diagram.

to gain insight in this, is through conformal diagrams. See for some further explanation the conformal diagrams in figure 7.1.

Higher-dimensional generalizations

The Reissner-Nordström black hole in 4d is not the only solution that contains AdS as its near horizon geometry. One can also obtain AdS geometries by taking the near-horizon geometries of given charged brane solutions in different types of string theories. These are higher-dimensional generalizations of the 4d Reissner-Nordström black hole discussed above. For some examples and classifications of these higher-dimensional generalizations (leading to higher-dimensional AdS geometries), see e.g. [77] and [85].

7.3 The weak gravity conjecture and AdS (in)stability

7.3.1 Sharpened version of the WGC

We now return to the weak gravity bound that we reviewed in section 7.1. States that have a mass or tension equal to their charge (i.e. states that saturate the bounds (7.1) or (7.5)) are well-known in string theory. These are BPS states.⁸ Recently, a stronger version of the WGC was proposed, stating that these BPS states are the only states that saturate the WGC [75] (see also [77, 76]). This sharpened version of the conjecture is therefore the statement that *the weak gravity conjecture is saturated if and only if the underlying theory is supersymmetric and the states under consideration are BPS with respect to the supersymmetry.*

It is argued that allowing the inequality in any other case does not seem natural [75]. Unless protected by supersymmetry, we wish to see extremal black holes decay. It is argued in [75] that the emission of extremal particles will have vanishing phase space in a non-supersymmetric setup. Therefore, the WGC (7.1) should be a strict inequality if we want extremal black holes to decay.

Aside from the above, extremal particles would obviously be on the brink of violating the WGC. Suppose we would allow the equality in (7.1) and we slightly perturb our theory. Then something should prevent the particle from becoming subextremal, since this would yield a violation of the WGC. Whereas in a supersymmetric theory the BPS condition prevents the particle from violating the WGC under such a small perturbation, we seem to have no similar tool in the non-supersymmetric case.⁹

7.3.2 Instability of non-supersymmetric AdS vacua

Although it might seem like the sharpening of the bound that was introduced in the previous section is just a small extension of the WGC, it implies that in a consistent theory of quantum gravity, all non-supersymmetric AdS geometries that are supported by fluxes must

⁸Very simply stated and without getting into details of supersymmetry, supersymmetric theories impose a lower bound on the mass of states that is given by the charge. This is the BPS bound. States that saturate the BPS bound are BPS states and the masses of these states do not receive quantum corrections. For a more detailed account of the BPS bound and BPS states, see e.g. [86].

⁹For further evidences for this version of the WGC, we refer to [75, 77]

be unstable. This follows from combining the sharpened WGC with the analysis done in [87]. The sharpened WGC demands that in non-supersymmetric theories, there must exist a brane that is charged with respect to the flux and that has a tension less than its charge. It was shown in [87] that if such branes exist in AdS, the geometry is unstable. This indeed seems to be true for all known constructions of non-supersymmetric AdS vacua in string theory. Multiple proposals have been formulated for such constructions, but not one of these has shown to be stable.

The instability of non-supersymmetric AdS can also be pictured in a different way, that suits better in the context of this thesis. Let us consider an extremal brane, whose near horizon geometry is AdS. If the brane is not protected by supersymmetry, then the sharpened WGC demands the existence of a (microscopic) superextremal brane. This means the extremal brane can decay through the emission of such a superextremal brane. A direct consequence of this decay is the instability of the AdS vacuum that is obtained from the brane's near horizon limit. So to conclude: a non-supersymmetric AdS vacuum that appears as the near horizon geometry of an extremal, but non-BPS, brane is unstable. The instability of this spacetime corresponds to the brane's ability to emit microscopic branes that obey the strict inequality of the weak gravity bound.

For a large extremal brane, the decay rate may be small. It could therefore exist as a quasi-stable state. In any case, the brane has a finite lifetime as viewed from far away. As we measure the decay rate closer to the brane's horizon, however, it becomes larger due to gravitational redshift. In the near horizon limit, observers are affected by an infinite redshift effect. Therefore, to an observer in AdS, the decay happens instantaneously.

In string theory, there are different approaches to obtain AdS vacua. In the above, we viewed AdS vacua as near horizon geometries of some given extremal brane solutions. We would like to know if the result extends to all AdS (flux) vacua in string theory, and not just those constructed with the use of branes. This essentially boils down to the question whether we may think of all AdS vacua as emerging as the near horizon geometry of a brane construction. In [77], it was argued that *“viewing AdS vacua as the near horizon limit of membranes is not merely a technical trick, but rather a physical statement and, as such, it may be used to analyze the stability of all AdS vacua.”* In other words, we may indeed use information about the (in)stability of extremal branes to find answers to questions concerning the (in)stability of the corresponding AdS vacua.

7.4 AdS₂ fragmentation

Our result does not forbid the emission of an extremal particle by an extremal black hole. However, if one follows the argument above, essentially stating that an extremal particle cannot exist in a non-supersymmetric theory, the amplitude for this process vanishes. In this section, we nevertheless discuss this possibility.

In [87] the fragmentation of an initial AdS₂ × S² geometry into two final AdS₂ × S² universes is discussed. The instanton that describes such a tunneling process was found by Brill, and is hence called the Brill instanton [88]. Here, we will not review his work, but simply use the results. Consider the fragmentation of an AdS₂ × S² space of charge (or equivalently: AdS radius) $Q = Q_1 + Q_2$ into two AdS₂ × S² spaces of charges Q_1 and Q_2 . In short we denote this as: AdS($Q_1 + Q_2$) → AdS(Q_1) + AdS(Q_2). The computed instanton action is

$$S_{inst} = -\frac{1}{2}\Delta S_{BH}, \quad (7.20)$$

where $S_{BH}(Q) = \pi Q^2$ is the Bekenstein-Hawking entropy of a extremal Reissner-Nordström black hole with charge Q and

$$\Delta S_{BH} = S_{BH}(Q_1) + S_{BH}(Q_2) - S_{BH}(Q_1 + Q_2) = -2\pi Q_1 Q_2. \quad (7.21)$$

This instanton provides us with the transition amplitude, so twice the factor (7.20) gives us the probability for this fragmentation to occur

$$\Gamma_{Q \rightarrow Q_1 + Q_2} \sim e^{-\Delta S_{BH}} = e^{-2\pi Q_1 Q_2}. \quad (7.22)$$

An assumption that has been made in deriving the above result is that either one of the charges Q_1 or Q_2 is very small compared to the other.

We can relate the above with the results we obtained in chapters 5 and 6. To do so we take our result in (5.87) and take the limit where $M \rightarrow Q$ and $\omega \rightarrow q$. This corresponds to the probability of an extremal Reissner-Nordström black hole of charge Q emitting an extremal particle of charge q . In this limit, our result reads

$$\Gamma_q \sim e^{\Delta S_{BH}} = e^{-2\pi(Qq - \frac{q^2}{2})}. \quad (7.23)$$

To see if our result agrees with the tunneling rate (7.22) we consider the probability for the emission of a particle with charge Q_2 from a black hole with charge $Q_1 + Q_2$ and focus on

the case where $Q_2 \ll Q_1$. Hence, we take (7.23) with $Q = Q_1 + Q_2$ and $q = Q_2$ to find

$$\begin{aligned} \Gamma(Q_1 + Q_2 \rightarrow Q_1) &\sim e^{S_{BH}(Q_1+Q_2-Q_1)-S_{BH}(Q_1+Q_2)} \\ &= e^{-2\pi(Q_1Q_2+\frac{Q_2^2}{2})} \\ &\simeq e^{-2\pi Q_1Q_2}, \end{aligned} \tag{7.24}$$

which equals the probability found in (7.22). Equally well, we could have considered the emission of a particle with charge Q_1 and $Q_1 \ll Q_2$. This would have given us the same result. Therefore, as far as our result is concerned, a non-supersymmetric extremal Reissner-Nordström may emit an extremal particle, with a probability that agrees with the probability for the fragmentation of $\text{AdS}_2 \times S^2$ geometry into two separate $\text{AdS}_2 \times S^2$ geometries, found in [87]. It might be interesting to further explore this link between the tunneling calculations performed in this thesis and gravitational instantons.

Chapter 8

Conclusions

We started this thesis with a review of some aspects of classical black hole physics and quantum fields in curved spacetime. In chapter 4, we merged these two concepts to discuss the semiclassical theory of black holes. We revisited Hawking's work [1, 25], who showed with strictly semiclassical methods that black holes radiate a purely thermal flux of particles, and can therefore evaporate. This discovery led to numerous puzzles, many of which have yet to be solved today. Nevertheless, black hole thought experiments have proved vital in leading us to our present understanding. Claims with regard to the quantum properties of gravity are often inferred from black hole physics, a particularly interesting example of which is the *weak gravity conjecture* (WGC). In short, it may safely be said that the process of black hole evaporation is far from fully understood and that a lot is still to be learned about black hole physics, even without a theory of quantum gravity at hand.

In this thesis we set out to gain a better understanding of the Hawking process in the presence of back reaction effects. Generally, this requires one to treat the metric as a quantum variable and therefore, quantum gravity. In [12, 13], however, an approach was suggested that allows for the inclusion of effects due to self-gravitation of the radiation in spherically symmetric setups, without the need for quantum gravity. The inclusion of these effects, probably the (quantitatively) most important back reaction effects, allows for the conservation of energy for the whole system throughout the emission process. Building on this approach, a large part of this thesis was devoted to the calculation of the s-wave emission probability for a black hole, while including effects of gravitational self-interactions.

In chapter 5, this analysis was performed for both massless and charged radiation from

Schwarzschild and Reissner-Nordström black holes. We showed that by properly taking into account the self-gravitational effects of the radiation one finds a modification of the emission probability away from thermality. In all cases considered in this thesis we found $\Gamma \sim e^{\Delta S_{BH}}$, where ΔS_{BH} is the change in the black hole's Bekenstein-Hawking entropy due to the emission. To lowest order in ω and q , respectively the emitted particle's energy and charge, this result yields the standard thermal spectrum. Higher order corrections drive the spectrum away from a strictly thermal one. It should be noted that this result differs from the results in [12, 13]. Our analysis may be thought of as correcting the one in these articles.

The route to our results furthermore exposes an intimate link with the tunneling description that is often used as an heuristic picture for Hawking radiation. It was shown that a quantum mechanical WKB tunneling calculation emerges from our field theory approach, essentially as we truncate to an effective particle description. This seems to imply that one may indeed naturally interpret the emission from a black hole as resulting from the tunneling of particles across the hole's horizon.

A particularly elegant derivation of black hole radiation, following this intuitive tunneling approach was proposed in [14], partly drawing on results from [12]. There, the tunneling of self-gravitating, massless shells across the black hole horizon is considered and a tunneling probability is obtained that agrees with our results reviewed above. In this thesis we showed in detail how the starting point of this tunneling analysis originates from the field theory approach and that the consistency of such a tunneling picture crucially depends on the enforcement of energy conservation. Therefore, the fact that the authors of [14] obtain similar results is to be expected. Nevertheless, the derivation of Hawking radiation as a tunneling process is elegant and allows one to avoid the more tedious Bogoliubov machinery. In chapter 6, this procedure was reviewed and generalized to include massive and charged radiation from Reissner-Nordström black holes. Again, we obtained the same result as with our field theory analysis, which also shows we were consistent.

In chapter 7 we reviewed the WGC and discussed our results in this context. One of the main motivations for the WGC originally was the notion to allow extremal black holes to decay. Such a decay process is not described by the strictly semi-classical Hawking effect. Our result explicitly shows a nonzero probability for an extremal Reissner-Nordström black hole to decay if and only if the WGC is obeyed. This should be expected for a correct

emission probability, and is equivalent to the statement that our result explicitly forbids the creation of a naked singularity by Hawking radiation.

Recently, some interesting work has linked the WGC to the instability non-supersymmetric AdS vacua [75, 76, 77]. As a closure of this thesis, we reviewed the interplay between the WGC, black hole (in)stability and the (in)stability of AdS. In this context it is noted that in the limit where an extremal black hole emits an extremal particle, our result for the emission probability matches the probability computed in [87] for an $\text{AdS}_2 \times S^2$ geometry to fragment into two disconnected $\text{AdS}_2 \times S^2$ geometries. It would be interesting to further investigate this relation.

The issues touched upon in chapter 7, concerning the WGC, AdS (in)stability, and their interplay with the evaporation of black holes and branes constitute an interesting direction for further research. For example, a better understanding of the evaporation of extremal black branes might shed light on the nature of the supposed instability of AdS vacua and the consequences for their dual CFTs. Of course, finding a proof of, or counterexample to, the WGC would be particularly valuable, as its implications reach far wider than just to the topics discussed in this thesis.

As for the analysis performed in chapters 5 and 6, we clarify once more that we only considered self-interactions. Taking into account interactions between subsequently emitted particles would be a logical next step. Considering multi-particle emission might also allow one to determine whether the inclusion of gravitating interactions leads to correlations in the radiation. Such an extension of the methods used in chapter 5, however, faces some difficulties, as was discussed in section 5.2.5.

As for the broader picture of this thesis, the ultimate goal would of course be to resolve the puzzles posed by the semiclassical study of black holes, and in particular to acquire a complete understanding of the information paradox. Fully resolving these issues, however, would very likely require a theory of quantum gravity. In the mean time, semiclassical black hole physics may continue to provide us with valuable clues.

Appendix A

Conformal diagrams

When working in a curved spacetime it is often challenging to imagine its global structure, even if this spacetime is highly symmetric. A useful tool to gain insight in this structure is a so called conformal diagram (or Penrose diagram), that can be drawn for sufficiently symmetric spacetimes [89]. A conformal diagram is a representation of a spacetime diagram, showing its global properties and causal structure.

In fact, a conformal diagram is nothing else than an ordinary spacetime diagram on which we have performed a clever coordinate transformation. Since we want to depict the causal structure of the manifold, we want the new coordinates to have at least the following two properties:

- there must be a ‘timelike’ and a ‘radial’ coordinate such that radial lightcones are consistently represented at 45° in the diagram, and
- ‘infinity’ must be at finite coordinate distance, in order for the structure of the full spacetime to be apparent in the diagram.

In order to satisfy these criteria, we use what is known as a conformal transformation. A conformal transformation has the form

$$g_{\mu\nu} \rightarrow \tilde{g}_{\mu\nu} = \omega(x)g_{\mu\nu}. \tag{A.1}$$

The metric is invariant under conformal transformations, up to a local change of scale. As such, transformations as in (A.1) leave angles between vectors invariant. For our purposes

it is a particularly crucial feature of conformal transformations that they leave null curves invariant. This is easily shown. Consider a null path $x^\mu(\lambda)$ parametrized by λ . Null paths must obey the condition

$$g_{\mu\nu} \frac{dx^\mu}{d\lambda} \frac{dx^\nu}{d\lambda} = 0. \quad (\text{A.2})$$

Performing now a conformal transformation yields for $x^\mu(\lambda)$

$$\tilde{g}_{\mu\nu} \frac{dx^\mu}{d\lambda} \frac{dx^\nu}{d\lambda} = \omega(x) g_{\mu\nu} \frac{dx^\mu}{d\lambda} \frac{dx^\nu}{d\lambda} = 0. \quad (\text{A.3})$$

Thus, a curve $x^\mu(\lambda)$ that is null with respect to the metric $g_{\mu\nu}$ is also null as defined by the conformally related metric $\tilde{g}_{\mu\nu}$. As conformal transformations leave null curves invariant, we will look for a set of coordinates in terms of which the metric is related by a conformal transformation to another metric, for which we know it has the property that lightcones are at 45° . Furthermore, we may choose the function $\omega(x)$ such that all points that are at ∞ in the old metric $g_{\mu\nu}$, are at finite coordinate distance in the new one $\tilde{g}_{\mu\nu}$.

To demonstrate how such conformal diagrams are constructed, we take the simplest possible example: Minkowski spacetime. In this procedure, we closely follow [15]. In polar coordinates the line element reads

$$ds^2 = -dt^2 + dr^2 + r^2 d\Omega^2. \quad (\text{A.4})$$

In this metric we already have the demanded feature that light cones are at 45° all over spacetime. All that remains is the transformation to coordinates that have finite ranges. To begin with, we switch to null coordinates

$$u = t - r, \quad v = t + r. \quad (\text{A.5})$$

Our original coordinates t and r had ranges

$$-\infty < t < \infty, \quad 0 \leq r < \infty \quad (\text{A.6})$$

and consequently our null coordinates cover ranges

$$-\infty < u < \infty, \quad -\infty < v < \infty, \quad u \leq v. \quad (\text{A.7})$$

In these coordinates the Minkowski line element is

$$ds^2 = -\frac{1}{2}(dudv - dvdu) + \frac{1}{4}(v - u)^2 d\Omega^2. \quad (\text{A.8})$$

Next, we bring the infinities to a finite coordinate value by defining

$$U = \arctan u, \quad V = \arctan v, \quad (\text{A.9})$$

where now

$$-\frac{\pi}{2} < U < \frac{\pi}{2}, \quad -\frac{\pi}{2} < V < \frac{\pi}{2}, \quad U \leq V \quad (\text{A.10})$$

In terms of these coordinates the metric (A.4) is given by

$$ds^2 = \frac{1}{4 \cos^2 U \cos^2 V} [-2(dU dV + dV dU) + \sin^2(V - U) d\Omega^2]. \quad (\text{A.11})$$

Finally, we switch to a timelike and radial coordinate

$$T = V + U, \quad R = V - U. \quad (\text{A.12})$$

T and R have corresponding ranges

$$0 \leq R < \pi, \quad |T| + R < \pi \quad (\text{A.13})$$

and the Minkowski metric now has the form

$$ds^2 = \omega^{-1}(T, R) (-dT^2 + dR^2 + \sin^2 R d\Omega^2) \quad (\text{A.14})$$

where $\Omega = (\cos T + \cos R)^{1/2}$. We see that the Minkowski metric ds^2 is conformally related to the metric \tilde{ds}^2

$$\tilde{ds}^2 = \omega(T, R) ds^2 = -dT^2 + dR^2 + \sin^2 R d\Omega^2. \quad (\text{A.15})$$

This is the metric of the spacetime $\mathbb{R} \times S^3$, with a spacelike, time-independent 3-sphere. Unlike Minkowski spacetime, this manifold is curved. However, the metric \tilde{ds}^2 is not physical. No matter what coordinates we choose, the truly physical metric is still the Minkowski one, which we obtain with a conformal transformation. The coordinates T and R only cover the ranges as defined by (A.13), instead of the full range on $\mathbb{R} \times S^3$ ($-\infty < T < \infty$, $0 \leq R \leq \pi$). This means Minkowski space is conformally mapped into a subspace of this manifold. If we draw $\mathbb{R} \times S^3$ as a cylinder, so that every circle of constant T in fact represents a spacelike 3-sphere, the dark region in figure A.1 represents Minkowski spacetime. This region can be ‘unrolled’ in order to represent Minkowski spacetime as a triangle in the T, R plane. This is done in figure A.2 and is what we call a conformal, or Penrose, diagram.

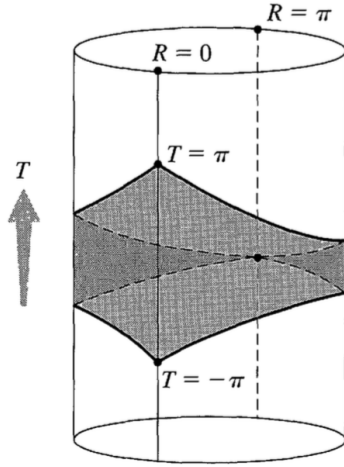


Figure A.1: This cylinder represents the manifold $\mathbb{R} \times S^3$, where every circle of constant T represents a spacelike 3-sphere. Minkowski space is conformally related to the interior of the shaded region. (Figure taken from [15])

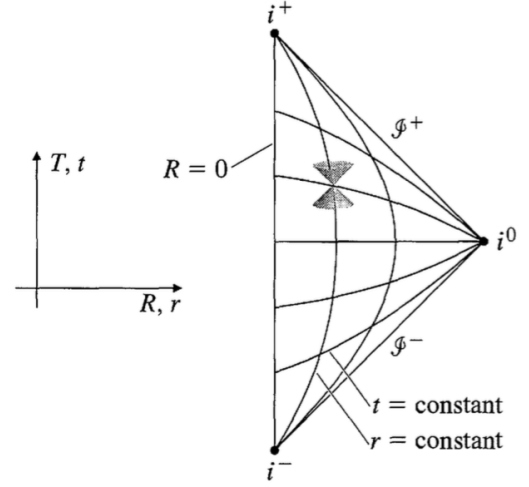


Figure A.2: This triangle is the conformal diagram of Minkowski spacetime. As depicted, lightcones are represented at 45° . (Figure taken from [15])

To be precise, Minkowski spacetime is just the interior of the shaded region in figure A.1 (as infinity is not part of the spacetime). We refer to the boundaries as conformal infinity. The union of conformal infinity and the physical spacetime under consideration is called the conformal compactification. As can be seen from the diagram A.2 conformal infinity comes in five pieces (where we added a heuristic description):

- i^+ , named *future timelike infinity*
 $t = \infty$, r is finite: timelike paths extend toward i^+ .
- i^- , named *past timelike infinity*.
 $t = -\infty$, r is finite: timelike paths start at i^- .
- i^0 , named *spacelike infinity*.
 $r = \infty$, t is finite: spacelike slices extend toward i^0 .
- \mathcal{I}^+ , named *future null infinity*.
 $t + r = \infty$, $t - r$ is finite: outgoing null paths extend toward \mathcal{I}^+ .

- \mathcal{I}^- , named *past null infinity*.

$t - r = -\infty$, $t + r$ is finite: ingoing null paths extend toward \mathcal{I}^+ .

Finally, let us mention some important characteristics of the conformal diagram A.2. As demanded beforehand, the radial null paths are at $\pm 45^\circ$. We see that all these null paths start at \mathcal{I}^- and end at \mathcal{I}^+ . All spacelike geodesics have i^0 as starting and ending point and all timelike geodesics start of at i^- and end at i^+ .

Minkowski serves as good example to show the meaning and construction of a conformal diagram. Apart from serving that purpose, it is a rather boring example. For more complicated spacetimes, conformal diagrams provide insight in their causal structure, which could be very interesting.

Appendix B

Solving to the Klein Gordon equation in a Schwarzschild geometry

We wish to find solutions to the massless Klein Gordon equation

$$\frac{1}{\sqrt{-g}}\partial_\mu(\sqrt{-g}g^{\mu\nu}\partial_\nu\phi) = 0, \quad (\text{B.1})$$

where $g = \det g_{\mu\nu}$. We are considering scalar fields in the Schwarzschild background, for which we have

$$g_{\mu\nu} = \begin{pmatrix} -f(r) & 0 & 0 & 0 \\ 0 & f(r)^{-1} & 0 & 0 \\ 0 & 0 & r^2 & 0 \\ 0 & 0 & 0 & r^2 \sin^2 \theta \end{pmatrix}, \quad g^{\mu\nu} = \begin{pmatrix} -f(r)^{-1} & 0 & 0 & 0 \\ 0 & f(r) & 0 & 0 \\ 0 & 0 & r^{-2} & 0 \\ 0 & 0 & 0 & r^{-2} \sin^{-2} \theta \end{pmatrix} \quad (\text{B.2})$$

and $g = -r^4 \sin^2 \theta$. We now substitute this data for the Schwarzschild geometry into (B.1) to obtain

$$\left[-\frac{1}{f(r)}\partial_t^2 + \frac{1}{r^2}\partial_r(r^2 f(r)\partial_r) + \frac{1}{r^2 \sin \theta} \left(\partial_\theta \sin \theta \partial_\theta + \frac{1}{\sin \theta} \partial_\varphi^2 \right) \right] \phi = 0. \quad (\text{B.3})$$

Now we recognize in the last term the Laplacian on the 2-sphere and write it in terms of the angular momentum operator, \hat{L}^2

$$\left[-\frac{1}{f(r)}\partial_t^2 + \frac{1}{r^2}\partial_r(r^2 f(r)\partial_r) - \frac{1}{r^2}\hat{L}^2 \right] \phi = 0. \quad (\text{B.4})$$

Since we have no mixed terms, we can solve this equation by separation of variables. The solution ϕ can be rewritten as

$$\phi = (Ae^{-i\omega t} + A^*e^{i\omega t}) R(r)\Theta(\theta, \varphi). \quad (\text{B.5})$$

We substitute this in (B.4), divide by $(Ae^{-i\omega t} + A^*e^{i\omega t})$, take one term to the left and divide by $R(r)\Theta(\theta, \varphi)/r^2$ to obtain

$$\frac{r^2}{R(r)} \left[\frac{\omega^2}{f(r)} + \frac{1}{r^2} \partial_r (r^2 f(r) \partial_r) \right] R(r) = \frac{1}{\Theta(\theta, \varphi)} \hat{L}^2 \Theta(\theta, \varphi). \quad (\text{B.6})$$

This equation is explicitly written in separable form, meaning both sides of the equation are constant. We take this constant to be $l(l+1)$. Firstly we take the angular part

$$\hat{L}^2 \Theta(\theta, \varphi) = l(l+1) \Theta(\theta, \varphi). \quad (\text{B.7})$$

The solutions to this equation are well known as

$$\Theta(\theta, \varphi) = \sum_m B_{lm} Y_{lm}(\theta, \varphi), \quad (\text{B.8})$$

where Y_{lm} are the spherical harmonics and B_{lm} are integration constants. On to the radial equation

$$\left[\frac{\omega^2}{f(r)} + \frac{1}{r^2} \partial_r (r^2 f(r) \partial_r) - \frac{l(l+1)}{r^2} \right] R(r) = 0. \quad (\text{B.9})$$

To solve this we switch variables to the *tortoise* coordinate $r_* = r + 2M \log \left| \frac{r}{2M} - 1 \right|$, such that

$$\partial_r = \frac{1}{f(r)} \partial_{r_*}, \quad (\text{B.10})$$

and introduce $\tilde{R}(r_*) = rR(r)$. In terms of these variables we have

$$\left[\frac{\omega^2}{f(r)} \frac{1}{f(r)} \partial_{r_*}^2 - \frac{2M}{r^3} - \frac{l(l+1)}{r^2} \right] \frac{\tilde{R}(r_*)}{r} = 0. \quad (\text{B.11})$$

Multiplying by $rf(r)$ gives us

$$\partial_{r_*}^2 \tilde{R}(r_*) + \left[\omega^2 - f(r) \left(\frac{2M}{r^3} + \frac{l(l+1)}{r^2} \right) \right] \tilde{R}(r_*) = 0 \quad (\text{B.12})$$

Now, we are interested in solutions at $r \rightarrow \infty$, as discussed in section (4.1). In this limit we have

$$\partial_{r_*}^2 \tilde{R}(r_*) + \omega^2 \tilde{R}(r_*) = 0, \quad r \rightarrow \infty. \quad (\text{B.13})$$

This equation has the solution

$$R(r) = \frac{\tilde{R}(r_*)}{r} = \frac{1}{r} (C_{\omega l} e^{-i\omega r_*} + C_{\omega l}^* e^{i\omega r_*}). \quad (\text{B.14})$$

Plugging this solution for $R(r)$ and (B.8) into our expression for ϕ (B.5) we have

$$\phi = \sum_{\omega, l, m} \frac{1}{r} [AC_{\omega l} e^{-i\omega(t+r_*)} + AC_{\omega l}^* e^{-i\omega(t-r_*)} + A^* C_{\omega l} e^{i\omega(t-r_*)} + A^* C_{\omega l}^* e^{i\omega(t+r_*)}] B_{lm} Y_{lm}(\theta, \varphi). \quad (\text{B.15})$$

We now switch to the affine parameters, used in section 4.1

$$v = t + r_* \quad u = t - r_*. \quad (\text{B.16})$$

We express our solutions in terms of these parameters and take all constants A, B, C together apart from a factor $\frac{1}{\sqrt{2\pi\omega}}$ (common in solutions to KG equation). We furthermore give our integration ‘constants’ a small r -dependence, to account for our approximate limit $r \rightarrow \infty$. We see that two partial wave solutions to the Klein Gordon equation in the Schwarzschild geometry are

$$\begin{aligned} f_{\omega lm} &= \frac{F_{\omega}(r)}{r\sqrt{2\pi\omega}} e^{i\omega v} Y_{lm}(\theta, \varphi) \\ p_{\omega lm} &= \frac{P_{\omega}(r)}{r\sqrt{2\pi\omega}} e^{i\omega u} Y_{lm}(\theta, \varphi). \end{aligned} \quad (\text{B.17})$$

Appendix C

Evaluating contour integrals

The integrals we encounter in chapters 5 and 6 can be evaluated using techniques of complex analysis. In particular, the methods of contour integration are useful. The integrals in chapter 6 have poles on the region of the real axis that we integrate over. The integrals in chapter 5 involve logarithms and therefore require some additional attention. In this appendix we review some of the basics necessary to perform the integrals in both chapters.

C.1 One pole on the real axis

In chapter, 6 the integrals want to evaluate are of the form

$$\int_A^B f(x)dx, \tag{C.1}$$

where the integrand diverges at a point that lies in the interval of integration. Let us call this point x_0 , then

$$\lim_{x \rightarrow x_0} |f(x)| = \infty. \tag{C.2}$$

The integral in (C.1) is defined as

$$\int_A^B f(x)dx = \lim_{\epsilon \rightarrow 0} \int_A^{x_0 - \epsilon} f(x)dx + \lim_{\eta \rightarrow 0} \int_{x_0 + \eta}^B f(x)dx. \tag{C.3}$$

Here ϵ and η go to zero through positive values and they do so independently. It might be that these limits do not exist. However, there is another limit that does exist, called the

Cauchy principal value

$$P \int_A^B f(x) dx = \lim_{\epsilon \rightarrow 0} \left[\int_A^{x_0 - \epsilon} f(x) dx + \int_{x_0 + \epsilon}^B f(x) dx \right]. \quad (\text{C.4})$$

If $f(z)$ falls off rapidly enough in the upper half plane, we can find a formula for the principal value of an integral with a simple pole on the real axis.

We pick a contour C that is a semicircle in the upper half plane. We deform this contour around the pole through the upper half plane. Since we consider the case in which we have no poles in the upper half plane, the integral along the entire contour will be zero

$$\oint_C f(z) dz = 0. \quad (\text{C.5})$$

Since we demanded the function $f(z)$ to fall off rapidly in the upper half plane, the value of the integral over the large semicircle approaches zero. Therefore

$$\oint_C f(z) dz = 0 = P \int_A^B f(x) dx - i\pi \text{Res}[f(z)], \quad (\text{C.6})$$

where $\text{Res}[f(x)]$ is the residue of $f(z)$ at z_0 .¹ The final term comes from the contribution of the small semicircle around the pole at x_0 . A proof of the value of this last term can be found in [90]. This means we can evaluate the integrals encountered in chapter 6 with the formula

$$\int_A^B f(x) dx = P \int_A^B f(x) dx = i\pi \text{Res}[f(z)]. \quad (\text{C.7})$$

C.2 Issues with logarithms

The integrals encountered in chapter 5 have to be treated a bit differently. These integrals involve logarithms and are of the form

$$\int_A^B f(x) \log \left| \frac{x-a}{x-b} \right| dx, \quad (\text{C.8})$$

where a and b lie within the interval of integration and $f(x)$ is regular on this interval. Here, $x = a$ and $x = b$ are branch points. Therefore, we have to be a bit more careful. We pick a

¹Methods for calculating residues can be found in e.g. [90]

branch cut that adjoins the branch points a and b . If we now choose a contour that encloses this branch cut, then the integrand will be analytic outside the contour. This means we may evaluate this integral using the residue at infinity. For some function $g(z)$, this is

$$\text{Res}[g(z), \infty] = -\text{Res} \left[\frac{1}{z^2} g \left(\frac{1}{z} \right), 0 \right]. \quad (\text{C.9})$$

If a and b are on the real axis, we may combine the above with similar techniques as in section C.1 to find

$$\int_A^B g(x) dx = -\pi i \text{Res} \left[\frac{1}{z^2} g \left(\frac{1}{z} \right), 0 \right], \quad (\text{C.10})$$

where $g(x) = f(x) \log \left| \frac{x-a}{x-b} \right| dx$.

The integrals in chapter 5 are of the form

$$\int_A^B r \log \left| \frac{\sqrt{r} - \sqrt{a}}{\sqrt{r} - \sqrt{b}} \right|. \quad (\text{C.11})$$

Substituting $u \equiv \sqrt{r}$ gives

$$\int_A^B 2u^3 \log \left| \frac{u - \sqrt{a}}{u - \sqrt{b}} \right| du. \quad (\text{C.12})$$

Hence, we find

$$\begin{aligned} \int_A^B 2u^3 \log \left| \frac{u - \sqrt{a}}{u - \sqrt{b}} \right| du &= -\pi i \text{Res} \left[\frac{2}{u^5} \log \left| \frac{1 - \sqrt{a}u}{1 - \sqrt{b}u} \right|, u = 0 \right] \\ &= -\frac{\pi i}{2} (b^2 - a^2) \end{aligned} \quad (\text{C.13})$$

Bibliography

- [1] S. W. Hawking. Black Hole Explosions? *Nature*, 248:30, 1974.
- [2] B. Carter. Black hole equilibrium states. In C. DeWitt and B.S. DeWitt, editors, *Black Holes*, pages 57–214. Gordon and Breach, New York, 1973.
- [3] J.M. Bardeen, B. Carter, and S.W. Hawking. The four laws of black hole mechanics. *Comm. Math. Phys.*, 31:161, 1973.
- [4] J.D. Bekenstein. Black holes and entropy. *Phys. Rev.*, D7:2333, 1973.
- [5] J.D. Bekenstein. Generalized second law of thermodynamics in black hole physics. *Phys. Rev.*, D9:3292, 1974.
- [6] A. Strominger and C. Vafa. Microscopic origin of the Bekenstein-Hawking entropy. *Phys. Lett.*, B379:99–104, 1996.
- [7] S. W. Hawking. Breakdown of Predictability in Gravitational Collapse. *Phys. Rev.*, D14:2460–2473, 1976.
- [8] G. 't Hooft. Dimensional reduction in quantum gravity. In *Salamfest 1993:0284-296*, pages 0284–296, 1993.
- [9] L. Susskind. The World as a hologram. *J. Math. Phys.*, 36:6377–6396, 1995.
- [10] J. Maldacena. The large N limit of superconformal field theories and supergravity. *Adv. Theor. Math. Phys.*, 2:231, 1998.
- [11] N. Arkani-Hamed, L. Motl, A. Nicolis, and C. Vafa. The String landscape, black holes and gravity as the weakest force. *JHEP*, 06:060, 2007.

-
- [12] P. Kraus and F. Wilczek. Self-interaction correction to black hole radiance. *Nucl. Phys.*, B433:403–420, 1995.
- [13] P. Kraus and F. Wilczek. Effect of self-interaction correction on charged black hole radiance. *Nucl. Phys.*, B437:231–242, 1995.
- [14] M.K. Parikh and F. Wilczek. Hawking radiation as tunneling. *Phys. Rev. Lett.*, 85:5042–5045, 2000.
- [15] S. Carrol. *Spacetime and Geometry*. Pearson, Harlow, England, 2014.
- [16] G.F.R. Ellis and S.W. Hawking. *The large scale structure of spacetime*. Cambridge University Press, Cambridge, England, 1973.
- [17] P.K. Townsend. Black holes. Lecture notes given as part of the Cambridge University Mathematical Tripos, 1997.
- [18] R.M. Wald. The thermodynamics of black holes. *Living Rev. in Rel.*, 4:6, 2001.
- [19] H.S. Reall. Part 3: Black holes. Lecture notes given as part of the Cambridge University Mathematical Tripos, 2014.
- [20] B. Carter. Properties of the Kerr metric. In C. DeWitt and B.S. DeWitt, editors, *Black Holes*. Gordon and Breach, New York, 1973.
- [21] S.W. Hawking. Gravitational radiation from colliding black holes. *Phys. Rev. Lett.*, 26:1344, 1971.
- [22] S.W. Hawking. Black holes in general relativity. *Commun. Math. Phys.*, 25:152, 1972.
- [23] G.D. Birkhoff. *Relativity and modern physics*. Harvard University Press, Harvard, United States, 1923.
- [24] C.W. Misner, K.S. Thorne, and J.A. Wheeler. *Gravitation*. W.H. Freeman and Company, New York, United States, 1973.
- [25] S.W. Hawking. Particle creation by black holes. *Commun. Math. Phys.*, 43:199, 1975.
- [26] T. Hartmann. Lectures on Quantum Gravity and Black Holes. Lecture notes Cornell Physics 7661, 1997.

-
- [27] P. Painlevé. La mécanique classique et la théorie de la relativité. *C. R. Acad. Sci. (Paris)*, 173:677, 1921.
- [28] P. Kraus and F. Wilczek. Some applications of a simple stationary line element for the Schwarzschild geometry. *Mod. Phys. Lett.*, A9:3713, 1994.
- [29] M.K. Parikh. New coordinates for de Sitter space and de Sitter radiation. *Phys. Lett.*, B546:189, 2002.
- [30] A.J.M. Medved. Radiation via tunneling from a de Sitter cosmological horizon. *Phys. Rev.*, D66:124009, 2002.
- [31] S. Hemming and E. Keski-Vakkuri. Hawking radiation from AdS black holes. *Phys. Rev.*, D64:044006, 2001.
- [32] E.C. Vagenas. Semiclassical corrections to the Bekenstein-Hawking entropy of the BTZ black hole via selfgravitation. *Phys. Lett.*, B533:302, 2002.
- [33] N.B. Birrel and P.C.W. Davies. *Quantum fields in curved space*. Cambridge University Press, Cambridge, England, 1992.
- [34] L. Parker and D. Toms. *Quantum field theory in curved spacetime: quantum fields and gravity*. Cambridge University Press, Cambridge, England, 2009.
- [35] V. Mukhanov and S. Winitzki. *Introduction to quantum effects in gravity*. Cambridge University Press, Cambridge, England, 2007.
- [36] T. Jacobsen. Introduction to quantum fields in curved space-time and the Hawking effect. Notes on lectures given at the CECS School on Quantum Gravity in Valdivia, Chile, January 2002, 2003.
- [37] S.A. Fulling. Non-uniqueness of canonical field quantization in Riemannian space-time. *Phys. Rev. D*, 7:2850, 1973.
- [38] N.N. Bogoliubov. A new method in the theory of superconductivity. *Sov. Phys. JETP.*, 34:58, 1958.
- [39] W.G. Unruh. Notes on black hole evaporation. *Phys. Rev. D*, 14:870, 1976.

-
- [40] J. Traschen. An Introduction to Black Hole Evaporation. In A. Bytsenko and F. Williams, editors, *Mathematical Methods of Physics, proceedings of the 1999 Londrina Winter School*. World Scientific, 2000.
- [41] K. Umetsu. *Recent Attempts in the Analysis of Black Hole Radiation*. PhD thesis, Nihon University, 2010.
- [42] J.B. Hartle and S.W. Hawking. Path integral derivation of black hole radiance. *Phys. Rev. D*, 13:2188, 1976.
- [43] G.W. Gibbons and S.W. Hawking. Action integrals and partition functions in quantum gravity. *Phys. Rev. D*, 15:2752, 1977.
- [44] S.M. Christensen and S.A. Fulling. Trace anomalies and the Hawking effect. *Phys. Rev. D*, 15:2088, 1977.
- [45] K. Fredenhagen and R. Haag. On the derivation of the Hawking radiation associated with the formation of a black hole. *Commun. Math. Phys.*, 127:273, 1990.
- [46] M. Banados, C. Teitelboim, and J. Zanelli. Black hole entropy and the dimensional continuation of the Gauss-Bonnet theorem. *Phys. Rev. Lett.*, 72:957, 1994.
- [47] R.M. Wald. On particle creation by black holes. *Commun. Math. Phys.*, 45:9, 1975.
- [48] J. Polchinski. The Black Hole Information Problem. In *Proceedings, Theoretical Advanced Study Institute in Elementary Particle Physics: New Frontiers in Fields and Strings (TASI 2015): Boulder, CO, USA, June 1-26, 2015*, pages 353–397, 2017.
- [49] S.D. Mathur. What Exactly is the Information Paradox? *Lect. Notes Phys.*, 769:3–48, 2009.
- [50] S.D. Mathur. The Information paradox: A Pedagogical introduction. *Class. Quant. Grav.*, 26:224001, 2009.
- [51] T. Banks, L. Susskind, and M.E. Peskin. Difficulties for the Evolution of Pure States Into Mixed States. *Nucl. Phys.*, B244:125–134, 1984.
- [52] S.B. Giddings. Constraints on black hole remnants. *Phys. Rev.*, D49:947–957, 1994.
- [53] L. Susskind. Trouble for remnants. 1995. hep-th/9501106.

-
- [54] A. Almheiri, D. Marolf, J. Polchinski, and J. Sully. Black Holes: Complementarity or Firewalls? *JHEP*, 02:062, 2013.
- [55] J. Preskill, P. Schwarz, A. D. Shapere, Sandip Trivedi, and Frank Wilczek. Limitations on the statistical description of black holes. *Mod. Phys. Lett.*, A6:2353–2362, 1991.
- [56] R. Arnowitt, S. Deser, and C.W. Misner. Dynamical structure and definition of energy in general relativity. *Phys. Rev.*, 116 (5):1322, 1959.
- [57] R. Arnowitt, S. Deser, and C.W. Misner. *The dynamics of general relativity*, chapter 7. Wiley, 1962.
- [58] R. Arnowit, S. Deser, and C.W. Misner. Republication of: The dynamics of general relativity. *Gen. Rel and Grav.*, 40 (9):1997, 2008.
- [59] B.K. Berger, D. M. Chitre, V. E. Moncrief, and Y. Nutku. Hamiltonian formulation of spherically symmetric gravitational fields. *Phys. Rev. D*, 5:2467–2470, 1972.
- [60] W. Fischler, D. Morgan, and J. Polchinski. Quantization of false-vacuum bubbles: a Hamiltonian treatment of gravitational tunneling. *Phys. Rev.*, D42:4042, 1990.
- [61] P. Kraus. *Nonthermal aspects of black hole radiance*. PhD thesis, Princeton University, 1995.
- [62] M.K. Parikh. Energy conservation and Hawking radiation. 2004. hep-th/0402166.
- [63] W. Israel and Z. Yun. Band-aid for information loss from black holes. *Phys. Rev.*, D 82:124036, 2010.
- [64] S. Massar and R. Parentani. On the gravitational back reaction to Hawking radiation. 1998. gr-qc/9801043.
- [65] M.K. Parikh. A secret tunnel through the horizon. 2004. hep-th/0405160.
- [66] J. Polchinski. *String theory*. Cambridge University Press, New York, United States, 2005.
- [67] M.B. Green, J.H. Schwarz, and E. Witten. *Superstring theory*. Cambridge University Press, Cambridge, England, 2012.
- [68] C. Vafa. The String landscape and the swampland. 2005. hep-th/0509212.

-
- [69] H. Ooguri and C. Vafa. On the geometry of the string landscape and the swampland. *Nucl. Phys. B*, 766:21, 2007.
- [70] L.D. Landau. In W. Pauli, editor, *Niels Bohr and the development of physics*. Pergamon Press, London, England, 1955.
- [71] C. Cheung and G.N. Remmen. Naturalness and the Weak Gravity Conjecture. *Phys. Rev. Lett.*, 113:051601, 2014.
- [72] Y. Nakayama and Y. Nomura. Weak gravity conjecture in the AdS/CFT correspondence. *Phys. Rev.*, D 92:126006, 2015.
- [73] J. Brown, W. Cottrell, G. Shiu, and P. Soler. Fencing in the swampland: quantum gravity constraints on large field inflation. *JHEP*, 10:23, 2015.
- [74] W. Cottrell, G. Shiu, and P. Soler. Weak gravity conjecture and extremal black holes. 2017. 1611.06270 [hep-th].
- [75] H. Ooguri and C. Vafa. Non-supersymmetric AdS and the swampland. 2016. 1610.01533 [hep-th].
- [76] B. Freivogel and M. Kleban. Vacua morghulis. 2016. 1610.04564 [hep-th].
- [77] U.H. Danielsson and G. Dibitetto. The fate of stringy AdS vacua and the WGC. 2016. 1611.01395 [hep-th].
- [78] T. Banks, M. Johnson, and A. Shomer. A note on gauge theories coupled to gravity. *JHEP*, 09:49, 2006.
- [79] T. Banks and N. Seiberg. Symmetries and strings in field theory and gravity. *Phys. Rev.*, D 83:084019, 2011.
- [80] R. Kallosh, A.D. Linde, D.A. Linde, and L. Susskind. Gravity and global symmetries. *Phys. Rev.*, D 52:912, 1995.
- [81] C. Cheung and G.N. Remmen. Infrared consistency and the weak gravity conjecture. *JHEP*, 12:87, 2014.
- [82] B. Bellazzini, C. Cheung, and G.N. Remmen. Quantum gravity constraints from unitarity and analyticity. *Phys. Rev. D*, 93:064076, 2016.

-
- [83] B. Heidenreich, M. Reece, and T. Rudelius. Evidence for a lattice weak gravity conjecture. 2016. hep-th/1606.08437.
- [84] Z. Fisher and C.J. Mogni. A semiclassical, entropic proof of the weak gravity conjecture. 2017. 1706.08257 [hep-th].
- [85] M. Cvetič, H. Lu, C.N. Pope, and J.F. Vazquez-Poritz. AdS in warped spacetimes. *Phys. Rev.*, D62:122003, 2000.
- [86] F. Quevedo, S. Krippendorf, and O. Schlotterer. Cambridge Lectures on supersymmetry and extra dimensions. Lectures given in Part III of the Mathematical Tripos at the University of Cambridge, 2010.
- [87] J.M. Maldacena, J. Michelson, and A. Strominger. Anti-de Sitter fragmentation. *JHEP*, 9902:011, 1999.
- [88] D. Brill. Splitting of an extremal Reissner-Nordström throat via quantum tunneling. *Phys. Rev.*, D 46:1560, 1992.
- [89] R. Penrose. Conformal treatment of infinity. In C. DeWitt and B.S. DeWitt, editors, *Relativity, groups and topology*, page 565. Gordon and Breach, New York, 1964.
- [90] E. Kreyszig. *Advanced engineering mathematics*. John Wiley and Sons, Hoboken, United States, 2006.